

## **Substituted Aromatic Pentaphosphole Ligands – A Journey Across the p-Block**

Christoph Riesinger, Gábor Bálazs, Michael Seidl and Manfred Scheer\*

### **Author Contributions**

Christoph Riesinger – performing experimental work, writing of original draft.

Gábor Balázs – consultation regarding DFT calculations.

Michael Seidl – consultation regarding X-ray data handling.

Manfred Scheer – project administration, funding acquisition.

All authors contributed in preparing the manuscript.

# Contents

Contents.....	2
1. Synthesis and analytical data .....	1
1.1. General Considerations.....	1
1.2. $[\{Cp^*Fe\}_2\{(\eta^5-P_5)_2BBr_2\}][TEF]$ (2) .....	2
1.3. $[\{Cp^*Fe\}_2\{(\eta^5-P_5)_2Gal_2\}][TEF]$ (3).....	3
1.4. $[Cp^*Fe(\eta^5-P_5CH_2Ph)][TEF]$ (4).....	4
1.5. $[Cp^*Fe(\eta^5-P_5CHPh_2)][TEF]$ (5).....	5
1.6. $[Cp^*Fe(\eta^5-P_5SiHPh_2)][B(C_6F_5)_4]$ (6) .....	6
1.7. $[Cp^*Fe(\eta^5-P_5AsCy_2)][TEF]$ (7).....	7
1.8. $[\{Cp^*Fe(\mu,\eta^{5:2}-P_5)\}SbICp'''][TEF]$ (8).....	8
1.9. $[Cp^*Fe(\eta^5-P_5SePh)][TEF]$ (9).....	9
1.10. $[Cp^*Fe(\eta^5-P_5TeMes)][TEF]$ (10) .....	10
1.11. $[Cp^*Fe(\eta^5-P_5Cl)][TEF]$ (11).....	11
1.12. $[Cp^*Fe(\eta^5-P_5Br)][TEF]$ (12) .....	12
1.14. $[\{Cp''Ta(CO)_2\}_2\{\mu,\eta^{4:4}-((P_4)_2BBr_2)\}][TEF]$ (15) .....	14
2. Xray .....	16
2.1. General remarks.....	16
2.2. $[\{Cp^*Fe\}_2\{(\eta^5-P_5)_2BBr_2\}][TEF]$ (2) .....	19
2.3. $[\{Cp^*Fe\}_2\{(\eta^5-P_5)_2Gal_2\}][TEF]$ (3).....	20
2.4. $[Cp^*Fe(\eta^5-P_5CH_2Ph)][TEF]$ (4).....	21
2.5. $[Cp^*Fe(\eta^5-P_5CHPh_2)][TEF]$ (5).....	22
2.6. $[Cp^*Fe(\eta^5-P_5SiHPh_2)][B(C_6F_5)_4]$ (6) .....	23
2.7. $[Cp^*Fe(\eta^5-P_5AsCy_2)][TEF]$ (7).....	24
2.8. $[\{Cp^*Fe(\mu,\eta^{5:2}-P_5)\}SbICp'''][TEF]$ (8).....	25
2.9. $[Cp^*Fe(\eta^5-P_5SePh)][TEF]$ (9).....	26
2.10. $[Cp^*Fe(\eta^5-P_5TeMes)][TEF]$ (10) .....	27
2.11. $[Cp^*Fe(\eta^5-P_5Cl)][TEF]$ (11).....	28
2.12. $[Cp^*Fe(\eta^5-P_5Br)][TEF]$ (12) .....	29
2.13. $[Cp^*Fe(\eta^5-P_5I)][TEF]$ (13).....	30
2.14. $[\{Cp''Ta(CO)_2\}_2\{\mu,\eta^{4:4}-((P_4)_2BBr_2)\}][TEF]$ (15) .....	31
3. NMR .....	32
3.1. $[\{Cp^*Fe\}_2\{(\eta^5-P_5)_2BBr_2\}][TEF]$ (2) .....	32
3.2. $[\{Cp^*Fe\}_2\{(\eta^5-P_5)_2Gal_2\}][TEF]$ (3).....	34

3.3.	[Cp*Fe( $\eta^5$ -P <sub>5</sub> CH <sub>2</sub> Ph)][TEF] (4).....	35
3.4.	[Cp*Fe( $\eta^5$ -P <sub>5</sub> CHPh <sub>2</sub> )][TEF] (5).....	38
3.5.	[Cp*Fe( $\eta^5$ -P <sub>5</sub> SiHPh <sub>2</sub> )][B(C <sub>6</sub> F <sub>5</sub> ) <sub>4</sub> ] (6) .....	41
3.6.	[Cp*Fe( $\eta^5$ -P <sub>5</sub> AsCy <sub>2</sub> )][TEF] (7).....	43
3.7.	[{Cp*Fe( $\mu$ , $\eta^{5:2}$ -P <sub>5</sub> )SbICp'''][TEF] (8) .....	44
3.8.	[Cp*Fe( $\eta^5$ -P <sub>5</sub> SePh)][TEF] (9) .....	45
3.9.	[Cp*Fe( $\eta^5$ -P <sub>5</sub> TeMes)][TEF] (10) .....	47
3.10.	[Cp*Fe( $\eta^5$ -P <sub>5</sub> Cl)][TEF] (11).....	48
3.11.	[Cp*Fe( $\eta^5$ -P <sub>5</sub> Br)][TEF] (12) .....	49
3.12.	[Cp*Fe( $\eta^5$ -P <sub>5</sub> I)][TEF] (13) .....	50
3.13.	[{Cp'''Ta(CO) <sub>2</sub> } <sub>2</sub> { $\mu$ , $\eta^{4:4}$ -((P <sub>4</sub> ) <sub>2</sub> BBr <sub>2</sub> )}][TEF] (15) .....	51
3.14.	Additional Data .....	52
4.	Computational Details .....	55
4.1.	General remarks.....	55
4.2.	NBO Analyses .....	55
4.3.	NICS Values .....	57
4.4.	Optimized Geometries .....	58
5.	References .....	92

## 1. Synthesis and analytical data

### 1.1. General Considerations

All manipulations were carried out using standard Schlenk techniques at a Stock apparatus under N<sub>2</sub> as an inert gas or in a glove box with Ar atmosphere. All glassware was dried with a heat gun (600 °C) for at least 30 min prior to use. o-DFB (1,2-difluorobenzene) was distilled from P<sub>2</sub>O<sub>5</sub>, CD<sub>2</sub>Cl<sub>2</sub> was distilled from CaH<sub>2</sub> and other solvents were directly taken from an MBraun SPS-800 solvent purification system and degassed at room temperature. Solution <sup>1</sup>H (400.130 MHz), <sup>11</sup>B (128.432 MHz) <sup>13</sup>C (100.627 MHz), <sup>19</sup>F (376.498 MHz), <sup>29</sup>Si (79.485 MHz), <sup>31</sup>P (161.976 MHz) and <sup>77</sup>Se (76.334 MHz) NMR spectra were recorded at an Avance400 (Bruker) spectrometer using (H<sub>3</sub>C)<sub>4</sub>Si (<sup>1</sup>H, <sup>13</sup>C, <sup>29</sup>Si), BF<sub>3</sub>·OEt<sub>2</sub> (<sup>11</sup>B) CFCl<sub>3</sub> (<sup>19</sup>F), SeMe<sub>2</sub> (<sup>77</sup>Se) or 85% phosphoric acid (<sup>31</sup>P), respectively, as external standards. Chemical shifts ( $\delta$ ) are provided in parts per million (ppm) and coupling constants ( $J$ ) are reported in Hertz (Hz). Chemical shifts and coupling constants for all <sup>31</sup>P{<sup>1</sup>H} and <sup>31</sup>P NMR spectra were derived from spectral simulation using the built-in simulation package of TopSpin3.2. The following abbreviations are used: s = singlet, d = doublet, dd = doublet of doublets, dt = doublet of triplets, t = triplet, td = triplet of doublets br = broad and m = multiplet. ESI mass spectra were recorded at the internal mass spectrometry department using a ThermoQuest Finnigan TSQ 7000 mass spectrometer or by the first author on a Waters Micromass LCT ESI-TOF mass-spectrometer and peak assignment was performed using the Molecular weight calculator 6.50.<sup>1</sup> Elemental analysis of the products was conducted by the elemental analysis department at the University of Regensburg using an Elementar Vario EL. The starting materials [Cp\*Fe( $\eta^5$ -P<sub>5</sub>)] (**1**),<sup>2</sup> Ti[TEF],<sup>3</sup> [Ph<sub>3</sub>C][B(C<sub>6</sub>F<sub>5</sub>)<sub>4</sub>],<sup>4</sup> Cy<sub>2</sub>AsCl,<sup>5</sup> PhSeBr,<sup>6</sup> MesTeBr<sup>7</sup>, NaCp'',<sup>8</sup> [Cp''Ta(CO)<sub>2</sub>( $\eta^4$ -P<sub>4</sub>)] (**14**)<sup>9</sup> were synthesized following literature procedures. All other chemicals were purchased from commercial vendors and used without further purification.

## 1.2. [{Cp\*Fe}2{(\eta<sup>5</sup>-P<sub>5</sub>)<sub>2</sub>BBr<sub>2</sub>}][TEF] (2)

[Cp\*Fe(η<sup>5</sup>-P<sub>5</sub>)] (0.2 mmol, 70 mg, 2 eq.) and Ti[TEF] (0.1 mmol, 117 mg, 1 eq.) were dissolved in 4 mL of o-DFB and cooled to -30 °C. BBr<sub>3</sub> (0.1 mmol, 10 μL, 1 eq.) was added with a syringe which afforded a rapid colour change to brownish green and the precipitation of white solid (TIBr). The resulting solution was stirred for 1.5 h, filtered, and then layered with 40 mL of *n*-hexane. After storage for eight days the product [{Cp\*Fe}2{(\eta<sup>5</sup>-P<sub>5</sub>)<sub>2</sub>BBr<sub>2</sub>}][TEF] (**2**) could be isolated as crystalline dark brownish green sticks, which were of X-ray quality.

Yield: 130 mg (0.070 mmol, 70%)

Elemental analysis: calc. (%) for [{Cp\*Fe}2{(\eta<sup>5</sup>-P<sub>5</sub>)<sub>2</sub>BBr<sub>2</sub>}][TEF]·(*n*-hex)<sub>0.4</sub> (C<sub>38.4</sub>H<sub>35.6</sub>BO<sub>4</sub>F<sub>36</sub>AlP<sub>10</sub>Fe<sub>2</sub>Br<sub>2</sub>): C: 24.74 H: 1.92

found (%): C: 25.13 H: 1.76

ESI(+) MS (o-DFB): *m/z* (%) = 345.92 (30%) [Cp\*Fe(η<sup>5</sup>-P<sub>5</sub>)]<sup>+</sup>, 417.98 (100%) [Cp\*FeP<sub>6</sub>·MeCN]<sup>+</sup>, (strong fragmentation)

NMR (CD<sub>2</sub>Cl<sub>2</sub>, 298 K): <sup>1</sup>H: δ/ppm = 1.76 (s, 15 H, Cp\*)

<sup>31</sup>P{<sup>1</sup>H}: AA'M<sub>2</sub>M'X<sub>2</sub>X' spin system δ/ppm = 165.8 (m, <sup>1</sup>J<sub>PA-PX/X'</sub> = 604.5/589.8 Hz, <sup>2</sup>J<sub>PA-PM/M'</sub> = 6.8/3.8 Hz, <sup>2</sup>J<sub>PA-PA'</sub> = 123.6 Hz, <sup>1</sup>J<sub>PA/A'-B</sub> = 64 Hz, 2 P, P<sup>A/A'</sup>), 145.6 (m, <sup>1</sup>J<sub>PM/M'-PX/X'</sub> = 447.5/436.8 Hz, <sup>1</sup>J<sub>PM-PM'</sub> = 415.3 Hz, <sup>2</sup>J<sub>PM/M'-PX'/X</sub> = -58.4/-47.0 Hz, <sup>2</sup>J<sub>PM/M'-PA</sub> = 6.8/3.8 Hz, 4 P, P<sup>M/M'</sup>), 58.4 (m, <sup>1</sup>J<sub>PX/X'-PA</sub> = 604.5/589.8 Hz, <sup>1</sup>J<sub>PX/X'-PM/M'</sub> = 447.5/436.8 Hz, <sup>2</sup>J<sub>PX/X'-PM'/M</sub> = -58.4/-47.0 Hz, <sup>2</sup>J<sub>PX-PX'</sub> = 36.9 Hz, 4 P, P<sup>X/X'</sup>)

<sup>31</sup>P: AA'M<sub>2</sub>M'X<sub>2</sub>X' spin system δ/ppm = 165.8 (m, <sup>1</sup>J<sub>PA-PX/X'</sub> = 604.5/589.8 Hz, <sup>2</sup>J<sub>PA-PM/M'</sub> = 6.8/3.8 Hz, <sup>2</sup>J<sub>PA-PA'</sub> = 123.6 Hz, <sup>1</sup>J<sub>PA/A'-B</sub> = 64 Hz, 2 P, P<sup>A/A'</sup>), 145.6 (m, <sup>1</sup>J<sub>PM/M'-PX/X'</sub> = 447.5/436.8 Hz, <sup>1</sup>J<sub>PM-PM'</sub> = 415.3 Hz, <sup>2</sup>J<sub>PM/M'-PX'/X</sub> = -58.4/-47.0 Hz, <sup>2</sup>J<sub>PM/M'-PA</sub> = 6.8/3.8 Hz, 4 P, P<sup>M/M'</sup>), 58.4 (m, <sup>1</sup>J<sub>PX/X'-PA</sub> = 604.5/589.8 Hz, <sup>1</sup>J<sub>PX/X'-PM/M'</sub> = 447.5/436.8 Hz, <sup>2</sup>J<sub>PX/X'-PM'/M</sub> = -58.4/-47.0 Hz, <sup>2</sup>J<sub>PX-PX'</sub> = 36.9 Hz, 4 P, P<sup>X/X'</sup>)

<sup>11</sup>B: δ/ppm = -15.6 (t, <sup>1</sup>J<sub>B-PA/A'</sub> = 64 Hz, 1 B, {BBr<sub>2</sub>})

<sup>19</sup>F{<sup>1</sup>H}: δ/ppm = -75.6 (s, [TEF]<sup>-</sup>)

### 1.3. [{Cp\*Fe}2{( $\eta^5$ -P<sub>5</sub>)<sub>2</sub>Gal<sub>2</sub>}][TEF] (3)

[Cp\*Fe( $\eta^5$ -P<sub>5</sub>)] (0.2 mmol, 70 mg, 2 eq.), Tl[TEF] (0.1 mmol, 117 mg, 1 eq.) and Gal<sub>3</sub> (0.1 mmol, 45 mg, 1 eq.) were dissolved in 5 mL of *o*-DFB, which afforded a brown solution, with the Gal<sub>3</sub> still being suspended. Stirring this solution for three days lead to a colour change to brownish green and the formation of a yellow precipitate (TII). After filtration, this solution was layered with 50 mL of *n*-hexane, which after nine days afforded [{Cp\*Fe}2{( $\eta^5$ -P<sub>5</sub>)<sub>2</sub>Gal<sub>2</sub>}][TEF] (3) as dark brownish green stick shaped crystals of X-ray quality.

Yield: 63 mg (0.032 mmol, 32%)

Elemental analysis: calc. (%) for [{Cp\*Fe}2{( $\eta^5$ -P<sub>5</sub>)<sub>2</sub>Gal<sub>2</sub>}][TEF]  
(C<sub>36</sub>H<sub>30</sub>O<sub>4</sub>F<sub>36</sub>AlP<sub>10</sub>Fe<sub>2</sub>Gal<sub>2</sub>): C: 21.81 H: 1.53

found (%): C: 22.17 H: 1.37

ESI(+) MS (*o*-DFB): *m/z* (%) = 345.92 (60%) [Cp\*Fe( $\eta^5$ -P<sub>5</sub>)]<sup>+</sup>, (strong fragmentation)

NMR (CD<sub>2</sub>Cl<sub>2</sub>, 298 K): <sup>1</sup>H:  $\delta$ /ppm = 1.63 (s, 15 H, Cp\*)

<sup>31</sup>P{<sup>1</sup>H}:  $\delta$ /ppm = 117.2 (br)

<sup>31</sup>P:  $\delta$ /ppm = 117.2 (br)

<sup>19</sup>F{<sup>1</sup>H}:  $\delta$ /ppm = -75.6 (s, [TEF]<sup>-</sup>)

NMR (CD<sub>2</sub>Cl<sub>2</sub>, 193 K): <sup>1</sup>H:  $\delta$ /ppm = 1.62 (s, 15 H, Cp\*)

<sup>31</sup>P{<sup>1</sup>H}:  $\delta$ /ppm = 92.7 (m(br), 6 P), 141.6 (m(br), 4 P)

#### 1.4. $[\text{Cp}^*\text{Fe}(\eta^5\text{-P}_5\text{CH}_2\text{Ph})]\text{[TEF]} \text{ (4)}$

$\text{PhCH}_2\text{Br}$  (0.2 mmol, 24  $\mu\text{L}$ , 1 eq.) was added dropwise to a solution of  $\text{Cp}^*\text{Fe}(\eta^5\text{-P}_5)$  (0.2 mmol, 70 mg, 1 eq.) and  $\text{Ti}[\text{TEF}]$  (0.1 mmol, 117 mg, 1 eq.) in 4 mL *o*-DFB, which resulted in a gradual colour change from brownish green to red and the formation of a white precipitate ( $\text{TiBr}$ ) over the course of 24 h. The resulting mixture was filtered and 20 mL of *n*-hexane were added, which afforded the precipitation of  $[\text{Cp}^*\text{Fe}(\eta^5\text{-P}_5\text{CH}_2\text{Ph})]\text{[TEF]} \text{ (4)}$  as a dark red solid. This solid was washed two times with 10 mL of *n*-hexane, each, dried and then dissolved in 2 mL of *o*-DFB. Layering this solution with 20 mL of *n*-hexane and storing it for one week resulted in the formation of large red crystals of **4** in X-ray quality.

Yield: 127 mg (0.09 mmol, 45%)

Elemental analysis: calc. (%) for  $[\text{Cp}^*\text{Fe}(\eta^5\text{-P}_5\text{CH}_2\text{Ph})]\text{[TEF]}$  ( $\text{C}_{33}\text{H}_{22}\text{O}_4\text{F}_{36}\text{AlP}_5\text{Fe}$ ): C: 28.23 H: 1.58  
found (%): C: 28.73 H: 1.36

ESI(+) MS (*o*-DFB):  $m/z$  (%) = 437.03 (100%)  $[\text{Cp}^*\text{Fe}(\eta^5\text{-P}_5\text{CH}_2\text{Ph})]^+$

NMR ( $\text{CD}_2\text{Cl}_2$ , 298 K):  $^1\text{H}$ :  $\delta/\text{ppm} = 1.73$ , (s, 15 H,  $\text{Cp}^*$ ), 4.42 (dt,  $^2J_{\text{H-PA}} = 11.2$  Hz,  $^3J_{\text{H-PX/X'}} = 3.2$  Hz, 2 H,  $\text{CH}_2\text{Ph}$ ), 7.40–7.55 (m, 5 H, Ph)

$^{31}\text{P}\{^1\text{H}\}$ :  $\delta/\text{ppm} = 126.8$  (m,  $^1J_{\text{PA-PX/X'}} = 615.4/615.2$  Hz,  $^2J_{\text{PA-PM/M'}} = 10.2/9.0$  Hz, 1 P,  $\text{P}^A$ ), 113.9 (m,  $^1J_{\text{PM/M'}-{\text{PX/X'}}} = 455.4/454.6$  Hz,  $^1J_{\text{PM-PM'}} = 407.0$  Hz,  $^2J_{\text{PM/M'}-{\text{PX/X'}}} = -56.0/-55.7$  Hz,  $^2J_{\text{PM/M'}-{\text{PA}}} = 10.2/9.0$  Hz, 2 P,  $\text{P}^{\text{MM'}}$ ), 75.7 (m,  $^1J_{\text{PX/X'}-{\text{PA}}} = 615.4/615.2$  Hz,  $^1J_{\text{PX/X'}-{\text{PM/M'}}} = 455.4/454.6$  Hz,  $^2J_{\text{PX/X'}-{\text{PM'/M}}} = -56.0/-55.7$  Hz,  $^2J_{\text{PX-X'}} = 42.3$  Hz, 2 P,  $\text{P}^{\text{XX'}}$ )

$^{31}\text{P}$ :  $\delta/\text{ppm} = 126.8$  (m,  $^1J_{\text{PA-PX/X'}} = 617.1/613.6$  Hz,  $^2J_{\text{PA-PM/M'}} = 10.5/9.1$  Hz,  $^2J_{\text{PA-H}} = 11.3$  Hz, 1 P,  $\text{P}^A$ ), 113.9 (m,  $^1J_{\text{PM/M'}-{\text{PX/X'}}} = 459.3/450.9$  Hz,  $^1J_{\text{PM-PM'}} = 407.0$  Hz,  $^2J_{\text{PM/M'}-{\text{PX/X'}}} = -60.6/-51.2$  Hz,  $^2J_{\text{PM/M'}-{\text{PA}}} = 10.5/9.1$  Hz, 2 P,  $\text{P}^{\text{MM'}}$ ), 75.7 (m,  $^1J_{\text{PX/X'}-{\text{PA}}} = 617.1/613.6$  Hz,  $^1J_{\text{PX/X'}-{\text{PM/M'}}} = 459.3/450.9$  Hz,  $^2J_{\text{PX/X'}-{\text{PM'/M}}} = -60.6/-51.2$  Hz,  $^2J_{\text{PX-X'}} = 42.1$  Hz, 2 P,  $\text{P}^{\text{XX'}}$ )

$^{13}\text{C}\{^1\text{H}\}$ :  $\delta/\text{ppm} = 11.0$  (s,  $\text{C}_5\text{Me}_5$ ), 26.1 (d,  $^1J_{\text{C-PA}} = 23$  Hz,  $\text{CH}_2\text{Ph}$ ), 97.7 (s,  $\text{C}_5\text{Me}_5$ ), 121.3 (q,  $^1J_{\text{C-F}} = 292$  Hz,  $[\text{Al}(\text{OC}(\text{CF}_3)_3)_4]^-$ ), 129.2 (s, Ph), 129.3 (s, Ph), 130.2 (s, Ph), 132.4 (s, Ph)

$^{19}\text{F}\{^1\text{H}\}$ :  $\delta/\text{ppm} = -75.6$  (s, [TEF] $^-$ )

### 1.5. $[\text{Cp}^*\text{Fe}(\eta^5\text{-P}_5\text{CHPh}_2)][\text{TEF}]$ (5)

$\text{Ph}_2\text{CHCl}$  (0.2 mmol, 36  $\mu\text{L}$ , 1 eq.) was added dropwise to a solution of  $\text{Cp}^*\text{Fe}(\eta^5\text{-P}_5)$  (0.2 mmol, 70 mg, 1 eq.) and  $\text{Ti}[\text{TEF}]$  (0.1 mmol, 117 mg, 1 eq.) in 4 mL *o*-DFB, which resulted in a gradual colour change from brownish green to red and the formation of a white precipitate ( $\text{TiCl}$ ) over the course of 3 h. The resulting mixture was filtered and 20 mL of *n*-hexane were added, which afforded the precipitation of  $[\text{Cp}^*\text{Fe}(\eta^5\text{-P}_5\text{CHPh}_2)][\text{TEF}]$  (5) as a dark red solid. This solid was washed two times with 10 mL of *n*-hexane, each, dried and then dissolved in 2 mL of *o*-DFB. Layering this solution with 40 mL of *n*-hexane and storing it for one week resulted in the formation of large red crystals of 5 in X-ray quality.

Note: The order of addition in this reaction can be exchanged and the reaction could be scaled up to 2 mmol, which allows the gram scale isolation of 5.

Yield: 230 mg (0.16 mmol, 80%)

Elemental analysis: calc. (%) for  $[\text{Cp}^*\text{Fe}(\eta^5\text{-P}_5\text{CHPh}_2)][\text{TEF}] \cdot (\text{C}_6\text{H}_4\text{F}_2)_{0.4}$  ( $\text{C}_{41.4}\text{H}_{27.6}\text{O}_4\text{F}_{36.8}\text{AlP}_5\text{Fe}$ ): C: 32.59 H: 1.82

found (%): C: 32.80 H: 1.89 (traces of *o*-DFB are also detected in the  $^1\text{H}$  NMR spectrum of isolated crystals)

ESI(+) MS (*o*-DFB):  $m/z$  (%) = 513.02 (100%)  $[\text{Cp}^*\text{Fe}(\eta^5\text{-P}_5\text{CHPh}_2)]^+$

NMR ( $\text{CD}_2\text{Cl}_2$ , 298 K):  $^1\text{H}$ :  $\delta/\text{ppm} = 1.64$  (s, 15 H,  $\text{Cp}^*$ ), 5.93 (d,  $^2J_{\text{H-P}} = 17.3$  Hz, 1 H,  $\text{CHPh}_2$ ), 7.43-7.72 (br, 10 H,  $\text{CHPh}_2$ )

$^{31}\text{P}\{^1\text{H}\}$ :  $\delta/\text{ppm} = 156.2$  (m,  $^1J_{\text{PA}-\text{PX/X'}} = 629.8/625.3$  Hz,  $^2J_{\text{PA-PM/M'}} = 17.5/6.0$  Hz, 1 P,  $\text{P}^\text{A}$ ), 115.0 (m,  $^1J_{\text{PM/M'}-\text{PX/X'}} = 450.4/449.5$  Hz,  $^1J_{\text{PM-PM'}} = 412.2$  Hz,  $^2J_{\text{PM/M'}-\text{PX/X'}} = -54.5/-54.0$  Hz,  $^2J_{\text{PM/M'}-\text{PA}} = 17.5/6.0$  Hz, 2 P,  $\text{P}^{\text{M/M}'}$ ), 77.0 (m,  $^1J_{\text{PX/X'}-\text{PA}} = 629.8/625.3$  Hz,  $^1J_{\text{PX/X'}-\text{PM/M'}} = 450.4/449.5$  Hz,  $^2J_{\text{PX/X'}-\text{PM/M'}} = -54.5/-54.0$  Hz,  $^2J_{\text{PX-PX'}} = 43.1$  Hz, 2 P,  $\text{P}^{\text{X/X}'})$

$^{31}\text{P}$ :  $\delta/\text{ppm} = 156.2$  (m,  $^1J_{\text{PA}-\text{PX/X'}} = 628.5/626.4$  Hz,  $^2J_{\text{PA-PM/M'}} = 14.9/9.6$  Hz,  $^2J_{\text{PA-H}} = 17.3$  Hz, 1 P,  $\text{P}^\text{A}$ ), 115.0 (m,  $^1J_{\text{PM/M'}-\text{PX/X'}} = 452.7/447.1$  Hz,  $^1J_{\text{PM-PM'}} = 412.1$  Hz,  $^2J_{\text{PM/M'}-\text{PX/X'}} = -56.5/-52.1$  Hz,  $^2J_{\text{PM/M'}-\text{PA}} = 14.9/9.6$  Hz, 2 P,  $\text{P}^{\text{M/M}'})$ , 77.0 (m,  $^1J_{\text{PX/X'}-\text{PA}} = 628.5/626.4$  Hz,  $^1J_{\text{PX/X'}-\text{PM/M'}} = 452.7/447.1$  Hz,  $^2J_{\text{PX/X'}-\text{PM/M'}} = -56.5/-52.1$  Hz,  $^2J_{\text{PX-PX'}} = ^2J_{\text{PX-X'}} = 42.9$  Hz, 2 P,  $\text{P}^{\text{X/X}'})$

$^{13}\text{C}\{^1\text{H}\}$ :  $\delta/\text{ppm} = 11.0$  (s,  $\text{C}_5\text{Me}_5$ ), 49.3 (d,  $^1J_{\text{C-P}} = 23$  Hz,  $\text{CHPh}_2$ ), 97.9 (s,  $\text{C}_5\text{Me}_5$ ), 121.3 (q,  $^1J_{\text{C-F}} = 292$  Hz,  $[\text{Al}\{\text{OC}(\text{CF}_3)_3\}_4]^-$ ), 128.7 (d,  $^2J_{\text{C-P}} = 8$  Hz, Ph), 129.6 (s, Ph), 130.1 (s, Ph)

$^{19}\text{F}\{^1\text{H}\}$ :  $\delta/\text{ppm} = -75.6$  (s, [TEF] $^-$ )

### 1.6. $[\text{Cp}^*\text{Fe}(\eta^5\text{-P}_5\text{SiHPh}_2)][\text{B}(\text{C}_6\text{F}_5)_4]$ (6)

$\text{Ph}_2\text{SiH}_2$  (0.2 mmol, 37  $\mu\text{L}$ , 1 eq.) were added to a mixture of  $\text{Cp}^*\text{Fe}(\eta^5\text{-P}_5)$  (0.2 mmol, 70 mg, 1 eq.) and  $[\text{Ph}_3\text{C}][\text{B}(\text{C}_6\text{F}_5)_4]$  (0.2 mmol, 185 mg, 1 eq.) in 3 mL of *o*-DFB which afforded a rapid colour change to brownish green. The mixture was stirred for one hour and then directly layered with 30 mL of *n*-hexane. Storing this mixture for one day at room temperature afforded  $[\text{Cp}^*\text{Fe}(\eta^5\text{-P}_5\text{SiHPh}_2)][\text{B}(\text{C}_6\text{F}_5)_4]$  (6) as brownish green plate shaped crystals of X-ray quality. After decanting the solution and thoroughly drying the crystals under reduced pressure ( $10^{-3}$  mbar), 6 could be isolated as a pure compound.

Yield: 205 mg (0.17 mmol, 85%)

Elemental analysis: calc. (%) for  $[\text{Cp}^*\text{Fe}(\eta^5\text{-P}_5\text{SiHPh}_2)][\text{B}(\text{C}_6\text{F}_5)_4]$  ( $\text{C}_{46}\text{H}_{26}\text{BF}_{20}\text{SiP}_5\text{Fe}$ ): C: 45.73 H: 2.17  
found (%): C: 45.38 H: 1.84

ESI(+) MS (*o*-DFB):  $m/z$  (%) = 347.01 (100%)  $[\text{Cp}^*\text{Fe}(\text{h}^5\text{-P}_5\text{H})]^+$  (formed by fragmentation in the mass spectrometer)

NMR ( $\text{CD}_2\text{Cl}_2$ , 300 K):  $^1\text{H}$ :  $\delta/\text{ppm} = 1.51$  (s(br), 15 H,  $\text{Cp}^*$ ), 6.45 (s,  $^1J_{\text{H-Si}} = 237.5$  Hz, 1 H,  $\text{SiHPh}_2$ ), 7.63 (m, 4 H,  $\text{SiHPh}_2^{\text{m}}$ ), 7.70 (m, 2 H  $\text{SiHPh}_2^{\text{p}}$ ), 8.00 (m, 4 H,  $\text{SiHPh}_2^{\text{o}}$ )

$^{31}\text{P}\{^1\text{H}\}$ , 300 K:  $\delta/\text{ppm} = 83.6$  (br,  $\omega_{1/2} = 1300$  Hz,  $\text{P}^{\text{X}}$ ), 104.0 (br, ,  $\omega_{1/2} = 1600$  Hz,  $\text{P}^{\text{M/M'}}$ ), 145.6 (br,  $\omega_{1/2} = 1400$  Hz,  $\text{P}^{\text{A/A'}}$ )

$^{19}\text{F}\{^1\text{H}\}$ :  $\delta/\text{ppm} = -167.1$  (t,  $^3J_{\text{F-F}} = 19$  Hz, 8 F, m- $\text{C}_6\text{F}_5$ ), -163.2 (t,  $^3J_{\text{F-F}} = 19$  Hz, 4 F, p- $\text{C}_6\text{F}_5$ ), -132.6 (br, 8 F, o- $\text{C}_6\text{F}_5$ )

NMR ( $\text{CD}_2\text{Cl}_2$ , 243 K):  $^{29}\text{Si}$ (DEPT135):  $\delta/\text{ppm} = -20$  (dm,  $^1J_{\text{Si-P}} = 239$  Hz,  $\text{SiHPh}_2$ )

NMR ( $\text{CD}_2\text{Cl}_2$ , 193 K):  $^1\text{H}$ :  $\delta/\text{ppm} = 1.40$  (s(br), 15 H,  $\text{Cp}^*$ ), 6.39 (s,  $^1J_{\text{H-Si}} = 237.5$  Hz, 1 H,  $\text{SiHPh}_2$ ), 7.59 (m, 4 H,  $\text{SiHPh}_2^{\text{m}}$ ), 7.65 (m, 2 H  $\text{SiHPh}_2^{\text{p}}$ ), 7.97 (m, 4 H,  $\text{SiHPh}_2^{\text{o}}$ )

$^{31}\text{P}\{^1\text{H}\}$ :  $\delta/\text{ppm} = 76.4$  (t (br),  $\text{P}^{\text{X}}$ ), 102.6 (m,  $\text{P}^{\text{M/M'}}$ ), 141.1 (m,  $\text{P}^{\text{A/A'}}$ )

$^{31}\text{P}$ :  $\delta/\text{ppm} = 76.4$  (t (br), 1 P,  $\text{P}^{\text{X}}$ ), 102.6 (m, 2 P,  $\text{P}^{\text{M/M'}}$ ), 141.1 (m, 2 P,  $\text{P}^{\text{A/A'}}$ )

### 1.7. $[\text{Cp}^*\text{Fe}(\eta^5\text{-P}_5\text{AsCy}_2)]\text{[TEF]}$ (7)

Cy<sub>2</sub>AsCl (0.2 mmol, 39 µL, 1 eq.) was added to a suspension of LiBr (3 mmol, 261 mg, 15 eq.) in 2 mL of toluene (Similar halogen exchange has been described for chlorophosphanes).<sup>10</sup> The mixture was stirred for two hours and the white precipitate allowed to settle. The resulting solution was filtered to a mixture of  $\text{Cp}^*\text{Fe}(\eta^5\text{-P}_5)$  (0.2 mmol, 70 mg, 1 eq.) and Ti[TEF] (0.2 mmol, 234 mg, 1 eq.) in 3 mL of *o*-DFB which afforded a rapid colour change to dark red and the precipitation of a colourless solid (TiBr). The suspension was stirred for 3 h and 20 mL of *n*-hexane were added to precipitate  $[\text{Cp}^*\text{Fe}(\eta^5\text{-P}_5\text{AsCy}_2)]\text{[TEF]}$  (7) as a dark red solid. The supernatant was decanted, the solid washed two times with 10 mL of toluene, each, one time with 10 mL of *n*-hexane, and then dried at reduced pressure ( $10^{-3}$  mbar). 2 mL of *o*-DFB were added to give a dark red solution above a colourless solid. The solution was filtered and 20 mL of *n*-hexane were added to precipitate 7 as a red solid, which was isolated after drying at reduced pressure ( $10^{-3}$  mbar). 7 could be recrystallized from *o*-DFB/*n*-hexane mixtures as red block shaped crystals of X-ray quality.

Yield: 210 mg (0.135 mmol, 68%)

Elemental analysis: calc. (%) for  $[\text{Cp}^*\text{Fe}(\eta^5\text{-P}_5\text{AsCy}_2)]\text{[TEF]}$  ( $\text{C}_{38}\text{H}_{37}\text{O}_4\text{F}_{36}\text{AlP}_5\text{FeAs}$ ): C: 29.36 H: 2.40  
found (%): C: 28.89 H: 2.28

ESI(+) MS (*o*-DFB):  $m/z$  (%) = 587.00 (100%)  $[\text{Cp}^*\text{Fe}(\eta^5\text{-P}_5\text{AsCy}_2)]^+$

NMR ( $\text{CD}_2\text{Cl}_2$ ):  $^1\text{H}$  (298 K):  $\delta/\text{ppm}$  = 1.62 (s, 15 H, Cp\*), 1.34-2.94 (br, 22 H, AsCy<sub>2</sub>)

$^{31}\text{P}\{^1\text{H}\}$  (273 K):  $\delta/\text{ppm}$  = 123.9 (m,  $^1J_{\text{PA/A'-PB/B'}} = 432.9/430.0$  Hz,  $^1J_{\text{PA-PA'}} = 420.1$  Hz,  $^2J_{\text{PA/A'-PB'/PB}} = -52.0/-50.5$  Hz,  $^2J_{\text{PA/A'-PX}} = 10.2/3.8$  Hz, 2 P, P<sup>A/A'</sup>), 117.1 (m,  $^1J_{\text{PB/B'-PX}} = 576.0/574.5$  Hz,  $^1J_{\text{PB/B'-PA/A'}} = 432.9/430.0$  Hz,  $^2J_{\text{PB/B'-PA/PA}} = -52.0/-50.5$  Hz,  $^2J_{\text{PB-PB'}} = 22.2$  Hz, 2 P, P<sup>B/B'</sup>), 86.6 (m,  $^1J_{\text{PX-PB/B'}} = 576.0/574.5$  Hz,  $^2J_{\text{PX-PA/A'}} = 10.2/3.8$  Hz, 1 P, P<sup>X</sup>)

$^{31}\text{P}$  (298 K):  $\delta/\text{ppm}$  = 123.9 (m,  $^1J_{\text{PA/A'-PB/B'}} = 432.9/430.0$  Hz,  $^1J_{\text{PA-PA'}} = 420.1$  Hz,  $^2J_{\text{PA/A'-PB'/PB}} = -52.0/-50.5$  Hz,  $^2J_{\text{PA/A'-PX}} = 10.2/3.8$  Hz, 2 P, P<sup>A/A'</sup>), 117.1 (m,  $^1J_{\text{PB/B'-PX}} = 576.0/574.5$  Hz,  $^1J_{\text{PB/B'-PA/A'}} = 432.9/430.0$  Hz,  $^2J_{\text{PB/B'-PA/PA}} = -52.0/-50.5$  Hz,  $^2J_{\text{PB-PB'}} = 22.2$  Hz, 2 P, P<sup>B/B'</sup>), 86.6 (m,  $^1J_{\text{PX-PB/B'}} = 576.0/574.5$  Hz,  $^2J_{\text{PX-PA/A'}} = 10.2/3.8$  Hz, 1 P, P<sup>X</sup>)

$^{19}\text{F}\{^1\text{H}\}$  (298 K):  $\delta/\text{ppm}$  = -75.6 (s, [TEF]<sup>-</sup>)

### **1.8. [{Cp\*Fe( $\mu$ , $\eta^{5:2}$ -P<sub>5</sub>)}SbICp''][TEF] (8)**

Cp\*Fe( $\eta^5$ -P<sub>5</sub>) (0.2 mmol, 70 mg, 1 eq.), Cp''SbI<sub>2</sub> (0.2 mmol, 122 mg, 1 eq.) and Ti[TEF] (0.2 mmol, 234 mg, 1 eq.) were dissolved in 5 mL of *o*-DFB, which gave a light brown solution and a pale yellow precipitate (TII). This mixture was stirred for 1 h, filtered and then directly layered with 50 mL of *n*-hexane. After 13 days of storage at room temperature [{Cp\*Fe( $\eta^{5:2}$ -P<sub>5</sub>)}SbICp''][TEF] (8) could be isolated as dark brown rod shaped crystals of X-ray quality.

Yield: 85 mg (0.048 mmol, 24%)

Elemental analysis: calc. (%) for [{Cp\*Fe( $\eta^{5:2}$ -P<sub>5</sub>)}SbICp''][TEF] (C<sub>43</sub>H<sub>44</sub>O<sub>4</sub>F<sub>36</sub>AlP<sub>5</sub>FeSbI): C: 28.77 H: 2.47  
found (%): C: 28.62 H: 2.25

ESI(+) MS (*o*-DFB): *m/z* (%) = 481.03 (5%) [Cp''SbI]<sup>+</sup>, 587.36 (10%) [Cp''<sub>2</sub>Sb]<sup>+</sup>  
(strong fragmentation)

NMR (CD<sub>2</sub>Cl<sub>2</sub>, 298 K): <sup>1</sup>H:  $\delta$ /ppm = 1.41 (s, 15 H, Cp\*), 1.51 (s, 9 H, C(CH<sub>3</sub>)<sub>3</sub>), 1.55 (s, 18 H, C(CH<sub>3</sub>)<sub>3</sub>), 6.72 (s, 2 H, C<sub>5</sub>H<sub>2</sub>tBu<sub>3</sub>)  
<sup>31</sup>P{<sup>1</sup>H}:  $\delta$ /ppm = 164.7 (s, 5 P, P<sub>5</sub>)  
<sup>31</sup>P:  $\delta$ /ppm = 164.7 (s, 5 P, P<sub>5</sub>)  
<sup>19</sup>F{<sup>1</sup>H}:  $\delta$ /ppm = - 75.6 (s, [TEF]<sup>-</sup>)

### 1.9. [Cp\*Fe( $\eta^5$ -P<sub>5</sub>SePh)][TEF] (9)

Cp\*Fe( $\eta^5$ -P<sub>5</sub>) (0.1 mmol, 35 mg, 1 eq.) and PhSeBr (0.1 mmol, 24 mg, 1 eq.) were dissolved in 4 mL of *o*-DFB to give an orange-green solution. Ti[TEF] (0.1 mmol, 117 mg, 1 eq.), dissolved in 2 mL of *o*-DFB, was added to afford a rapid colour change to dark brown and the precipitation of a white solid (TiBr). This mixture was stirred for 5 h at room temperature and then filtered. The resulting dark reddish-brown solution was concentrated to 2 mL under reduced pressure (10<sup>-3</sup> mbar) and 20 mL of *n*-hexane were added to precipitate [Cp\*Fe( $\eta^5$ -P<sub>5</sub>SePh)][TEF] (**9**) as a dark brown solid. This solid was washed two times with 10 mL of *n*-hexane, each, and then dissolved in 3 mL of *o*-DFB. Layering this solution with 20 mL of *n*-hexane and storing it for 12 days at room temperature afforded dark brown rod shaped crystals of **9** in X-ray quality.

Yield: 95 mg (0.065 mmol, 65%)

Elemental analysis: calc. (%) for [Cp\*Fe( $\eta^5$ -P<sub>5</sub>SePh)][TEF] (C<sub>32</sub>H<sub>20</sub>O<sub>4</sub>F<sub>36</sub>AlP<sub>5</sub>FeSe): C: 26.16 H: 1.37

found (%): C: 26.49 H: 1.43

ESI(+) MS (*o*-DFB): *m/z* (%) = 502.96 (100%) [Cp\*Fe(h<sup>5</sup>-P<sub>5</sub>SePh)]<sup>+</sup>

NMR (CD<sub>2</sub>Cl<sub>2</sub>, 298 K): <sup>1</sup>H: δ/ppm = 1.75 (s, 15 H, Cp\*), 7.47-7.90(m, 5 H, Ph)

<sup>31</sup>P{<sup>1</sup>H}: δ/ppm = 135.5 (m, <sup>1</sup>J<sub>PA/A'-PX</sub> = 596.9/595.4 Hz, <sup>1</sup>J<sub>PA/A'-PM/M'</sub> = 448.4/441.1 Hz, <sup>2</sup>J<sub>PA/A'-PM'/M</sub> = -54.2/-48.3 Hz, <sup>2</sup>J<sub>PA-PA'</sub> = 37.3 Hz, 2 P, P<sup>A/A'</sup>), 113.8 (m, <sup>1</sup>J<sub>PM/M'-PA/A'</sub> = 448.4/441.1 Hz, <sup>1</sup>J<sub>PM-PM'</sub> = 413.3 Hz, <sup>2</sup>J<sub>PM/M'-PA'/A</sub> = -54.2/-48.3 Hz, <sup>2</sup>J<sub>PM/M'-PX</sub> = -1.9/-0.6 Hz, 2 P, P<sup>M/M'</sup>), 70.4 (m, <sup>1</sup>J<sub>PX-PA/A'</sub> = 596.9/595.4 Hz, <sup>2</sup>J<sub>PX-PM/M'</sub> = 7.8/2.4 Hz, <sup>1</sup>J<sub>PX-Se</sub> = 418 Hz, 1 P, P<sup>X</sup>)

<sup>31</sup>P: δ/ppm = 135.5 (m, <sup>1</sup>J<sub>PA/A'-PX</sub> = 596.9/595.4 Hz, <sup>1</sup>J<sub>PA/A'-PM/M'</sub> = 448.4/441.1 Hz, <sup>2</sup>J<sub>PA/A'-PM'/M</sub> = -54.2/-48.3 Hz, <sup>2</sup>J<sub>PA-PA'</sub> = 37.3 Hz, 2 P, P<sup>A/A'</sup>), 113.8 (m, <sup>1</sup>J<sub>PM/M'-PA/A'</sub> = 448.4/441.1 Hz, <sup>1</sup>J<sub>PM-PM'</sub> = 413.3 Hz, <sup>2</sup>J<sub>PM/M'-PA'/A</sub> = -54.2/-48.3 Hz, <sup>2</sup>J<sub>PM/M'-PX</sub> = -1.9/-0.6 Hz, 2 P, P<sup>M/M'</sup>), 70.4 (m, <sup>1</sup>J<sub>PX-PA/A'</sub> = 596.9/595.4 Hz, <sup>2</sup>J<sub>PX-PM/M'</sub> = 7.8/2.4 Hz, <sup>1</sup>J<sub>PX-Se</sub> = 418 Hz, 1 P, P<sup>X</sup>)

<sup>77</sup>Se{<sup>1</sup>H}: δ/ppm = 287.3 (d, <sup>1</sup>J<sub>Se-P</sub> = 418 Hz, SePh)

<sup>19</sup>F{<sup>1</sup>H}: d/ppm = -75.5 (s, [TEF]<sup>-</sup>)

### 1.10. $[\text{Cp}^*\text{Fe}(\eta^5\text{-P}_5\text{TeMes})]\text{[TEF]} \quad (\mathbf{10})$

$\text{Cp}^*\text{Fe}(\eta^5\text{-P}_5)$ ] (0.2 mmol, 70 mg, 1 eq.) and MesTeBr (0.2 mmol, 65 mg, 1 eq.) were dissolved in 4 mL of *o*-DFB to give a brownish-green solution. Ti[TEF] (0.2 mmol, 234 mg, 1 eq.), dissolved in 2 mL of *o*-DFB, was added to afford a rapid colour change to dark brown and the precipitation of a white solid (TiBr). This mixture was stirred for 18 h at room temperature and then filtered. The resulting dark reddish-brown solution was concentrated to 4 mL under reduced pressure ( $10^{-3}$  mbar) and 20 mL of *n*-hexane were added to precipitate  $[\text{Cp}^*\text{Fe}(\eta^5\text{-P}_5\text{TeMes})]\text{[TEF]} \quad (\mathbf{10})$  as a dark brown solid. This solid was washed two times with 10 mL of toluene and two times with 10 mL of *n*-hexane and then dried under reduced pressure to afford **10** as a pure compound. Dissolving **10** in 3 mL of *o*-DFB and layering the solution with 20 mL of *n*-hexane after storage for 12 days at room temperature afforded dark brownish red rod shaped crystals in X-ray quality.

Yield: 177 mg (0.114 mmol, 57%)

Elemental analysis: calc. (%) for  $[\text{Cp}^*\text{Fe}(\eta^5\text{-P}_5\text{TeMes})]\text{[TEF]}$   
( $\text{C}_{35}\text{H}_{26}\text{O}_4\text{F}_{36}\text{AlP}_5\text{FeTe}$ ): C: 26.95 H: 1.68  
found (%): C: 27.19 H: 1.68

ESI(+) MS (*o*-DFB):  $m/z$  (%) = 537.02 (100%)  $[(\text{Cp}^*\text{Fe})_2(\mu,\eta^{5:5}\text{-P}_5)]^+$ , 593.00 (5%)  
 $[\text{Cp}^*\text{Fe}(\eta^5\text{-P}_5\text{TeMes})]^+$

NMR ( $\text{CD}_2\text{Cl}_2$ , 298 K):  $^1\text{H}$ :  $\delta/\text{ppm} = 1.70$  (s, 15 H,  $\text{Cp}^*$ ), 2.27 (s, 3 H,  $\text{Mes}_{\text{para}}$ ), 2.84 (s, 6 H,  $\text{Mes}_{\text{ortho}}$ ), 7.12 (s, 2 H,  $\text{Mes}_{\text{meta}}$ )

$^{31}\text{P}\{\text{H}\}$ :  $\delta/\text{ppm} = 126.3$  (br,  $\omega_{1/2} = 2500$  Hz)

$^{31}\text{P}$ :  $\delta/\text{ppm} = 126.3$  (br,  $\omega_{1/2} = 2500$  Hz)

$^{19}\text{F}\{\text{H}\}$ : d/ppm = -75.5 (s, [TEF]<sup>-</sup>)

NMR ( $\text{CD}_2\text{Cl}_2$ , 193 K):  $^{31}\text{P}\{\text{H}\}$ :  $\delta/\text{ppm} = 10.0$  (br,  $\omega_{1/2} = 1100$  Hz), 124.9 (br,  $\omega_{1/2} = 1000$  Hz), 139.3 (br,  $\omega_{1/2} = 1500$  Hz)

### 1.11. $[\text{Cp}^*\text{Fe}(\eta^5\text{-P}_5\text{Cl})]\text{[TEF]} \text{ (11)}$

$\text{PCl}_5$  (0.2 mmol, 42 mg, 1 eq.) and  $\text{Ti}[\text{TEF}]$  (0.2 mmol, 234 mg, 1 eq.) were dissolved in 4 mL of *o*-DFB and stirred for 1.5 h. The resulting colourless solid ( $\text{TiCl}$ ) was allowed to settle from the clear solution. The latter was then filtered into a solution of  $[\text{Cp}^*\text{Fe}(\eta^5\text{-P}_5)]$  (0.2 mmol, 70 mg, 1 eq.) in 2 mL of *o*-DFB resulting in an immediate colour change from green to dark brownish red. This solution was stirred for 2 h, concentrated under reduced pressure ( $10^{-3}$  mbar) and then 30 mL of *n*-hexane were added to precipitate  $[\text{Cp}^*\text{Fe}(\eta^5\text{-P}_5\text{Cl})]\text{[TEF]} \text{ (11)}$  as a dark brownish red solid. The solid was washed two times with 10 mL of *n*-hexane, each, then dried and dissolved in 2 mL of *o*-DFB. The resulting solution was layered with 20 mL of *n*-hexane and then stored at -30 °C for five days, which afforded dark red block shaped crystals of **11** in X-ray quality.

Yield: 175 mg (0.13 mmol, 65%)

Elemental analysis: calc. (%) for  $[\text{Cp}^*\text{Fe}(\eta^5\text{-P}_5\text{Cl})]\text{[TEF]}\cdot(\text{C}_6\text{H}_4\text{F}_2)_{0.1}$  ( $\text{C}_{26.6}\text{H}_{15.4}\text{O}_4\text{F}_{36.2}\text{AlP}_5\text{FeCl}$ ):  
C: 23.49 H: 1.14  
found (%): C: 23.84 H: 0.95

ESI(+) MS (*o*-DFB):  $m/z$  (%) = 536.97 (100%)  $[(\text{Cp}^*\text{Fe})_2(\mu,\eta^{5:5}\text{-P}_5)]^+$

NMR ( $\text{CD}_2\text{Cl}_2$ , 300 K):  $^1\text{H}$ :  $\delta/\text{ppm} = 1.73$  (s,  $\text{Cp}^*$ )

$^{31}\text{P}\{\text{H}\}$ :  $\delta/\text{ppm} = 156.1$  (m,  $^1J_{\text{PA/A'-PM}} = 637.3/626.9$  Hz,  $^1J_{\text{PA/A'-PX/X'}} = 461.8/426.0$  Hz,  $^2J_{\text{PA/A'-PX'/X}} = -71.2/-37.6$  Hz,  $^2J_{\text{PA-PA'}} = 41.7$  Hz, 2 P,  $\text{P}^{\text{A/A}'}$ ), 84.9 (m,  $^1J_{\text{PM-PA/A'}} = 637.3/626.9$  Hz,  $^2J_{\text{PM-PX/X'}} = 6.1/2.0$  Hz, 1 P,  $\text{P}^{\text{M}}$ ), 70.7 (m,  $^1J_{\text{PX/X'-PA/A'}} = 461.8/426.0$  Hz,  $^1J_{\text{PX-PX'}} = 406.2$  Hz,  $^2J_{\text{PX/X'-PA/A'}} = -71.2/-37.6$  Hz,  $^2J_{\text{PX/X'-PM}} = 6.1/2.0$  Hz, 2 P,  $\text{P}^{\text{X/X}'})$

$^{31}\text{P}$ :  $\delta/\text{ppm} = 156.1$  (m,  $^1J_{\text{PA/A'-PM}} = 637.3/626.9$  Hz,  $^1J_{\text{PA/A'-PX/X'}} = 461.8/426.0$  Hz,  $^2J_{\text{PA/A'-PX'/X}} = -71.2/-37.6$  Hz,  $^2J_{\text{PA-PA'}} = 41.7$  Hz, 2 P,  $\text{P}^{\text{A/A}'}$ ), 84.9 (m,  $^1J_{\text{PM-PA/A'}} = 637.3/626.9$  Hz,  $^2J_{\text{PM-PX/X'}} = 6.1/2.0$  Hz, 1 P,  $\text{P}^{\text{M}}$ ), 70.7 (m,  $^1J_{\text{PX/X'-PA/A'}} = 461.8/426.0$  Hz,  $^1J_{\text{PX-PX'}} = 406.2$  Hz,  $^2J_{\text{PX/X'-PA/A'}} = -71.2/-37.6$  Hz,  $^2J_{\text{PX/X'-PM}} = 6.1/2.0$  Hz, 2 P,  $\text{P}^{\text{X/X}'})$

$^{19}\text{F}\{\text{H}\}$ :  $\delta/\text{ppm} = -75.5$  (s, [TEF]<sup>-</sup>)

## 1.12. $[\text{Cp}^*\text{Fe}(\eta^5\text{-P}_5\text{Br})]\text{[TEF]} \text{ (12)}$

$\text{Br}_2$  (0.2 mmol, 10  $\mu\text{L}$ , 1 eq.) was added dropwise to a solution of  $\text{Cp}^*\text{Fe}(\eta^5\text{-P}_5)$  (0.2 mmol, 70 mg, 1 eq.) and  $\text{Ti}[\text{TEF}]$  (0.1 mmol, 117 mg, 1 eq.) in 3 mL of  $\text{CH}_2\text{Cl}_2$  at  $-80^\circ\text{C}$  affording an immediate colour change to dark brownish red and the precipitation of a white solid ( $\text{TiBr}$ ). The resulting mixture was stirred at room temperature for 1.5 h, then filtered and addition of 20 mL of *n*-pentane afforded the precipitation of  $[\text{Cp}^*\text{Fe}(\eta^5\text{-P}_5\text{Br})]\text{[TEF]} \text{ (12)}$  as a dark brown powder. This powder was dissolved in 3 mL of *o*-DFB to give a dark brown solution, which was layered with 30 mL of *n*-pentane and stored for 7 days to afford dark reddish brown crystals (rod shaped) of **12** in X-ray quality.

Yield: 181 mg (0.13 mmol, 65%)

Elemental analysis: calc. (%) for  $[\text{Cp}^*\text{Fe}(\eta^5\text{-P}_5\text{Br})]\text{[TEF]}$  ( $\text{C}_{26}\text{H}_{15}\text{O}_4\text{F}_{36}\text{AlP}_5\text{FeBr}$ ):  
C: 22.42 H: 1.09  
found (%): C: 22.71 H: 0.72

ESI(+) MS (*o*-DFB):  $m/z$  (%) = 536.97 (100%)  $[(\text{Cp}^*\text{Fe})_2(\mu,\eta^{5:5}\text{-P}_5)]^+$

NMR ( $\text{CD}_2\text{Cl}_2$ , 300 K):  $^1\text{H}$ :  $\delta/\text{ppm} = 1.73$  (s,  $\text{Cp}^*$ )

$^{31}\text{P}\{^1\text{H}\}$ :  $\delta/\text{ppm} = 157.6$  (m,  $^1J_{\text{PA}/\text{A}'\text{-PX}} = 616.4/615.2$  Hz,  $^1J_{\text{PA}/\text{A}'\text{-PM/M'}} = 439.0/436.5$  Hz,  $^2J_{\text{PA}/\text{A}'\text{-PM'/M}} = -58.0/-49.4$  Hz,  $^2J_{\text{PA-PA}'} = 34.4$  Hz, 2 P,  $\text{P}^{\text{AA}'}$ ), 77.4 (m,  $^1J_{\text{PM/M}'\text{-PA/A}'} = 439.0/436.5$  Hz,  $^1J_{\text{PM-PM}'} = 415.6$  Hz,  $^2J_{\text{PM/M}'\text{-PA}'\text{/A}} = -58.0/-49.4$  Hz,  $^2J_{\text{PM/M}'\text{-PX}} = -1.8/-1.4$  Hz, 2 P,  $\text{P}^{\text{MM}'}$ ), 64.2 (m,  $^1J_{\text{PX-PA/A}'} = 616.4/615.2$  Hz,  $^2J_{\text{PX-PM/M}'} = -1.8/-1.4$  Hz, 1 P,  $\text{P}^X$ )

$^{31}\text{P}$ :  $\delta/\text{ppm} = 157.6$  (m,  $^1J_{\text{PA}/\text{A}'\text{-PX}} = 616.4/615.2$  Hz,  $^1J_{\text{PA}/\text{A}'\text{-PM/M}'} = 439.0/436.5$  Hz,  $^2J_{\text{PA}/\text{A}'\text{-PM'/M}} = -58.0/-49.4$  Hz,  $^2J_{\text{PA-PA}'} = 34.4$  Hz, 2 P,  $\text{P}^{\text{AA}'}$ ), 77.4 (m,  $^1J_{\text{PM/M}'\text{-PA/A}'} = 439.0/436.5$  Hz,  $^1J_{\text{PM-PM}'} = 415.6$  Hz,  $^2J_{\text{PM/M}'\text{-PA}'\text{/A}} = -58.0/-49.4$  Hz,  $^2J_{\text{PM/M}'\text{-PX}} = -1.8/-1.4$  Hz, 2 P,  $\text{P}^{\text{MM}'}$ ), 64.2 (m,  $^1J_{\text{PX-PA/A}'} = 616.4/615.2$  Hz,  $^2J_{\text{PX-PM/M}'} = -1.8/-1.4$  Hz, 1 P,  $\text{P}^X$ )

$^{19}\text{F}\{^1\text{H}\}$ :  $\delta/\text{ppm} = -75.5$  (s, [TEF])

### 1.13. $[\text{Cp}^*\text{Fe}(\eta^5\text{-P}_5\text{I})]\text{[TEF]}$ (13)

$\text{I}_2$  (0.2 mmol, 51 mg, 1 eq.) and  $\text{Ti}[\text{TEF}]$  (0.2 mmol, 234 mg, 1 eq.) were dissolved in 8 mL of *o*-DFB and cooled to  $-30^\circ\text{C}$ . Addition of this solution to another solution of  $[\text{Cp}^*\text{Fe}(\eta^5\text{-P}_5)]$  (0.2 mmol, 70 mg, 1 eq.) in 3 mL of *o*-DFB ( $-30^\circ\text{C}$ ) afforded a rapid colour change to brown and the formation of a yellow precipitate (TII). This mixture was stirred for another 2 h at  $-30^\circ\text{C}$  and then the solvent was removed under reduced pressure ( $10^{-3}$  mbar). The resulting dark brown residue was washed two times with 20 mL of *n*-pentane, each, and then dissolved in 3 mL of cold ( $-30^\circ\text{C}$ ) *o*-DFB. After filtration, this solution was layered with 30 mL of *n*-pentane and stored at  $-30^\circ\text{C}$ , which after 14 days afforded formation  $[\text{Cp}^*\text{Fe}(\eta^5\text{-P}_5\text{I})]\text{[TEF]}$  (13) as dark brown crystals in X-ray quality.

Yield: 178 mg (0.124 mmol, 62%)

Elemental analysis: calc. (%) for  $[\text{Cp}^*\text{Fe}(\eta^5\text{-P}_5\text{I})]\text{[TEF]}$  ( $\text{C}_{26}\text{H}_{15}\text{O}_4\text{F}_{36}\text{AlP}_5\text{FeI}$ ):

C: 21.69 H: 1.05

found (%): C: 22.14 H: 1.06

ESI(+) MS (*o*-DFB):  $m/z$  (%) = 536.97 (80%)  $[(\text{Cp}^*\text{Fe})_2(\mu,\eta^{5:5}\text{-P}_5)]^+$

NMR ( $\text{CD}_2\text{Cl}_2$ , 300 K):  $^1\text{H}$ :  $\delta/\text{ppm} = 1.67$  (s (br),  $\text{Cp}^*$ )

$^{31}\text{P}\{\text{H}\}$ :  $\delta/\text{ppm} = 106$  (br,  $\omega_{1/2} = 5600$  Hz)

$^{31}\text{P}$ :  $\delta/\text{ppm} = 106$  (br,  $\omega_{1/2} = 5600$  Hz)

$^{19}\text{F}\{\text{H}\}$ :  $\delta/\text{ppm} = -75.5$  (s, [TEF] $^-$ )

NMR ( $\text{CD}_2\text{Cl}_2$ , 193 K):  $^1\text{H}$ :  $\delta/\text{ppm} = 1.60$  (s,  $\text{Cp}^*$ )

$^{31}\text{P}\{\text{H}\}$ :  $\delta/\text{ppm} = 153$  (br,  $\omega_{1/2} = 4100$  Hz), 90 (br,  $\omega_{1/2} = 1060$  Hz) 19 (br,  $\omega_{1/2} = 4350$  Hz)

### 1.14. [{Cp'''}Ta(CO)<sub>2</sub>]<sub>2</sub>{μ,η<sup>4:4</sup>-((P<sub>4</sub>)<sub>2</sub>BBr<sub>2</sub>)}][TEF] (15)

[Cp'''Ta(CO)<sub>2</sub>(η<sup>4</sup>-P<sub>4</sub>)] (59 mg, 0.1 mmol, 2 eq.) and BBr<sub>3</sub> (5 μL, 0.05 mmol, 1 eq.) were dissolved in 5 mL of *o*-DFB to give a yellow solution. Ti[TEF] (59 mg, 0.05 mmol, 1 eq.) dissolved in 2 mL of *o*-DFB was added slowly under strong stirring. An immediate colour change to pale orange occurred and precipitation of a white solid (TiBr) can be observed. The mixture was stirred for six hours, then filtered and directly layered with 40 mL of *n*-pentane. Storage of this mixture for one day at room temperature affords [{Cp'''}Ta(CO)<sub>2</sub>]<sub>2</sub>{μ,η<sup>4:4</sup>-((P<sub>4</sub>)<sub>2</sub>BBr<sub>2</sub>)}][TEF] (15) as clear yellow crystals in X-ray quality. Further storage at -30 °C for several weeks leads to quantitative precipitation of **15** as orange powder.

Yield: 87 mg (0.037 mmol, 74%)

Elemental analysis: calc. (%) for [{Cp'''}Ta(CO)<sub>2</sub>]<sub>2</sub>{μ,η<sup>4:4</sup>-((P<sub>4</sub>)<sub>2</sub>BBr<sub>2</sub>)}][TEF] (C<sub>54</sub>H<sub>58</sub>BO<sub>8</sub>F<sub>36</sub>AlP<sub>8</sub>Br<sub>2</sub>Ta<sub>2</sub>):

C: 27.88 H: 2.51

calc. (%) for [{Cp'''}Ta(CO)<sub>2</sub>]<sub>2</sub>{μ,η<sup>4:4</sup>-((P<sub>4</sub>)<sub>2</sub>BBr<sub>2</sub>)}][TEF]·(TiBr)<sub>0.4</sub> (C<sub>54</sub>H<sub>58</sub>BO<sub>8</sub>F<sub>36</sub>AlP<sub>8</sub>Br<sub>2</sub>Ta<sub>2</sub>) ·(TiBr)<sub>0.4</sub>:

C: 26.58 H: 2.40

found (%): C: 26.23 H: 2.11

Traces of TiBr are inseparable from the crystals of the product by filtration or washing.

NMR (CD<sub>2</sub>Cl<sub>2</sub>, 300 K): <sup>1</sup>H: δ/ppm = 1.12 (s, 9 H, C<sub>5</sub>H<sub>2</sub><sup>t</sup>Bu<sub>3</sub>), 1.56 (s, 18 H, C<sub>5</sub>H<sub>2</sub><sup>t</sup>Bu<sub>3</sub>), 6.33 (s, 1 H, C<sub>5</sub>H<sub>2</sub><sup>t</sup>Bu<sub>3</sub>), 6.34 (s, 1 H, C<sub>5</sub>H<sub>2</sub><sup>t</sup>Bu<sub>3</sub>)

<sup>31</sup>P{<sup>1</sup>H}: δ/ppm = -15.4 (m, <sup>1</sup>J<sub>PA/A'-PM/M'</sub> = 350 Hz, <sup>1</sup>J<sub>PA/A'-PX/X'</sub> = 293 Hz, 4 P, P<sup>A/A'</sup>), -37.1 (m (br), <sup>1</sup>J<sub>PM/M'-PA/A'</sub> = 350 Hz, <sup>2</sup>J<sub>PM/M'-PX/X'</sub> = 117 Hz, , <sup>2</sup>J<sub>PM-M'</sub> = 120 Hz, <sup>1</sup>J<sub>PM-B</sub> = 61 Hz, 2 P, P<sup>A/A'</sup>) and -80.8 (m, <sup>1</sup>J<sub>PX/X'-PA/A'</sub> = 293 Hz, <sup>1</sup>J<sub>PX/X'-PM/M'</sub> = 117 Hz)

<sup>31</sup>P: δ/ppm = -15.4 (m, <sup>1</sup>J<sub>PA/A'-PM/M'</sub> = 350 Hz, <sup>1</sup>J<sub>PA/A'-PX/X'</sub> = 293 Hz, 4 P, P<sup>A/A'</sup>), -37.1 (m (br), <sup>1</sup>J<sub>PM/M'-PA/A'</sub> = 350 Hz, <sup>2</sup>J<sub>PM/M'-PX/X'</sub> = 117 Hz, , <sup>2</sup>J<sub>PM-M'</sub> = 120 Hz, <sup>1</sup>J<sub>PM-B</sub> = 61 Hz, 2 P, P<sup>A/A'</sup>) and -80.8 (m, <sup>1</sup>J<sub>PX/X'-PA/A'</sub> = 293 Hz, <sup>1</sup>J<sub>PX/X'-PM/M'</sub> = 117 Hz)

<sup>11</sup>B{<sup>1</sup>H}: δ/ppm = -10.2 (t, 1 B, <sup>1</sup>J<sub>B-P</sub> = 61 Hz, {BBr<sub>2</sub>})

<sup>19</sup>F{<sup>1</sup>H}: δ/ppm = -75.6 (s, [TEF]<sup>-</sup>)

### 1.15. Cp<sup>'''</sup>SbI<sub>2</sub>

To a solution of 9.80 g (19.5 mmol) SbI<sub>3</sub> in 200 mL THF a solution of 5.00 g (19.5 mmol) Cp<sup>'''</sup>Na in 100 mL THF was added at -80°C. The reaction mixture was warmed to room temperature and stirred for 18 hours. The solvent was removed in vacuo and the residue extracted with hexane. The hexane solution was concentrated until beginning of crystallization and stored over night at -28°C. Large orange crystals were formed. Yield 10.03 g (85%).

Elemental analysis:                    calc. (%) for Cp<sup>'''</sup>SbI<sub>2</sub> (C<sub>17</sub>H<sub>29</sub>SbI<sub>2</sub>): C: 33.53 H: 4.80  
    found (%): C: 33.43 H: 4.73

NMR (C<sub>6</sub>D<sub>6</sub>, 300 K): <sup>1</sup>H: δ/ppm = 1.22 (s, 18H, C(CH<sub>3</sub>)<sub>3</sub>), 1.29 (s, 9 H, C(CH<sub>3</sub>)<sub>3</sub>), 6.55 (s, 2H, CH).

<sup>13</sup>C{<sup>1</sup>H}: δ/ppm = 30.59 (s, C(CH<sub>3</sub>)<sub>3</sub>), 32.99 (s, C(CH<sub>3</sub>)<sub>3</sub>), 34.31 (s, C(CH<sub>3</sub>)<sub>3</sub>), 35.30 (s, C(CH<sub>3</sub>)<sub>3</sub>), 116.76 (s, CSbI<sub>2</sub>), 123.65 (s, CCH), 145.97 (s, CC(CH<sub>3</sub>)<sub>3</sub>)

## 2. X-ray

### 2.1. General remarks

The crystallographic data for all described compounds were collected on a SuperNova diffractometer (Rigaku) with a Titan<sup>S2</sup> detector using Cu-K $\alpha$  radiation (micro-focus sealed tube) (**7**), on a GV50 diffractometer (Rigaku) with a Titan<sup>S2</sup> detector using Cu-K $\beta$  radiation obtained by using customised optics (**13**), an Xcalibur Gemini Ultra diffractometer with an Atlas<sup>S2</sup> detector using Mo-K $\alpha$  (**9**) radiation (sealed tube) or a standard Cu-K $\alpha$  sealed tube (**2, 3, 5, 8**), or an XtalAB Synergy R, DW System with a HyPix-Arc 150 detector using Cu-K $\alpha$  radiation from a rotating anode (**4, 6, 10, 12**). Data reduction and absorption correction were performed with the CrysAlisPro software package.<sup>11</sup> Structure solution and refinement was conducted in Olex2 (1.3-alpha)<sup>12</sup> with ShelXT<sup>13</sup> (solution) and ShelXL-2018/3<sup>14</sup> (least squares refinement (F<sup>2</sup>)). All non-H atoms were refined with anisotropic displacement parameters (except the minor disordered part of **7**) and H atoms were treated as riding models with isotropic displacement parameters and fixed C–H bond lengths (sp<sup>3</sup>: 0.96 (CH<sub>3</sub>), 0.97 (CH<sub>2</sub>); sp<sup>2</sup>: 0.93 (CH)). Visualisation of the crystal structures was performed with Olex2 (1.3-alpha).<sup>12</sup>

CIF files with comprehensive information on the details of the diffraction experiments and full tables of bond lengths and angles for **2, 3, 4, 5, 6, 7, 8, 9, 10, 13** and **15** are deposited in Cambridge Crystallographic Data Centre under the deposition codes CCDC-2083554, CCDC-2083555, CCDC-2083556, CCDC-2083557, CCDC-2083558, CCDC-2083559, CCDC-2083560, CCDC-2083561, CCDC-2083562, CCDC-2083563, and CCDC-2101248 respectively.

Table S 1: X-ray crystallographic data on all crystallographically characterised compounds.

Compound	<b>2</b>	<b>3</b>	<b>4</b>	<b>5</b>
Formula	AlBB <sub>2</sub> C <sub>39.6</sub> F <sub>36</sub> Fe <sub>2</sub> H <sub>38.4</sub> O <sub>4</sub> P <sub>1</sub>	C <sub>36</sub> H <sub>30</sub> AlF <sub>36</sub> Fe <sub>2</sub> Gal <sub>2</sub> O <sub>4</sub> P <sub>10</sub>	C <sub>33</sub> H <sub>22</sub> AlF <sub>36</sub> FeO <sub>4</sub> P <sub>5</sub>	C <sub>39</sub> H <sub>26</sub> AlF <sub>36</sub> FeO <sub>4</sub> P <sub>5</sub>
<i>D</i> <sub>calc</sub> / g cm <sup>-3</sup>	1.937	2.074	1.896	1.830
$\mu$ /mm <sup>-1</sup>	8.892	15.621	4.279	5.382
Formula Weight	1881.31	1982.50	1404.18	1480.28
Colour	clear light green	dark brown	clear dark red	clear dark red
Shape	prism	plate	block	block-shaped
Size/mm <sup>3</sup>	0.36×0.12×0.06	0.42×0.37×0.12	0.32×0.28×0.19	0.63×0.38×0.21
T/K	123(1)	123(1)	123.00(10)	123(1)
Crystal System	monoclinic	triclinic	monoclinic	triclinic
Space Group	<i>C</i> 2	<i>P</i> 1	<i>P</i> 2 <sub>1</sub> / <i>n</i>	<i>P</i> 1
<i>a</i> /Å	40.0184(7)	12.8777(2)	15.0993(7)	15.4816(4)
<i>b</i> /Å	9.7379(10)	16.0557(2)	18.0632(8)	16.9548(5)
<i>c</i> /Å	18.3964(4)	18.4470(3)	18.8351(10)	21.6022(6)
$\alpha$ /°	90	112.4860(10)	90	86.014(2)
$\beta$ /°	115.870(2)	95.1250(10)	106.706(5)	71.751(2)
$\gamma$ /°	90	110.9810(10)	90	88.928(2)
V/Å <sup>3</sup>	6450.6(2)	3175.29(9)	4920.3(4)	5372.1(3)
Z	4	2	4	4
Z'	1	1	1	2
Wavelength/Å	1.54184	1.54184	1.39222	1.54184
Radiation type	Cu K $\alpha$	Cu K $\alpha$	Cu K $\beta$	Cu K $\alpha$
$\Theta_{min}$ /°	4.346	3.830	2.999	3.500
$\Theta_{max}$ /°	72.039	71.666	75.377	71.857
Measured Refl's.	23789	33614	26352	58001
Indep't Refl's	12143	12088	13101	20392
Refl's I≥2 σ(I)	11912	11702	10904	18475
<i>R</i> <sub>int</sub>	0.0362	0.0473	0.0306	0.0433
Parameters	921	1145	1385	2252
Restraints	88	851	608	1556
Largest Peak	0.730	1.421	0.612	1.211
Deepest Hole	-0.429	-1.030	-0.667	-0.506
GooF	1.037	1.035	1.087	1.044
w <i>R</i> <sub>2</sub> (all data)	0.1117	0.1314	0.1640	0.1939
w <i>R</i> <sub>2</sub>	0.1109	0.1301	0.1462	0.1882
<i>R</i> <sub>1</sub> (all data)	0.0432	0.0487	0.0667	0.0722
<i>R</i> <sub>1</sub>	0.0425	0.0477	0.0559	0.0675
Flack Parameter	0.386(5)	/	/	/
Hooft Parameter	0.387(2)	/	/	/

---

<b>Compound</b>	<b>6</b>	<b>7</b>	<b>8</b>	<b>9</b>
Formula	C <sub>46</sub> H <sub>26</sub> BF <sub>20</sub> FeP <sub>5</sub> Si	AlAsC <sub>41.5</sub> F <sub>36</sub> FeH <sub>41</sub> O <sub>4</sub> P <sub>5</sub>	Al <sub>2</sub> C <sub>92</sub> F <sub>72</sub> Fe <sub>2</sub> H <sub>98</sub> I <sub>2</sub> O <sub>8</sub> P <sub>10</sub> Sb <sub>2</sub>	C <sub>32</sub> H <sub>20</sub> AlF <sub>36</sub> FeO <sub>4</sub> P <sub>5</sub> Se
D <sub>calc.</sub> / g cm <sup>-3</sup>	1.707	1.812	1.837	1.944
μ/mm <sup>-1</sup>	5.490	5.578	11.213	1.374
Formula Weight	1208.27	1600.34	3672.36	1469.12
Colour	clear light green	clear dark red	light brown	clear dark red
Shape	plate	block-shaped	rod-shaped	block-shaped
Size/mm <sup>3</sup>	0.22×0.15×0.05	0.48×0.28×0.22	0.53×0.10×0.08	0.52×0.44×0.28
T/K	123.00(10)	123.15(1)	123(1)	123(1)
Crystal System	monoclinic	monoclinic	monoclinic	triclinic
Space Group	P2 <sub>1</sub> /c	P2 <sub>1</sub> /n	P2 <sub>1</sub> /n	P1
a/Å	17.0141(2)	28.0092(2)	21.0539(2)	12.1286(4)
b/Å	14.79290(10)	21.7375(2)	16.5834(2)	12.6674(5)
c/Å	20.3007(3)	10.53850(10)	38.0631(4)	17.2846(8)
α/°	90	90	90	107.670(4)
β/°	113.070(2)	113.8980(10)	92.2010(10)	96.922(3)
γ/°	90	90	90	90.247(3)
V/Å <sup>3</sup>	4700.82(11)	5866.28(10)	13279.7(2)	2509.49(18)
Z	4	4	4	2
Z'	1	1	1	1
Wavelength/Å	1.54184	1.54184	1.54184	0.71073
Radiation type	Cu K <sub>α</sub>	Cu K <sub>α</sub>	Cu K <sub>α</sub>	Mo K <sub>α</sub>
Θ <sub>min</sub> /°	2.823	4.007	3.394	3.379
Θ <sub>max</sub> /°	73.459	66.906	71.750	32.286
Measured Refl's.	33445	61278	75069	22005
Indep't Refl's	9127	10404	25253	15499
Refl's I>2 σ(I)	8217	9640	18923	11637
R <sub>int</sub>	0.0288	0.0393	0.0782	0.0296
Parameters	696	1182	2570	924
Restraints	48	368	1318	164
Largest Peak	0.649	0.842	1.024	0.770
Deepest Hole	-0.540	-0.807	-0.980	-0.555
GooF	1.091	1.024	1.008	1.059
wR <sub>2</sub> (all data)	0.1029	0.1469	0.1737	0.1329
wR <sub>2</sub>	0.1008	0.1429	0.1570	0.1169
R <sub>1</sub> (all data)	0.0396	0.0572	0.0875	0.0743
R <sub>1</sub>	0.0359	0.0537	0.0649	0.0508

---

---

<b>Compound</b>	<b>10</b>	<b>13</b>	<b>15</b>
Formula	$\text{Al}_3\text{C}_{123}\text{F}_{114}\text{Fe}_3\text{H}_{90}\text{O}_{12}\text{P}_{15}\text{Te}_3$	$\text{C}_{29}\text{H}_{17}\text{AlF}_{37}\text{FeI}\text{O}_4\text{P}_5$	$\text{C}_{54}\text{H}_{58}\text{AlBBr}_2\text{F}_{36}\text{O}_8\text{P}_8\text{Ta}_2$
$D_{calc}/\text{g cm}^{-3}$	1.917	2.071	1.973
$\mu/\text{mm}^{-1}$	8.965	8.267	9.149
Formula Weight	5021.78	1497.01	2326.27
Colour	dark red	dark brown	clear yellow
Shape	block-shaped	block-shaped	rods-shaped
Size/mm <sup>3</sup>	0.21×0.17×0.14	0.41×0.28×0.14	0.38×0.14×0.07
T/K	122.99(10)	122.99(10)	122.93(19)
Crystal System	triclinic	monoclinic	triclinic
Space Group	$P\bar{1}$	$C2/c$	$P\bar{1}$
$a/\text{\AA}$	18.1681(7)	31.0024(8)	10.70454(17)
$b/\text{\AA}$	19.4877(7)	19.5946(3)	17.1553(4)
$c/\text{\AA}$	28.8463(10)	19.9635(6)	22.3411(6)
$\alpha/^\circ$	77.316(3)	90	73.344(2)
$\beta/^\circ$	72.113(3)	127.644(4)	86.2377(16)
$\gamma/^\circ$	64.085(4)	90	85.9405(15)
$V/\text{\AA}^3$	8698.6(6)	9602.7(6)	3916.28(15)
Z	2	8	2
Z'	1	1	1
Wavelength/\AA	1.54184	1.39222	1.54184
Radiation type	Cu K $\alpha$	Cu K $\beta$	Cu K $\alpha$
$\Theta_{min}/^\circ$	3.543	2.605	3.832
$\Theta_{max}/^\circ$	73.781	74.464	74.898
Measured Refl's.	59952	39627	54888
Indep't Refl's	33498	13047	15822
Refl's $\geq 2 \sigma(I)$	25725	11680	14586
$R_{int}$	0.0555	0.0295	0.0744
Parameters	3526	942	1297
Restraints	1862	173	328
Largest Peak	1.133	0.662	3.643
Deepest Hole	-1.172	-0.479	-5.026
GooF	1.010	1.021	1.037
wR <sub>2</sub> (all data)	0.1815	0.1174	0.1950
wR <sub>2</sub>	0.1662	0.1133	0.1915
R <sub>1</sub> (all data)	0.0844	0.0478	0.0775
R <sub>1</sub>	0.0675	0.0431	0.0736

---

## 2.2. [{Cp\*Fe}2{( $\eta^5$ -P<sub>5</sub>)<sub>2</sub>BBr<sub>2</sub>}][TEF] (2)

Large pale greenish brown rod shaped crystals of [{Cp\*Fe}2{( $\eta^5$ -P<sub>5</sub>)<sub>2</sub>BBr<sub>2</sub>}][TEF] (2) are obtained by layering a concentrated solution in *o*-DFB with *n*-hexane (1:7) and storing it at room temperature for two weeks. **2** crystallises as inversion twins in the monoclinic space group C2 with one cation, one anion and 0.6 hexane solvent molecules present in the asymmetric unit (*Figure S 1*). Due to the heavy disorder of the hexane molecule a solvent mask was calculated with the in Olex2 implemented masking tool and 120 electrons were found in a volume of 550 Å<sup>3</sup> in 2 voids per unit cell. This is consistent with the presence of 0.6 hexane molecules per asymmetric unit, which account for 120 electrons per unit cell. Disorder within the anion was treated with appropriate geometric and ADP (Anisotropic Displacement Parameter) restraints.

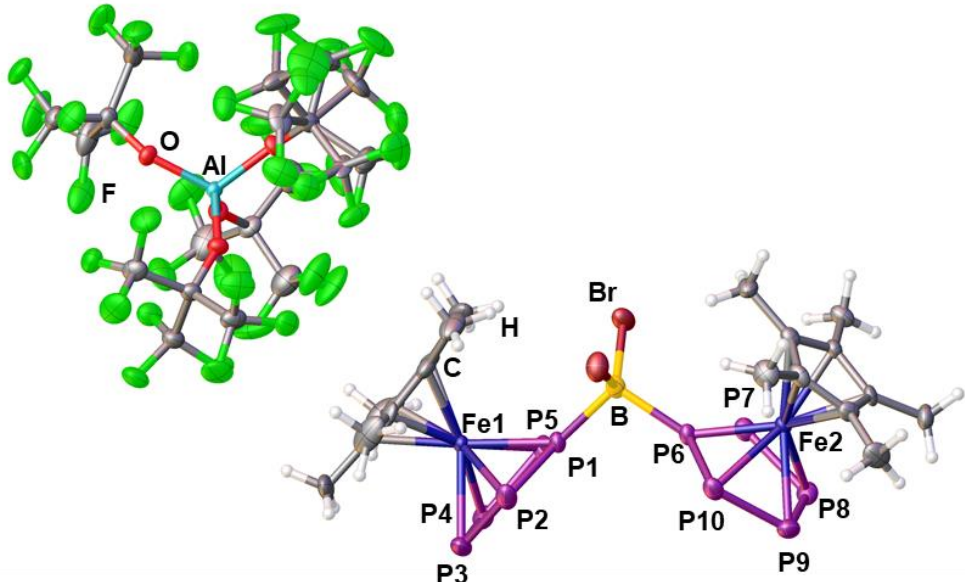


*Figure S 1: Solid state structure of **2**; Depicted is the asymmetric unit and ADPs are drawn at 50% probability; Selected bond lengths and angles: d(P1-P2) = 2.098(2) Å, d(P2-P3) = 2.117(3) Å, d(P3-P4) = 2.121(4) Å, d(P4-P5) = 2.103(3) Å, d(P1-P5) = 2.108(2) Å, d(P6-P7) = 2.105(2) Å, d(P7-P8) = 2.110(3) Å, d(P8-P9) = 2.120(3) Å, d(P9-P10) = 2.111(3) Å, d(P6-P10) = 2.110(2) Å, d(P1-B) = 1.985(7) Å, d(P6-B) = 1.985(8) Å, d(P1-Fe1) = 2.289(2) Å, d(P2-Fe1) = 2.408(2) Å, d(P3-Fe1) = 2.383(2) Å, d(P4-Fe1) = 2.379(3) Å, d(P5-Fe1) = 2.395(2) Å, d(P6-Fe2) = 2.275(2) Å, d(P7-Fe2) = 2.289(2) Å, d(P8-Fe2) = 2.380(3) Å, d(P9-Fe2) = 2.387(2) Å, d(P10-Fe2) = 2.397(2) Å,  $\alpha$ (P1-B-P6) = 100.9(3)°,  $\alpha$ (P3-P5-P2-P1) = 174.31(18)°,  $\alpha$ (P8-P10-P7-P6) = 173.10(14)°.*

### 2.3. $\{Cp^*Fe\}_2\{(\eta^5-P_5)_2Gal_2\}[TEF]$ (3)

Dark brown crystalline plates of  $\{Cp^*Fe(\eta^5-P_5)_2Gal_2\}[TEF]$  (3) are obtained by layering a concentrated solution in *o*-DFB with *n*-hexane (1:7) and storing it at room temperature for one week. **3** crystallises in the triclinic space group  $P\bar{1}$  with one cation and one anion present in the asymmetric unit (*Figure S 2*). Disorder within the anion was treated with appropriate geometric and ADP restraints.

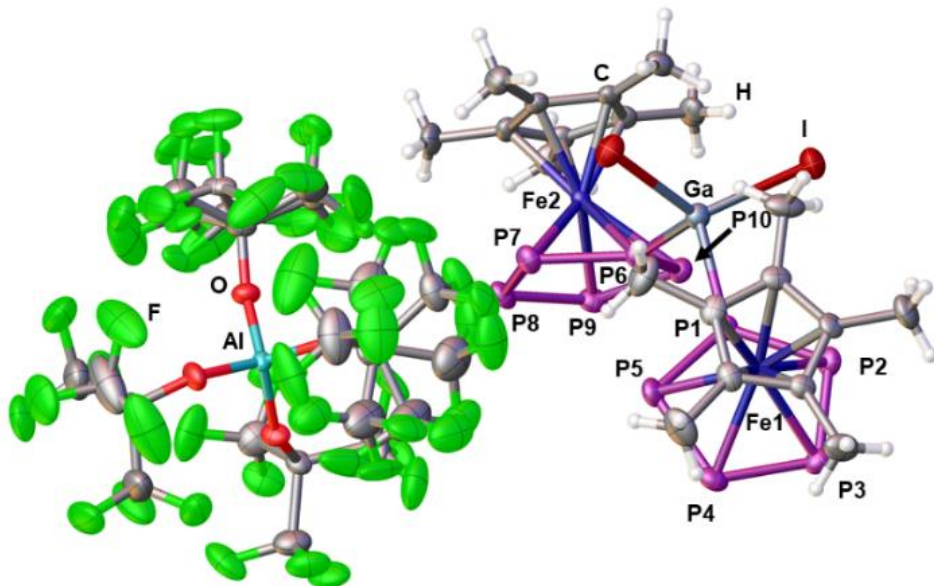


*Figure S 2: Solid state structure of **3**; Depicted is the asymmetric unit and ADPs are drawn at 50% probability; Selected bond lengths and angles:  $d(P1-P2) = 2.1054(15)$  Å,  $d(P2-P3) = 2.1076(16)$  Å,  $d(P3-P4) = 2.1175(17)$  Å,  $d(P4-P5) = 2.1179(15)$  Å,  $d(P1-P5) = 2.1076(16)$  Å,  $d(P6-P7) = 2.1116(15)$  Å,  $d(P7-P8) = 2.1174(17)$  Å,  $d(P8-P9) = 2.1123(17)$  Å,  $d(P9-P10) = 2.1127(17)$  Å,  $d(P6-P10) = 2.1044(15)$  Å,  $d(P1-Ga) = 2.3871(11)$  Å,  $d(P6-Ga) = 2.4102(12)$  Å,  $d(P1-Fe1) = 2.310(1)$  Å,  $d(P2-Fe1) = 2.375(2)$  Å,  $d(P3-Fe1) = 2.394(1)$  Å,  $d(P4-Fe1) = 2.368(2)$  Å,  $d(P5-Fe1) = 2.370(1)$  Å,  $d(P6-Fe2) = 2.308(1)$  Å,  $d(P7-Fe2) = 2.367(2)$  Å,  $d(P8-Fe2) = 2.391(2)$  Å,  $d(P9-Fe2) = 2.386(1)$  Å,  $d(P10-Fe2) = 2.375(1)$  Å,  $\alpha(P1-Ga-P6) = 97.31(4)$ °,  $\alpha(P3-P5-P2-P1) = 170.04(10)$ °,  $\alpha(P8-P10-P7-P6) = 171.61(12)$ °.*

## 2.4. $[\text{Cp}^*\text{Fe}(\eta^5\text{-P}_5\text{CH}_2\text{Ph})]\text{[TEF]} \text{ (4)}$

$[\text{Cp}^*\text{Fe}(\eta^5\text{-P}_5\text{CH}_2\text{Ph})]\text{[TEF]} \text{ (4)}$  can be obtained as dark red crystalline blocks after layering a concentrated solution in *o*-DFB with *n*-hexane (1:8) and storing it at room temperature for one week. **4** crystallises in the monoclinic space group  $P2_1/n$  with one cation and one anion present in the asymmetric unit (*Figure S 3*). Disorder within the anion and the cation was treated with appropriate geometric and ADP restraints.

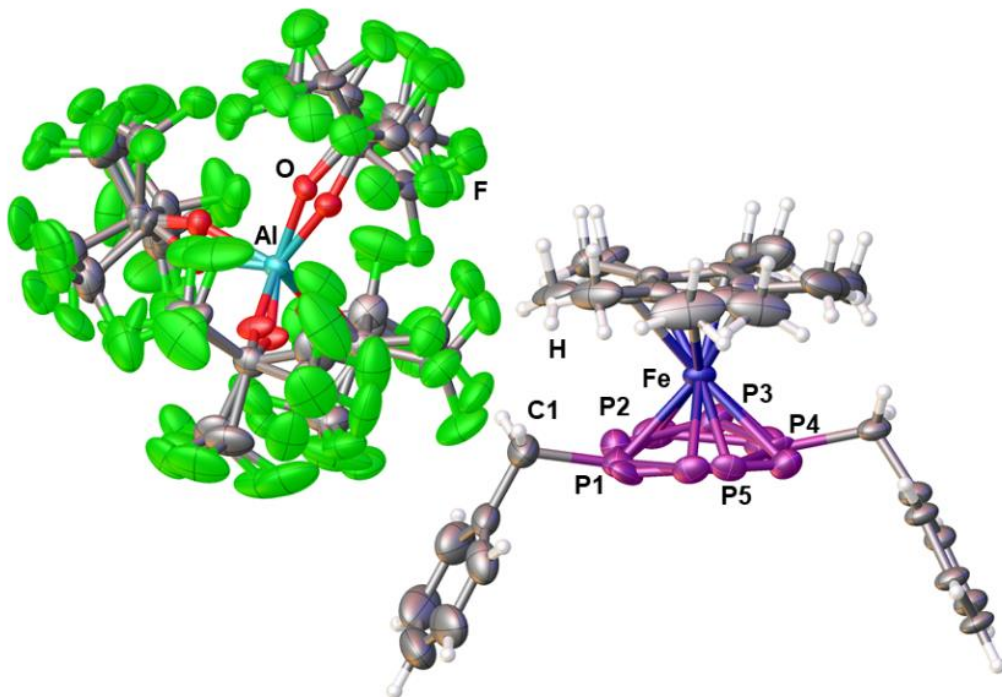


*Figure S 3: Solid state structure of **4**; Depicted is the asymmetric unit and ADPs are drawn at 50% probability; Selected bond lengths and angles:  $d(\text{P1-P2}) = 2.0893(18)$  Å,  $d(\text{P2-P3}) = 2.1091(17)$  Å,  $d(\text{P3-P4}) = 2.1273(14)$  Å,  $d(\text{P4-P5}) = 2.1032(15)$  Å,  $d(\text{P1-P5}) = 2.0928(17)$  Å,  $d(\text{P1-C1}) = 1.853(4)$  Å,  $d(\text{P1-Fe1}) = 2.282(1)$  Å,  $d(\text{P2-Fe1}) = 2.358(1)$  Å,  $d(\text{P3-Fe1}) = 2.391(1)$  Å,  $d(\text{P4-Fe1}) = 2.389(1)$  Å,  $d(\text{P5-Fe1}) = 2.359(1)$  Å,  $\alpha(\text{P1-C1-C2}) = 109.6(3)$ °,  $\alpha(\text{P3-P5-P2-P1}) = 166.00(9)$ °.*

## 2.5. $[\text{Cp}^*\text{Fe}(\eta^5\text{-P}_5\text{CHPh}_2)]\text{[TEF]} \text{ (5)}$

$[\text{Cp}^*\text{Fe}(\eta^5\text{-P}_5\text{CHPh}_2)]\text{[TEF]} \text{ (5)}$  can also be obtained as red crystalline blocks after layering a concentrated solution in *o*-DFB with *n*-hexane (1:8) and storing it at -30 °C for eleven days. **5** crystallises in the triclinic space group  $P\bar{1}$  with two cations and two anions present in the asymmetric unit (*Figure S 4*). Disorder within the anions was treated with appropriate geometric and ADP restraints.

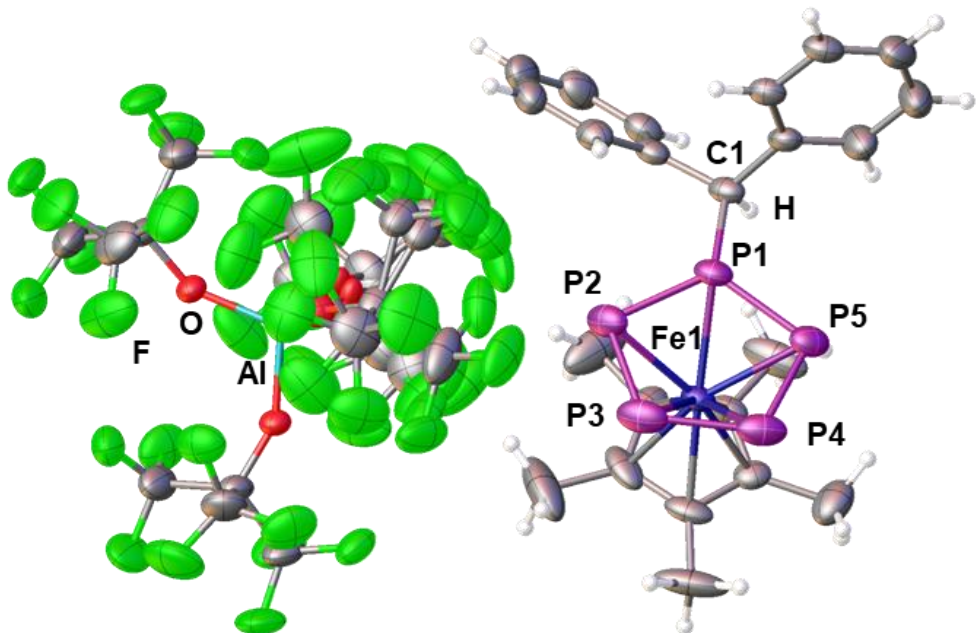


*Figure S 4:* Solid state structure of **5**; Depicted is half of the asymmetric unit and ADPs are drawn at 50% probability; Selected bond lengths and angles:  $d(\text{P1-P2}) = 2.0957(13)$  Å,  $d(\text{P2-P3}) = 2.1198(18)$  Å,  $d(\text{P3-P4}) = 2.1195(17)$  Å,  $d(\text{P4-P5}) = 2.1170(20)$  Å,  $d(\text{P1-P5}) = 2.0984(15)$  Å,  $d(\text{P1-C1}) = 1.866(4)$  Å,  $d(\text{P1-Fe1}) = 2.2944(10)$  Å,  $d(\text{P2-Fe1}) = 2.3679(13)$  Å,  $d(\text{P3-Fe1}) = 2.3829(12)$  Å,  $d(\text{P4-Fe1}) = 2.3863(18)$  Å,  $d(\text{P5-Fe1}) = 2.3520(12)$  Å,  $\alpha(\text{P1-C1-C2}) = 107.0(3)$  °,  $\alpha(\text{P3-P5-P2-P1}) = 162.96(10)$  °.

## 2.6. $[\text{Cp}^*\text{Fe}(\eta^5\text{-P}_5\text{SiHPh}_2)]\text{[B(C}_6\text{F}_5)_4]$ (6)

Crystals of  $[\text{Cp}^*\text{Fe}(\eta^5\text{-P}_5\text{SiHPh}_2)]\text{[B(C}_6\text{F}_5)_4]$  (6) can be obtained as clear greenish brown plates after layering a concentrated solution in *o*-DFB with *n*-hexane (1:10) and storing it at room temperature for two days. 6 crystallises in the monoclinic space group  $P2_1/c$  with one cation and one anion present in the asymmetric unit (*Figure S 5*). Disorder within the  $\text{Cp}^*$  ligand was treated with appropriate geometric and ADP restraints.

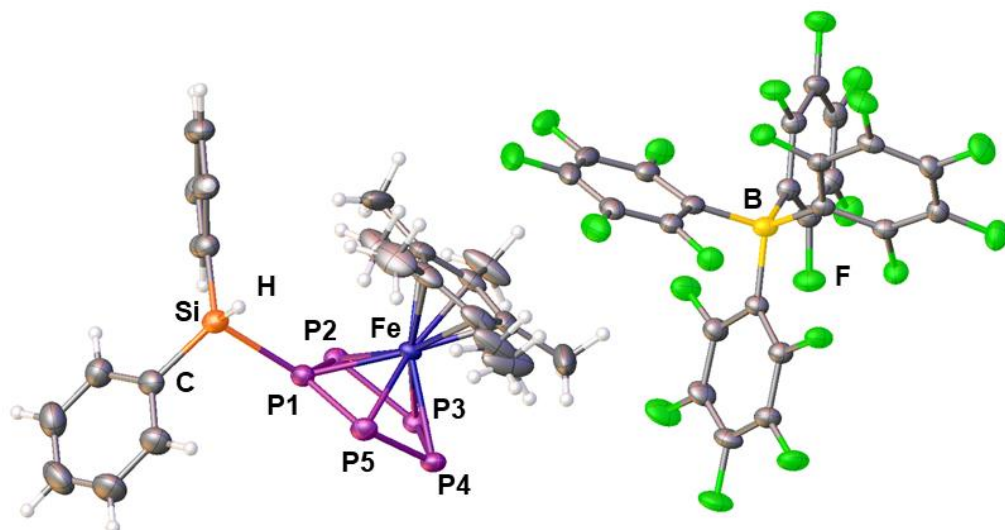


*Figure S 5:* Solid state structure of 6; Depicted is the asymmetric unit and ADPs are drawn at 50% probability; Selected bond lengths and angles:  $d(\text{P1-P2}) = 2.1047(8)$  Å,  $d(\text{P2-P3}) = 2.1124(8)$  Å,  $d(\text{P3-P4}) = 2.1150(8)$  Å,  $d(\text{P4-P5}) = 2.1151(8)$  Å,  $d(\text{P1-P5}) = 2.1027(8)$  Å,  $d(\text{P1-Si}) = 2.3053(8)$  Å,  $d(\text{P1-Fe1}) = 2.3080(8)$  Å,  $d(\text{P2-Fe1}) = 2.3640(8)$  Å,  $d(\text{P3-Fe1}) = 2.3683(6)$  Å,  $d(\text{P4-Fe1}) = 2.3963(6)$  Å,  $d(\text{P5-Fe1}) = 2.3544(7)$  Å,  $\alpha(\text{P1-Si-H1}) = 97.4(12)^\circ$ ,  $\alpha(\text{P3-P5-P2-P1}) = 167.74(5)^\circ$ .

## 2.7. $[\text{Cp}^*\text{Fe}(\eta^5\text{-P}_5\text{AsCy}_2)]\text{[TEF]} (7)$

Dark red block shaped crystals of  $[\text{Cp}^*\text{Fe}(\eta^5\text{-P}_5\text{AsCy}_2)]\text{[TEF]} (7)$  can be obtained after layering a concentrated solution in *o*-DFB with *n*-hexane (1:10) and storing it at -30 °C for two weeks. **7** crystallises in the monoclinic space group  $P2_1/n$  with one cation, one anion and one half of a toluene molecule present in the asymmetric unit (*Figure S 6*). The toluene could not be modelled properly and was therefore treated with the in Olex2 implemented masking tool. A solvent mask was calculated and 100 electrons were found in a volume of 348 Å<sup>3</sup> in 1 void per unit cell. This is consistent with the presence of half a toluene molecule per asymmetric unit, which accounts for 100 electrons per unit cell. Disorder within the anion and one of the cyclohexyl groups was treated with appropriate geometric and ADP restraints. Further, is the complete cationic part disordered over two positions (0.96 : 0.4). Due to the low occupancy of the second part it was only possible to model the heavy atom framework consisting of  $\text{FeP}_5\text{As}$ .

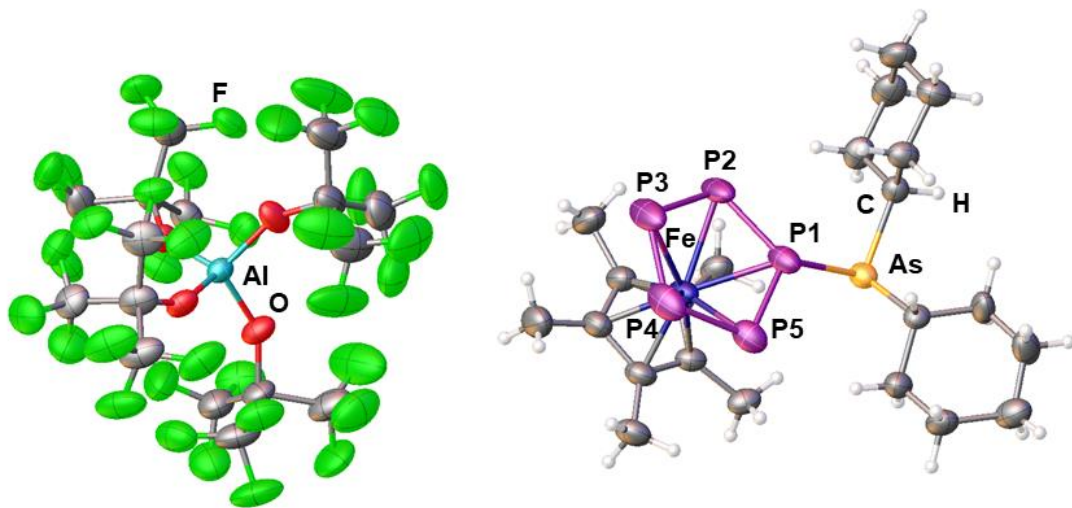


*Figure S 6:* Solid state structure of **7**; Depicted is the asymmetric unit and ADPs are drawn at 50% probability; Selected bond lengths and angles:  $d(\text{P1-P2}) = 2.110(2)$  Å,  $d(\text{P2-P3}) = 2.119(2)$  Å,  $d(\text{P3-P4}) = 2.121(3)$  Å,  $d(\text{P4-P5}) = 2.106(2)$  Å,  $d(\text{P1-P5}) = 2.116(2)$  Å,  $d(\text{P1-As}) = 2.348(1)$  Å,  $d(\text{P1-Fe1}) = 2.353(1)$  Å,  $d(\text{P2-Fe1}) = 2.335(2)$  Å,  $d(\text{P3-Fe1}) = 2.393(1)$  Å,  $d(\text{P4-Fe1}) = 2.386(2)$  Å,  $d(\text{P5-Fe1}) = 2.335(1)$  Å,  $\angle(\text{P3-P5-P2-P1}) = 162.66(8)$  °.

## 2.8. [{Cp\*Fe( $\mu$ , $\eta^{5:2}$ -P<sub>5</sub>)SbICp'''][TEF] (8)

Clear light greenish brown crystalline plates of [{Cp\*Fe( $\mu$ , $\eta^{5:2}$ -P<sub>5</sub>)SbICp'''][TEF] (8) can be obtained after layering a concentrated solution in o-DFB with *n*-hexane (1:10) and storing it at room temperature for ten days. **8** crystallises in the monoclinic space group *P*2<sub>1</sub>/*n* with two formula units and two times half a hexane molecule present in the asymmetric unit (*Figure S 7*). Disorder within the anions and the cations was treated with appropriate geometric and ADP restraints. The *n*-hexane molecules could not be modelled appropriately and therefore were treated with the in Olex2 implemented masking tool. A solvent mask was calculated and 204 electrons were found in a volume of 1206 Å<sup>3</sup> in 3 voids per unit cell. This is consistent with the presence of two half hexane molecules per asymmetric unit, which account for 200 electrons per unit cell.

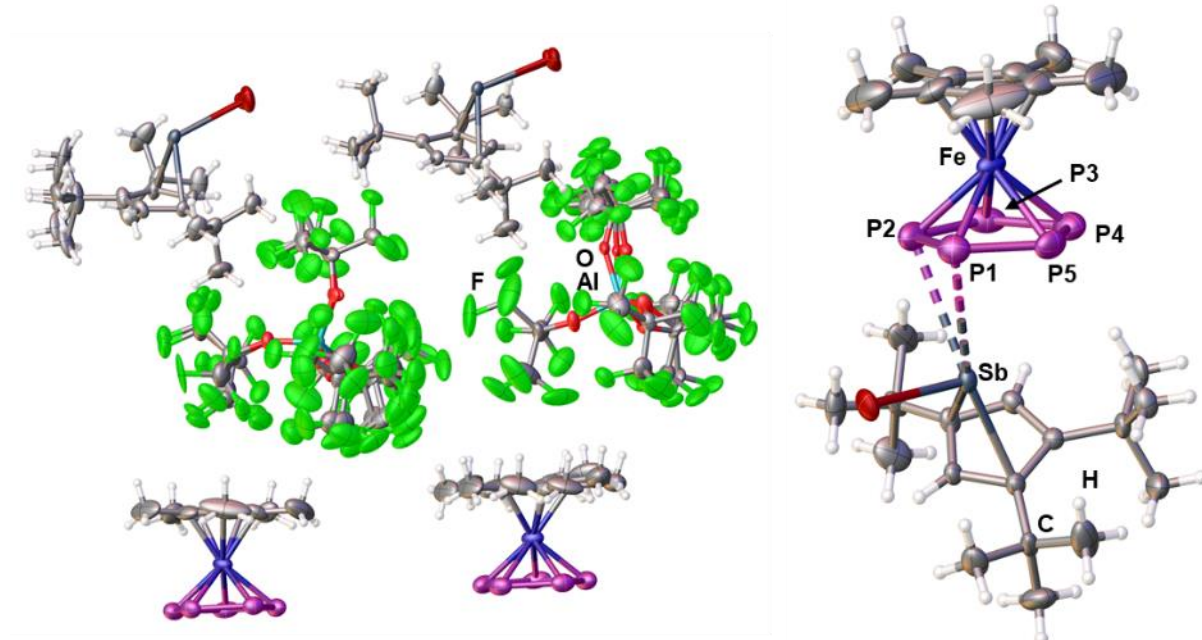


*Figure S 7:* Solid state structure of **8**; Depicted is the asymmetric unit (left), an excerpt of the cation (right) and ADPs are drawn at 50% probability; Selected bond lengths and angles:  $d(P1-P2) = 2.105(3)$  Å,  $d(P2-P3) = 2.137(4)$  Å,  $d(P3-P4) = 2.143(3)$  Å,  $d(P4-P5) = 2.119(3)$  Å,  $d(P1-P5) = 2.107(3)$  Å,  $d(P3-Sb) = 3.236(2)$  Å,  $d(P4-Sb) = 3.400(2)$  Å,  $d(Sb-I) = 2.787(3)$  Å,  $d(P1-Fe1) = 2.348(3)$  Å,  $d(P2-Fe1) = 2.329(2)$  Å,  $d(P3-Fe1) = 2.347(2)$  Å,  $d(P4-Fe1) = 2.328(2)$  Å,  $d(P5-Fe1) = 2.345(2)$  Å,  $\alpha(P5-Sb-C5) = 128.51(8)$  °.

## 2.9. $[\text{Cp}^*\text{Fe}(\eta^5\text{-P}_5\text{SePh})]\text{[TEF]} \text{ (9)}$

Clear dark red block shaped crystals of  $[\text{Cp}^*\text{Fe}(\eta^5\text{-P}_5\text{SePh})]\text{[TEF]} \text{ (9)}$  can be obtained after layering a concentrated solution in *o*-DFB with *n*-hexane (1:7) and storing it at room temperature for twelve days. **9** crystallises in the triclinic space group  $P\bar{1}$  with one cation and one anion present in the asymmetric unit (*Figure S 8*). Disorder within the anion was treated with appropriate geometric and ADP restraints.

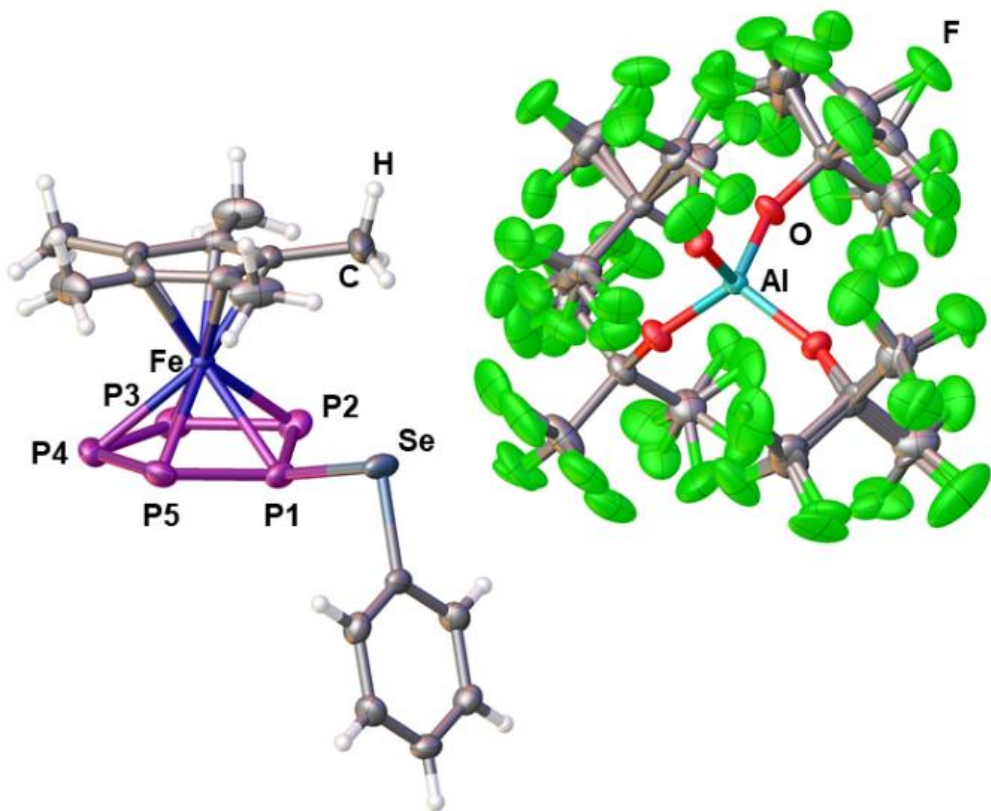


*Figure S 8:* Solid state structure of **9**; Depicted is the asymmetric unit and ADPs are drawn at 50% probability; Selected bond lengths and angles:  $d(\text{P1-P2}) = 2.1201(11)$  Å,  $d(\text{P2-P3}) = 2.1109(11)$  Å,  $d(\text{P3-P4}) = 2.1395(12)$  Å,  $d(\text{P4-P5}) = 2.1098(12)$  Å,  $d(\text{P1-P5}) = 2.1220(10)$  Å,  $d(\text{P1-Se}) = 2.2234(7)$  Å,  $d(\text{P1-Fe1}) = 2.3061(9)$  Å,  $d(\text{P2-Fe1}) = 2.3489(8)$  Å,  $d(\text{P3-Fe1}) = 2.3923(8)$  Å,  $d(\text{P4-Fe1}) = 2.3967(8)$  Å,  $d(\text{P5-Fe1}) = 2.3401(10)$  Å,  $\alpha(\text{P3-P5-P2-P1}) = 163.19(6)$ °.

## 2.10. $[\text{Cp}^*\text{Fe}(\eta^5\text{-P}_5\text{TeMes})]\text{[TEF]} \textbf{(10)}$

$[\text{Cp}^*\text{Fe}(\eta^5\text{-P}_5\text{TeMes})]\text{[TEF]} \textbf{(10)}$  can be obtained as crystalline dark red blocks after layering a concentrated solution in *o*-DFB with *n*-pentane (1:6) and storing it at room temperature for two weeks. **10** crystallises in the triclinic space group  $P\bar{1}$  with three cations, three anions and one *o*-DFB molecule present in the asymmetric unit (*Figure S 9*). Disorder within the anions and the solvent molecule was treated with appropriate geometric and ADP restraints.

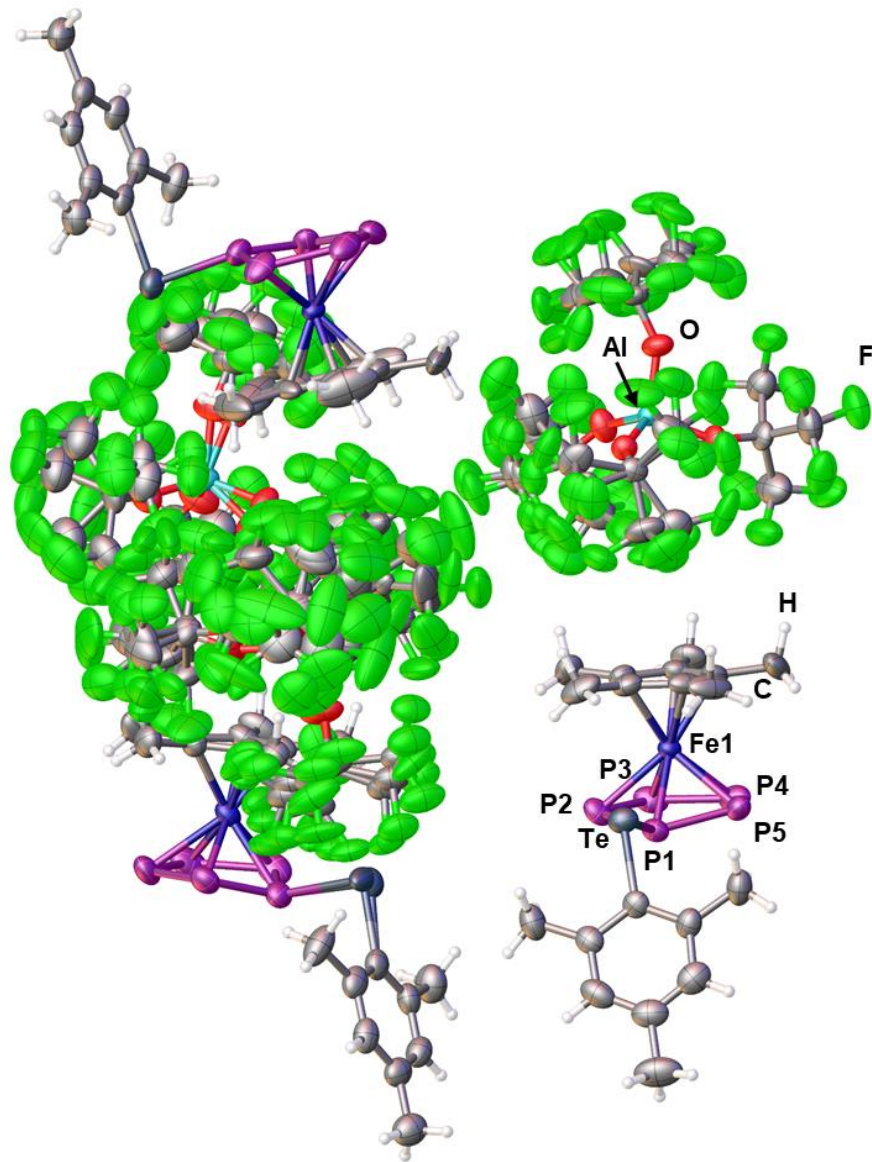


*Figure S 9:* Solid state structure of **10**; Depicted is the asymmetric unit and ADPs are drawn at 50% probability; Selected bond lengths and angles within the labelled cation:  $d(\text{P1-P2}) = 2.123(3)$  Å,  $d(\text{P2-P3}) = 2.092(4)$  Å,  $d(\text{P3-P4}) = 2.126(3)$  Å,  $d(\text{P4-P5}) = 2.123(4)$  Å,  $d(\text{P1-P5}) = 2.105(2)$  Å,  $d(\text{P1-Te}) = 2.438(2)$  Å,  $d(\text{P1-Fe1}) = 2.314(2)$  Å,  $d(\text{P2-Fe1}) = 2.340(2)$  Å,  $d(\text{P3-Fe1}) = 2.393(3)$  Å,  $d(\text{P4-Fe1}) = 2.376(2)$  Å,  $d(\text{P5-Fe1}) = 2.344(2)$  Å,  $\alpha(\text{P3-P5-P2-P1}) = 164.93(13)$  °.

## 2.11. [Cp\*Fe( $\eta^5$ -P<sub>5</sub>Cl)][TEF] (11)

Dark red block shaped crystals of [Cp\*Fe( $\eta^5$ -P<sub>5</sub>Cl)][TEF] (**11**) can easily be obtained from storing mixtures of concentrated solutions in *o*-DFB or CH<sub>2</sub>Cl<sub>2</sub> and *n*-hexane at -30 °C for several days. However, the crystal structure of **11** appears to be incommensurate modulated with a 1<sup>st</sup> order modulation vector of (0.201/-0.032/-0.230). Despite many attempts of recrystallisation and variation of experiment parameters during data collection (e. g. temperature), this modulation could not be resolved. Thus, the solid state structure of **11** cannot be provided within this report and only the cell parameters are given within *Table S 2*.

*Table S 2: Cell parameters for the average unit cell of **11**.*

Empirical formula	C <sub>26</sub> H <sub>15</sub> O <sub>4</sub> F <sub>36</sub> AlP <sub>5</sub> ClFe
Formula weight	1348.51
Temperature/K	122.96(13)
Crystal system	monoclinic
Space group	<i>Pc</i>
a/Å	20.4081(10)
b/Å	20.4729(11)
c/Å	21.4055(9)
α/°	90
β/°	93.162(4)
γ/°	90
Volume/Å <sup>3</sup>	8929.9(8)

## 2.12. $[\text{Cp}^*\text{Fe}(\eta^5\text{-P}_5\text{Br})]\text{[TEF]} \text{ (12)}$

$[\text{Cp}^*\text{Fe}(\eta^5\text{-P}_5\text{Br})]\text{[TEF]} \text{ (12)}$  can be obtained as crystalline dark brownish red plates after layering a concentrated solution in  $\text{CH}_2\text{Cl}_2$  with *n*-hexane (1:7) and storing it at -30 °C for three weeks. **12** crystallises in the monoclinic space group *C*2/c with one cation, one anion and one third of a  $\text{CH}_2\text{Cl}_2$  molecule present in the asymmetric unit. Despite using appropriate geometric and ADP restraints and constraints for handling the severe disorder within both the anion and the cation, proper refinement of the crystal structure was not feasible. Thus, only the major disordered parts of the anion and the cation are depicted in Figure S 10 as structural proof. The unit cell parameters of **12** are provided in Table S 3.

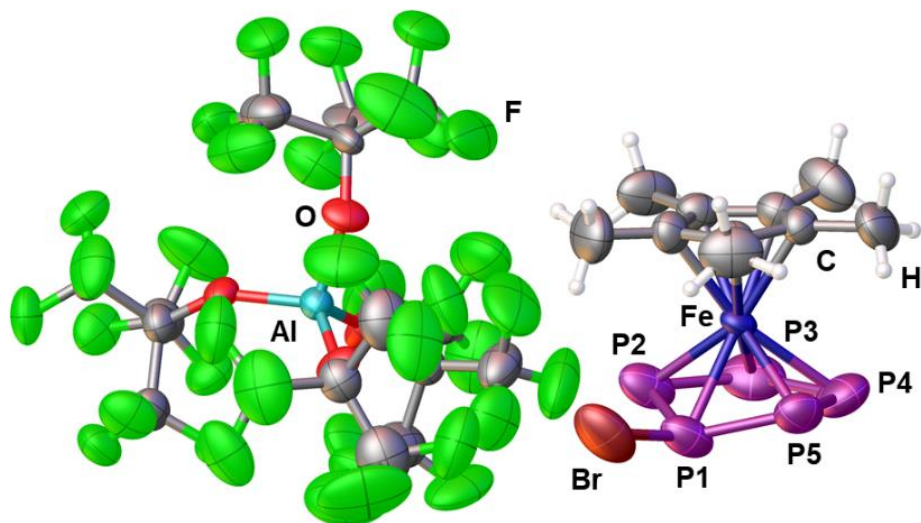


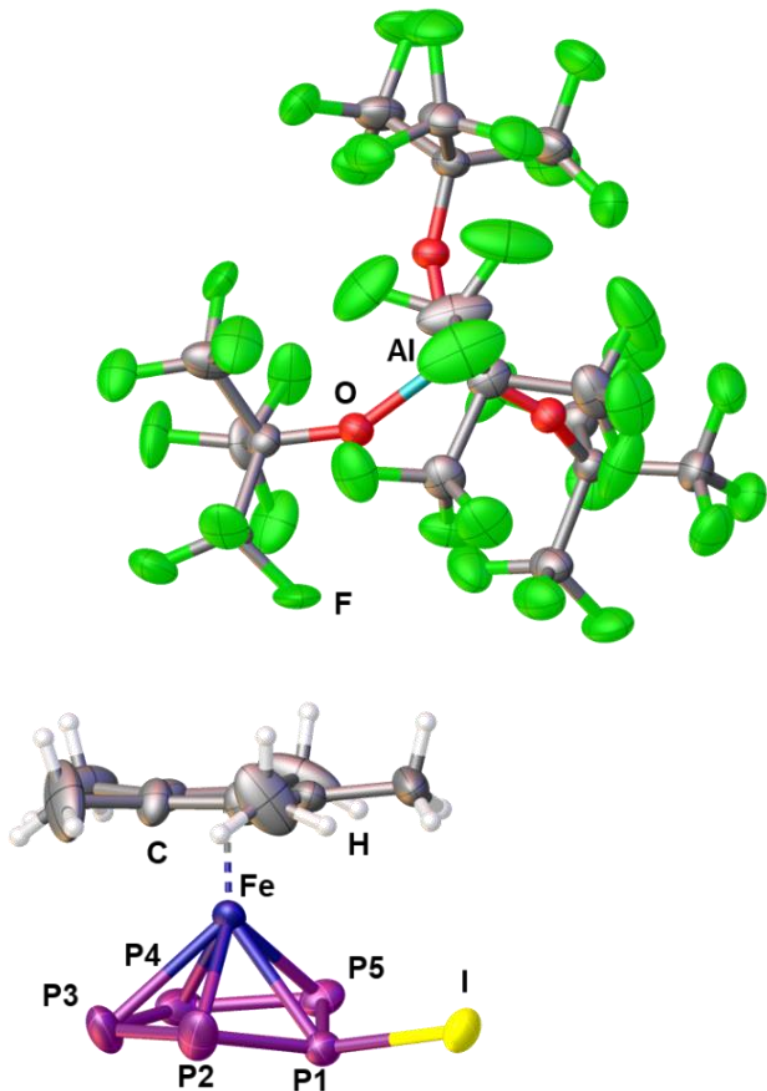
Figure S 10: Solid state structure of **12**; Depicted is the asymmetric unit and disorder, and solvent molecules are omitted for clarity.

Table S 3: Cell parameters for the unit cell of **12**.

Empirical formula	$\text{C}_{26.33}\text{H}_{15.66}\text{AlBrCl}_{0.66}\text{F}_{36}\text{FeO}_4\text{P}_5$
Formula weight	1420.99
Temperature/K	123.01(10)
Crystal system	monoclinic
Space group	<i>C</i> 2/c
a/Å	30.3586(19)
b/Å	19.7750(4)
c/Å	23.3649(16)
$\alpha/^\circ$	90
$\beta/^\circ$	138.494(13)
$\gamma/^\circ$	90
Volume/Å <sup>3</sup>	9295.6(18)

### 2.13. $[\text{Cp}^*\text{Fe}(\eta^5\text{-P}_5\text{I})]\text{[TEF]} \text{ (13)}$

$[\text{Cp}^*\text{Fe}(\eta^5\text{-P}_5\text{I})]\text{[TEF]} \text{ (13)}$  can be obtained as crystalline dark brown blocks after layering a concentrated solution in *o*-DFB with *n*-pentane (1:10) and storing it at -30 °C for three days. **13** crystallises in the monoclinic space group  $C2/c$  with one cation, one anion and half an equivalent of *o*-DFB present in the asymmetric unit (*Figure S 11*). Disorder within the anion was treated with appropriate geometric and ADP restraints.



*Figure S 11:* Solid state structure of **13**; Depicted is the asymmetric unit and ADPs are drawn at 50% probability; Selected bond lengths and angles within the labelled cation:  $d(\text{P1-P2}) = 2.107(4)$  Å,  $d(\text{P2-P3}) = 2.106(6)$  Å,  $d(\text{P3-P4}) = 2.147(6)$  Å,  $d(\text{P4-P5}) = 2.102(3)$  Å,  $d(\text{P1-P5}) = 2.112(3)$  Å,  $d(\text{P1-I}) = 2.385(1)$  Å,  $d(\text{P1-Fe1}) = 2.363(1)$  Å,  $d(\text{P2-Fe1}) = 2.301(6)$  Å,  $d(\text{P3-Fe1}) = 2.422(4)$  Å,  $d(\text{P4-Fe1}) = 2.494(3)$  Å,  $d(\text{P5-Fe1}) = 2.403(2)$  Å,  $\alpha(\text{P3-P5-P2-P1}) = 156.4(3)$  °.

## 2.14. $\left[\{\text{Cp}'''\text{Ta}(\text{CO})_2\}_2\{\mu,\eta^{4:4}\text{-}((\text{P}_4)_2\text{BBr}_2)\}\right]\text{[TEF]} \textbf{(15)}$

$\left[\{\text{Cp}'''\text{Ta}(\text{CO})_2\}_2\{\mu,\eta^{4:4}\text{-}((\text{P}_4)_2\text{BBr}_2)\}\right]\text{[TEF]} \textbf{(15)}$  can be obtained as clear yellow crystals after layering a concentrated solution in *o*-DFB with *n*-pentane (1:6) and storing it at room temperature for one day. **15** crystallises in the triclinic space group  $P\bar{1}$  with one cation and one anion in the asymmetric unit (*Figure S 12*). Disorder within the anion was treated with appropriate geometric and ADP restraints.

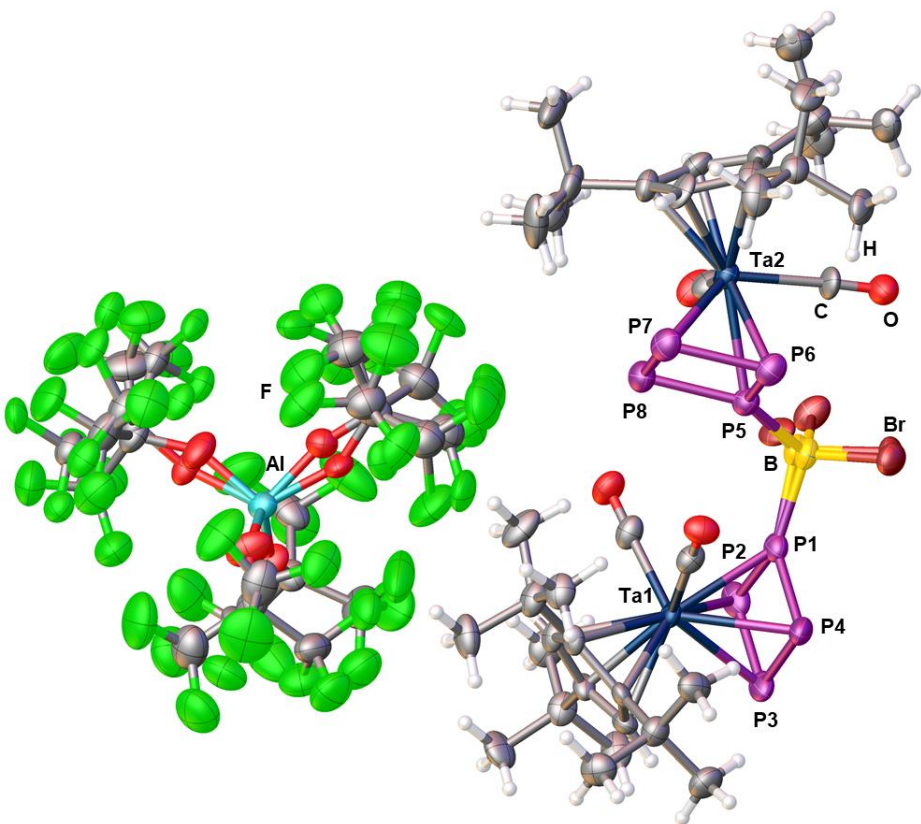


*Figure S 12:* Solid state structure of **15**; Depicted is the asymmetric unit and ADPs are drawn at 50% probability; Selected bond lengths and angles within the labelled cation:  $d(\text{P}1\text{-P}2) = 2.133(4)$  Å,  $d(\text{P}2\text{-P}3) = 2.171(4)$  Å,  $d(\text{P}3\text{-P}4) = 2.164(4)$  Å,  $d(\text{P}1\text{-P}4) = 2.124(4)$  Å,  $d(\text{P}5\text{-P}6) = 2.129(4)$  Å,  $d(\text{P}6\text{-P}7) = 2.171(4)$  Å,  $d(\text{P}7\text{-P}8) = 2.170(4)$  Å,  $d(\text{P}5\text{-P}8) = 2.149(3)$  Å,  $d(\text{P}1\text{-B}) = 1.997(10)$  Å,  $d(\text{P}5\text{-B}) = 1.996(9)$  Å,  $\angle(\text{P}1\text{-B}\text{-P}5) = 112.3(5)$  °.

### 3. NMR

#### 3.1. $\{(\text{Cp}^*\text{Fe})_2\{(\eta^5\text{-P}_5)_2\text{BBr}_2\}\}[\text{TEF}]$ (2)

While the  $^1\text{H}$  NMR spectrum recorded at room temperature only shows one singlet at  $\delta = 1.76$  ppm for the  $\text{Cp}^*$  ligands, its  $^{31}\text{P}$  NMR spectrum (Figure S 13) reveals a complex  $\text{AA}'\text{M}_2\text{M}'_2\text{X}_2\text{X}'_2$  spin system with an additional  $^{11}\text{B}$ - $\text{P}$  coupling (chemical shifts and coupling constants provided in Table S 4). Consistently, the  $^{11}\text{B}\{^1\text{H}\}$  NMR spectrum (Figure S 14) of **2** reveals a triplet at  $\delta = -15.6$  with a  $^1\text{J}_{\text{B-P}} = 64$  Hz coupling constant.

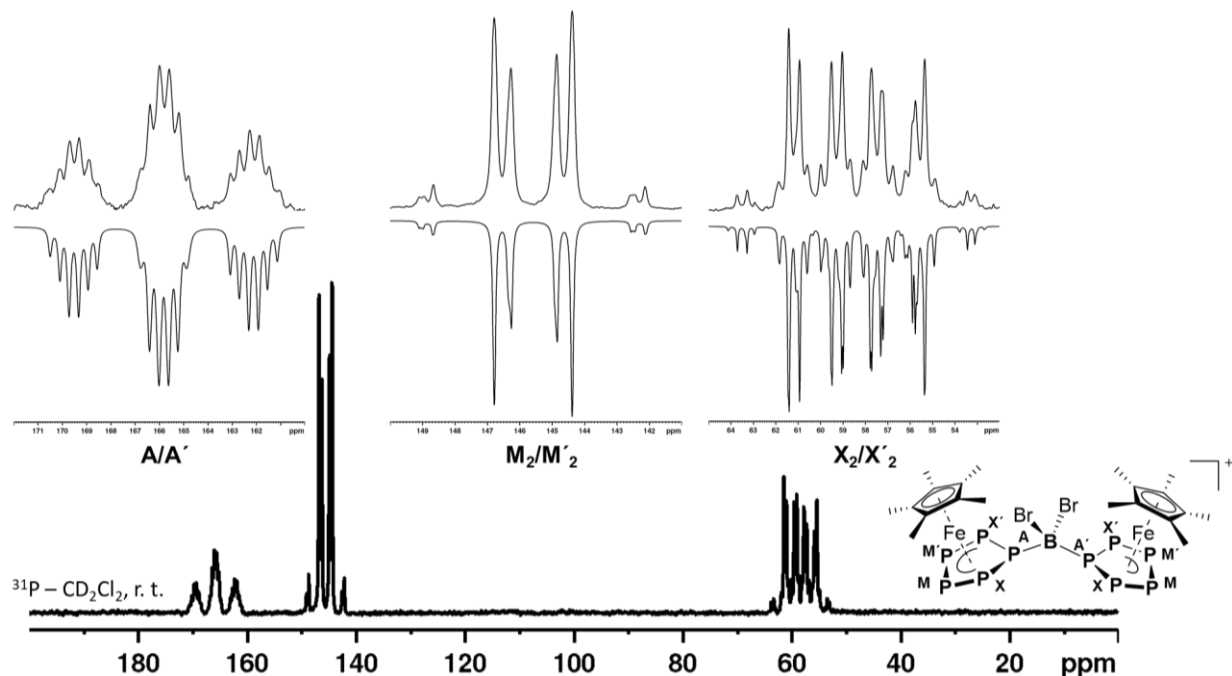


Figure S 13: Experimental (top) and simulated (bottom)  $^{31}\text{P}$  NMR spectrum of **2** in  $\text{CD}_2\text{Cl}_2$  at room temperature and assignment of the spin system (right).

Table S 4: Coupling constants (left) and chemical shifts (right) of **2** in  $\text{CD}_2\text{Cl}_2$  solution obtained from spectral simulation of the respective  $^{31}\text{P}$  NMR spectrum.

$J/\text{Hz}$	$\delta/\text{ppm}$
$^1\text{J}_{\text{PA/A'-PX/X'}}$	$\text{P}^{\text{A/A}'} \quad 165.8$
$^1\text{J}_{\text{PM/M'-PX/X'}}$	$\text{P}^{\text{M/M}'} \quad 145.6$
$^1\text{J}_{\text{PM-PM'}}$	$\text{P}^{\text{X/X}'} \quad 58.4$
$^2\text{J}_{\text{PM/M'-PX/X'}}$	$-58.4/-47.0$
$^2\text{J}_{\text{PA/A'-PM/M'}}$	$6.8/3.8$
$^2\text{J}_{\text{PX-X'}}$	$36.9$
$^1\text{J}_{\text{PA-A'}}$	$123.6$
$^1\text{J}_{\text{PA/A'-B}}$	$64$

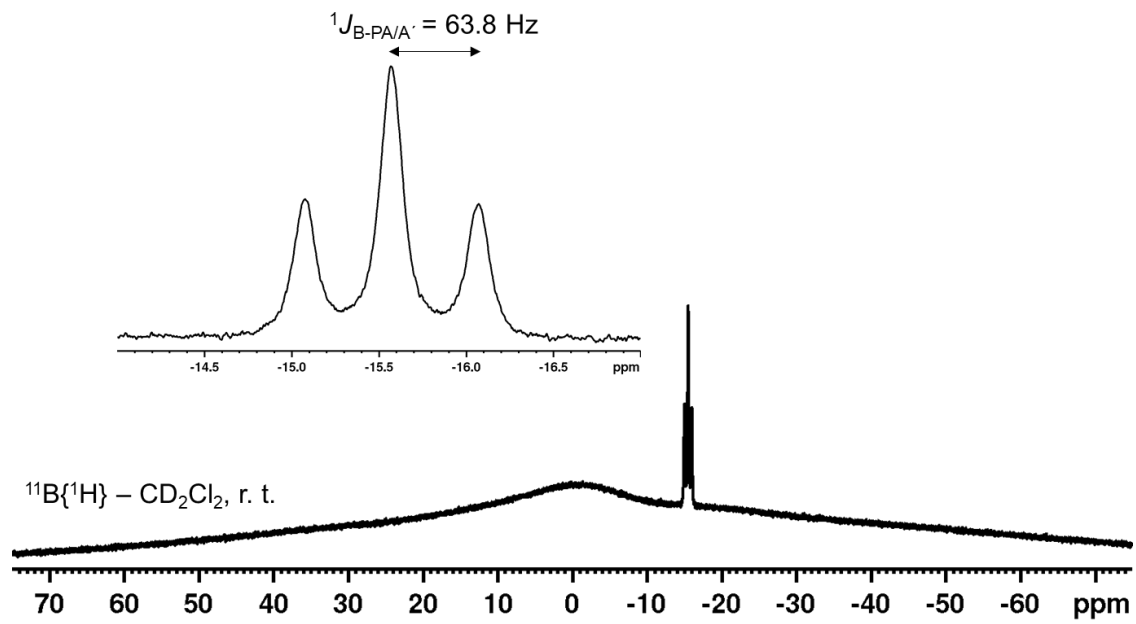


Figure S 14:  $^{11}\text{B}\{^1\text{H}\}$  NMR spectrum of **2** in  $\text{CD}_2\text{Cl}_2$  at room temperature.

### 3.2. $\{[\text{Cp}^*\text{Fe}]_2\{(\eta^5-\text{P}_5)_2\text{Gal}_2\}\}[\text{TEF}]$ (3)

**3** is well soluble in o-DFB, but shows rapid dynamic behaviour in solution, leading to observation of only one broad signal at room temperature. Even when a crystalline sample of **3**, dissolved in  $\text{CD}_2\text{Cl}_2$ , is cooled to -80 °C this dynamic behaviour is not completely resolved. The  $^{31}\text{P}\{^1\text{H}\}$  NMR spectrum of **3** recorded at -80 °C shows two signals I and II (Figure S 15) at  $\delta = 92.7$  and 141.6 ppm integrating in a ratio of 4:6, respectively, thus indicating overlap of two out of the three expected signals. However, **3** slowly decomposes in  $\text{CD}_2\text{Cl}_2$  solution, which is indicated by the presence of degradation products, such as  $[\text{Cp}^*\text{Fe}(\eta^5-\text{P}_5\text{H})]^+$ ,<sup>14</sup> in its  $^{31}\text{P}\{^1\text{H}\}$  NMR spectrum.

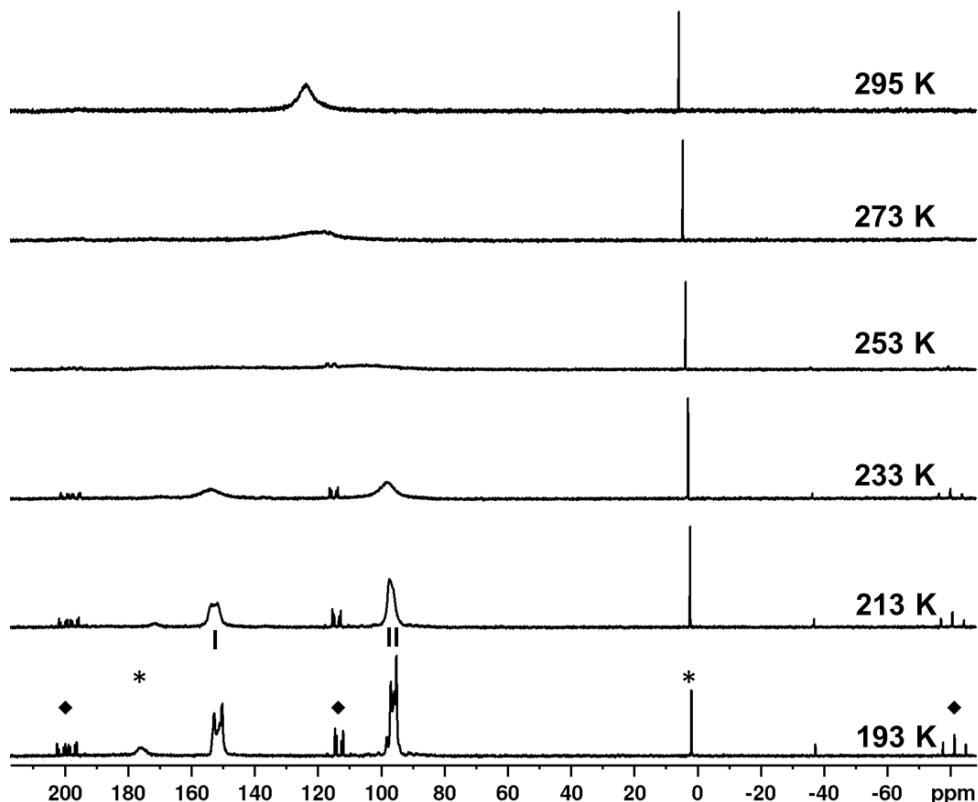


Figure S 15:  $^{31}\text{P}\{^1\text{H}\}$  NMR spectra of **3** in  $\text{CD}_2\text{Cl}_2$  recorded at indicated temperatures, revealing its dynamic behaviour in solution (even at -80 °C); ♦ marks the signals assigned to  $[\text{Cp}^*\text{Fe}(\eta^5-\text{P}_5\text{H})]^+$  and \* those assigned to corresponding, yet unidentified decomposition products.

### 3.3. $[\text{Cp}^*\text{Fe}(\eta^5\text{-P}_5\text{CH}_2\text{Ph})]\text{[TEF]} (4)$

**4** is well soluble in  $\text{CD}_2\text{Cl}_2$ , allowing its NMR spectra to be recorded easily. The  $^1\text{H}$  NMR spectrum (Figure S 18) recorded at room temperature reveals a singlet at  $\delta = 1.73$  ppm for the  $\text{Cp}^*$  ligand, a doublet of triplets at  $\delta = 4.42$  ppm for the benzylic protons and a multiplet of at  $\delta = 7.40\text{--}7.55$  ppm for the Ph group. Its  $^{31}\text{P}\{^1\text{H}\}$  NMR spectrum (Figure S 16) reveals an AMM'XX' spin system (chemical shifts and coupling constants provided in Table S 5), of which the signals for  $\text{P}^A$  shows additional coupling in the  $^{31}\text{P}$  NMR spectrum (Figure S 17 and Table S 6). The  $^{13}\text{C}\{^1\text{H}\}$  NMR spectrum (Figure S 19) of **4** additionally reveals a small doublet ( $\delta = 26.1$  ppm) for the benzylic carbon with a  $^1\text{J}_{\text{C-P}} = 23$  Hz coupling constant.

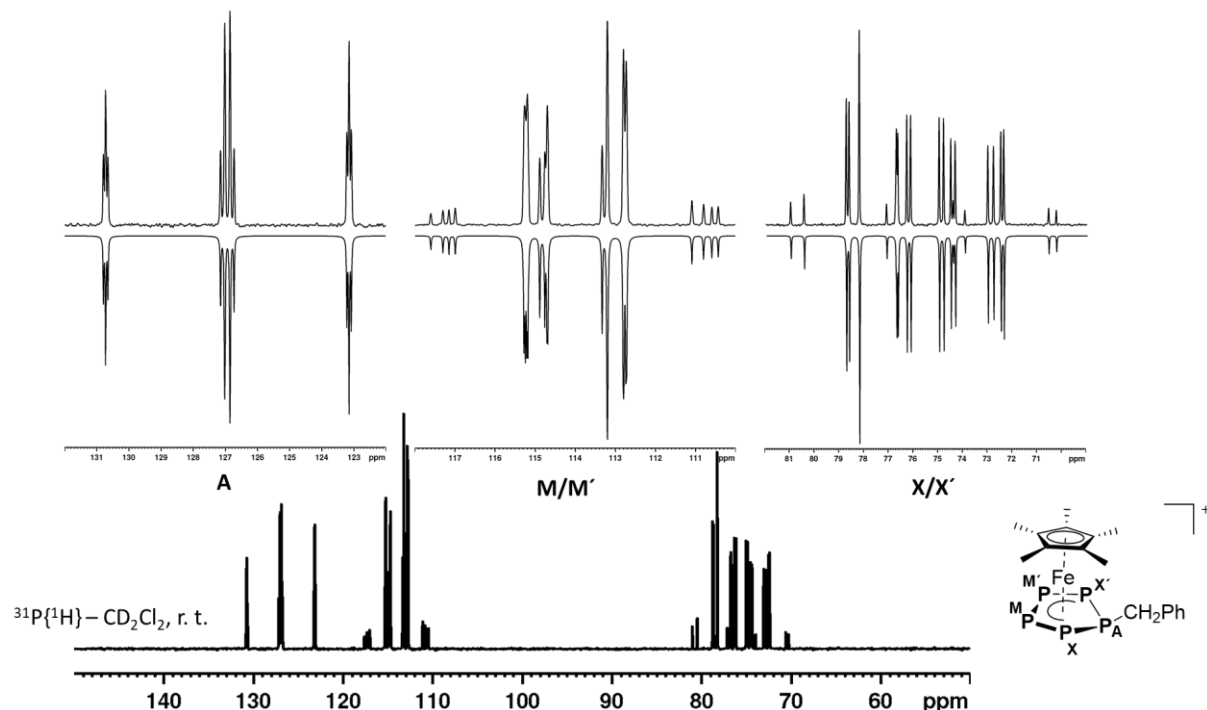


Figure S 16: Experimental (top) and simulated (bottom)  $^{31}\text{P}\{^1\text{H}\}$  NMR spectrum of **4** in  $\text{CD}_2\text{Cl}_2$  at room temperature and assignment of the spin system (right).

Table S 5: Coupling constants (left) and chemical shifts (right) of **4** in  $\text{CD}_2\text{Cl}_2$  solution obtained from spectral simulation of the respective  $^{31}\text{P}\{^1\text{H}\}$  NMR spectrum.

$J$ / Hz		$\delta$ / ppm
$^1\text{J}_{\text{PA-PX'/X'}}$	615.4/615.2	$\text{P}^A$ 126.8
$^1\text{J}_{\text{PM/M'-PX/X'}}$	455.4/454.6	$\text{P}^{\text{M/M}'}$ 113.9
$^1\text{J}_{\text{PM-PM'}}$	407.0	$\text{P}^{\text{X/X}'}$ 75.7
$^2\text{J}_{\text{PM/M'-PX'/X'}}$	-56.0/-55.7	
$^2\text{J}_{\text{PA-PM/M'}}$	10.2/9.0	
$^2\text{J}_{\text{PX-X'}}$	42.3	

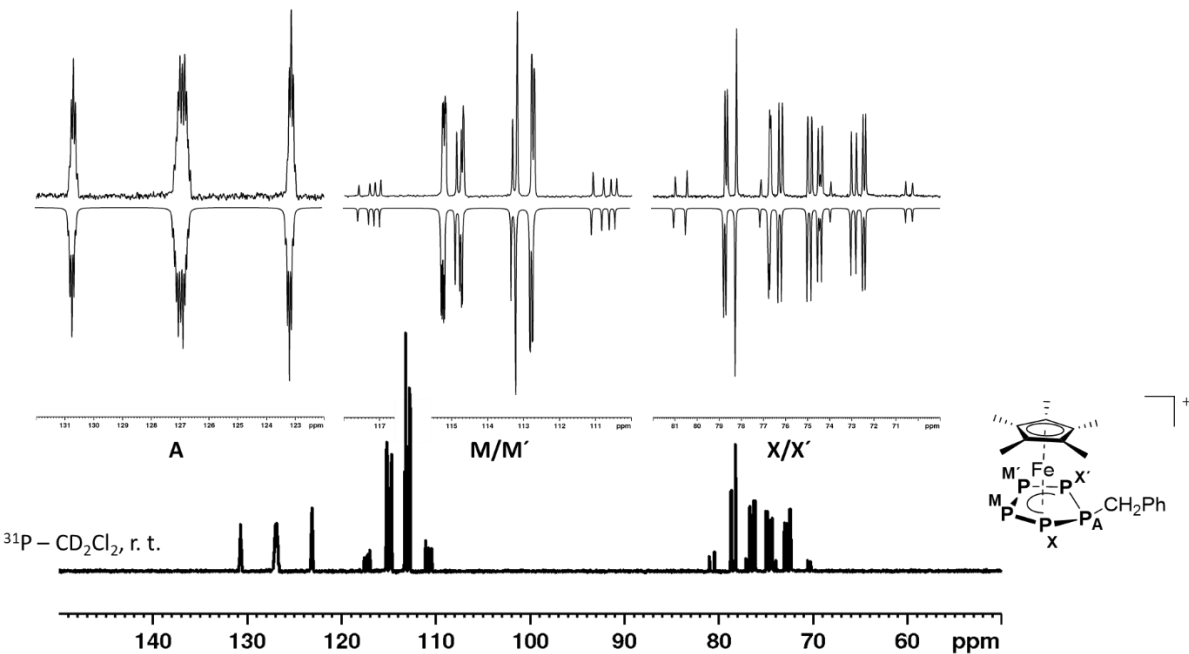


Figure S 17: Experimental (top) and simulated (bottom)  $^{31}\text{P}$  NMR spectrum of **4** in  $\text{CD}_2\text{Cl}_2$  at room temperature and assignment of the spin system (right).

Table S 6: Coupling constants (left) and chemical shifts (right) of **4** in  $\text{CD}_2\text{Cl}_2$  solution obtained from spectral simulation of the respective  $^{31}\text{P}$  NMR spectrum.

$J/\text{Hz}$		$\delta/\text{ppm}$	
$^1J_{\text{PA}-\text{PX}/\text{X}'}$	617.1/613.6	$\text{P}^{\text{A}}$	126.8
$^1J_{\text{PM}/\text{M}'-\text{PX}/\text{X}'}$	459.3/450.9	$\text{P}^{\text{M/M}'}$	113.9
$^1J_{\text{PM}-\text{PM}'}$	407.0	$\text{P}^{\text{X/X}'}$	75.7
$^2J_{\text{PM}/\text{M}'-\text{PX}/\text{X}'}$	-60.6/-51.2		
$^2J_{\text{PA}-\text{PM}/\text{M}'}$	10.5/9.1		
$^2J_{\text{PX}-\text{X}'}$	42.1		
$^2J_{\text{PA}-\text{H}}$	11.3		

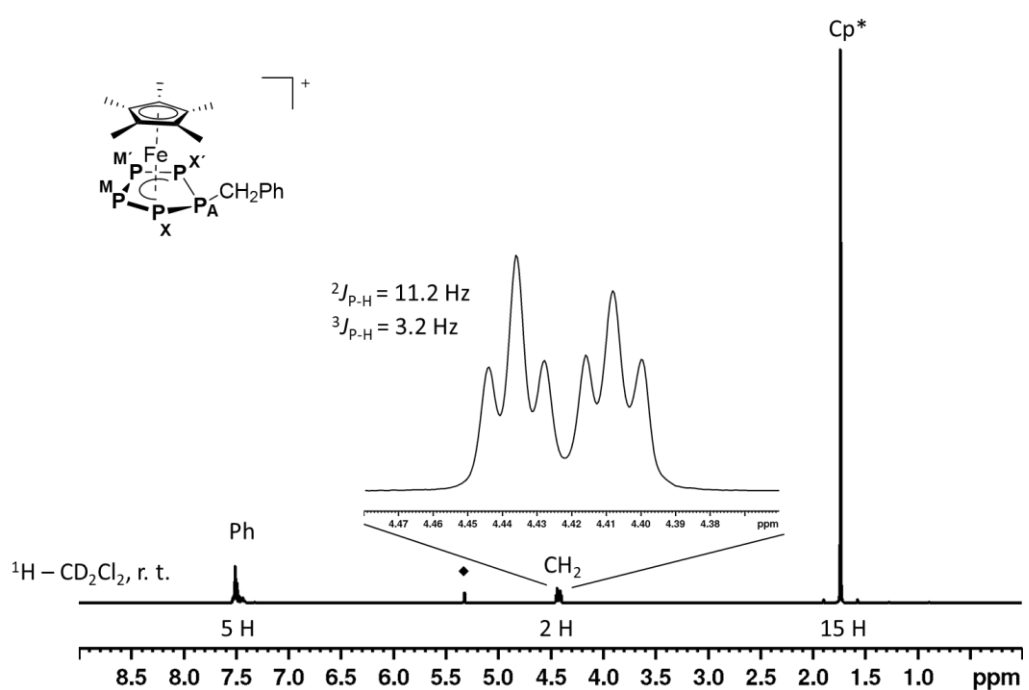


Figure S 18:  $^1\text{H}$  NMR spectrum of **4** in  $\text{CD}_2\text{Cl}_2$  at room temperature; ♦ marks the residual solvent signal for  $\text{CD}_2\text{Cl}_2$ .

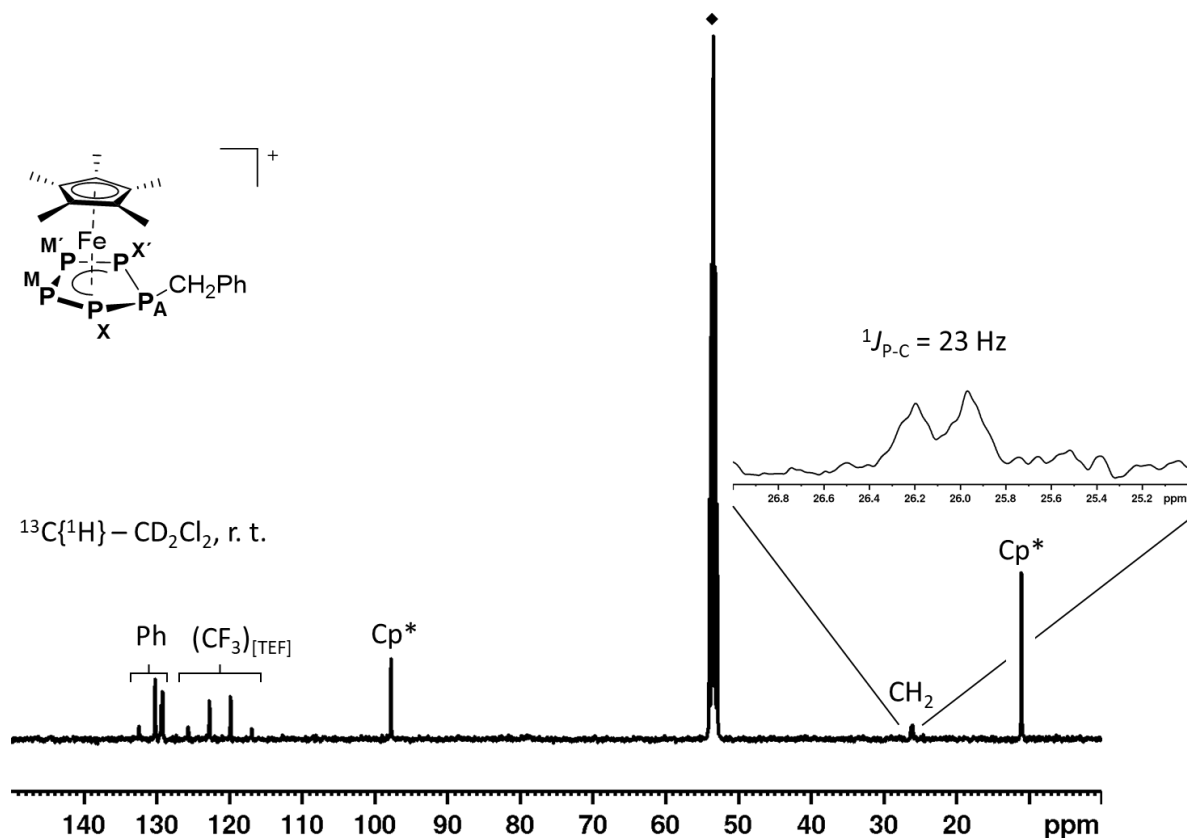


Figure S 19:  $^{13}\text{C}\{^1\text{H}\}$  NMR spectrum of **4** in  $\text{CD}_2\text{Cl}_2$  at room temperature; ♦ marks the residual solvent signal for  $\text{CD}_2\text{Cl}_2$ .

### 3.4. $[\text{Cp}^*\text{Fe}(\eta^5\text{-P}_5\text{CHPh}_2)]\text{[TEF]} (5)$

Similar to **4**, compound **5** is well soluble in  $\text{CD}_2\text{Cl}_2$  and its  $^1\text{H}$  NMR spectrum (Figure S 22) recorded at room temperature reveals a sharp singlet at  $\delta = 1.64$  ppm for the  $\text{Cp}^*$  ligand, a doublet of triplets at  $\delta = 5.93$  ppm for the benzylic proton and a set of multiplets in between  $\delta = 7.43\text{-}7.72$  ppm for the Ph groups. The  $^{31}\text{P}\{^1\text{H}\}$  NMR spectrum (Figure S 20) again shows an AMM'XX' spin system (chemical shifts and coupling constants provided in Table S 7), of which the  $\text{P}^A$  signal shows further coupling in the  $^{31}\text{P}$  NMR spectrum (Figure S 21 and Table S 8). In agreement, the  $^{13}\text{C}\{^1\text{H}\}$  NMR spectrum (Figure S 23) of **5** reveals a doublet at  $\delta = 49.3$  ppm with a distinct  $^1J_{\text{C-P}} = 23$  Hz coupling constant.

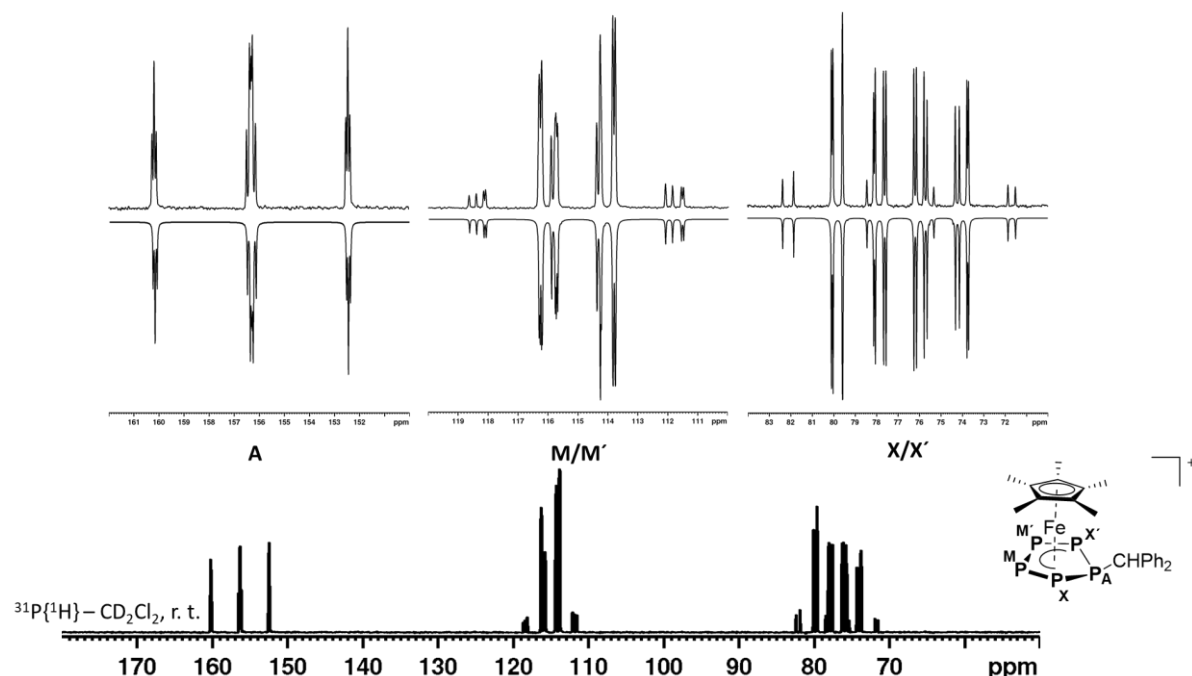


Figure S 20: Experimental (top) and simulated (bottom)  $^{31}\text{P}\{^1\text{H}\}$  NMR spectrum of **5** in  $\text{CD}_2\text{Cl}_2$  at room temperature and assignment of the spin system (right).

Table S 7: Coupling constants (left) and chemical shifts (right) of **5** in  $\text{CD}_2\text{Cl}_2$  solution obtained from spectral simulation of the respective  $^{31}\text{P}\{^1\text{H}\}$  NMR spectrum.

$J/\text{Hz}$		$\delta/\text{ppm}$
$^1J_{\text{PA-PX/X'}}$	629.8/625.3	$\text{P}^A$ 156.2
$^1J_{\text{PM/M'-PX/X'}}$	450.4/449.5	$\text{P}^{\text{M/M}'}$ 115.0
$^1J_{\text{PM-PM'}}$	412.2	$\text{P}^{\text{X/X}'}$ 77.0
$^2J_{\text{PM/M'-PX/X'}}$	-54.5/-54.0	
$^2J_{\text{PA-PM/M'}}$	17.5/6.0	
$^2J_{\text{PX-X'}}$	43.1	

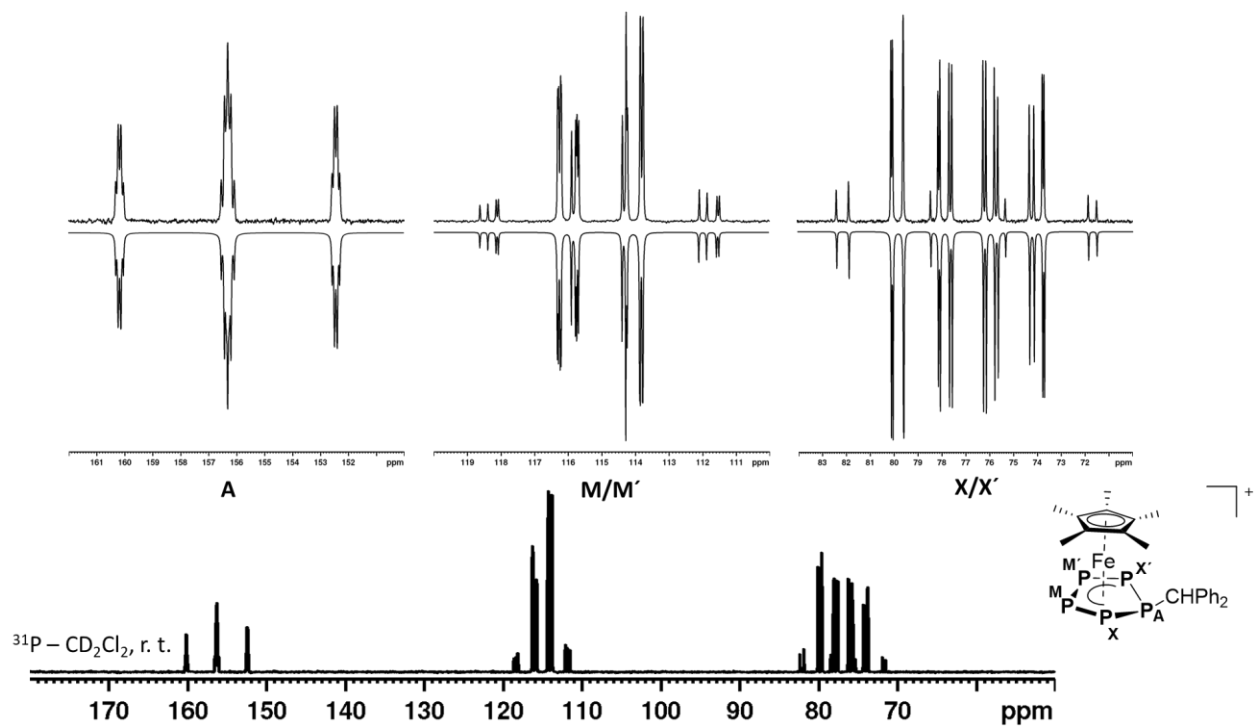


Figure S 21: Experimental (top) and simulated (bottom)  $^{31}\text{P}$  NMR spectrum of **5** in  $\text{CD}_2\text{Cl}_2$  at room temperature and assignment of the spin system (right).

Table S 8: Coupling constants (left) and chemical shifts (right) of **5** in  $\text{CD}_2\text{Cl}_2$  solution obtained from spectral simulation of the respective  $^{31}\text{P}$  NMR spectrum.

$J/\text{Hz}$	$\delta/\text{ppm}$
$^1J_{\text{PA}-\text{PX}/\text{X}'}$	$\text{P}^{\text{A}}$ 156.2
$^1J_{\text{PM}/\text{M}'-\text{PX}/\text{X}'}$	$\text{P}^{\text{M}/\text{M}'}$ 115.0
$^1J_{\text{PM}-\text{PM}'}$	$\text{P}^{\text{X}/\text{X}'}$ 77.0
$^2J_{\text{PM}/\text{M}'-\text{PX}/\text{X}'}$	
$^2J_{\text{PA}-\text{PM}/\text{M}'}$	
$^2J_{\text{PX}-\text{X}'}$	
$^2J_{\text{PA}-\text{H}}$	

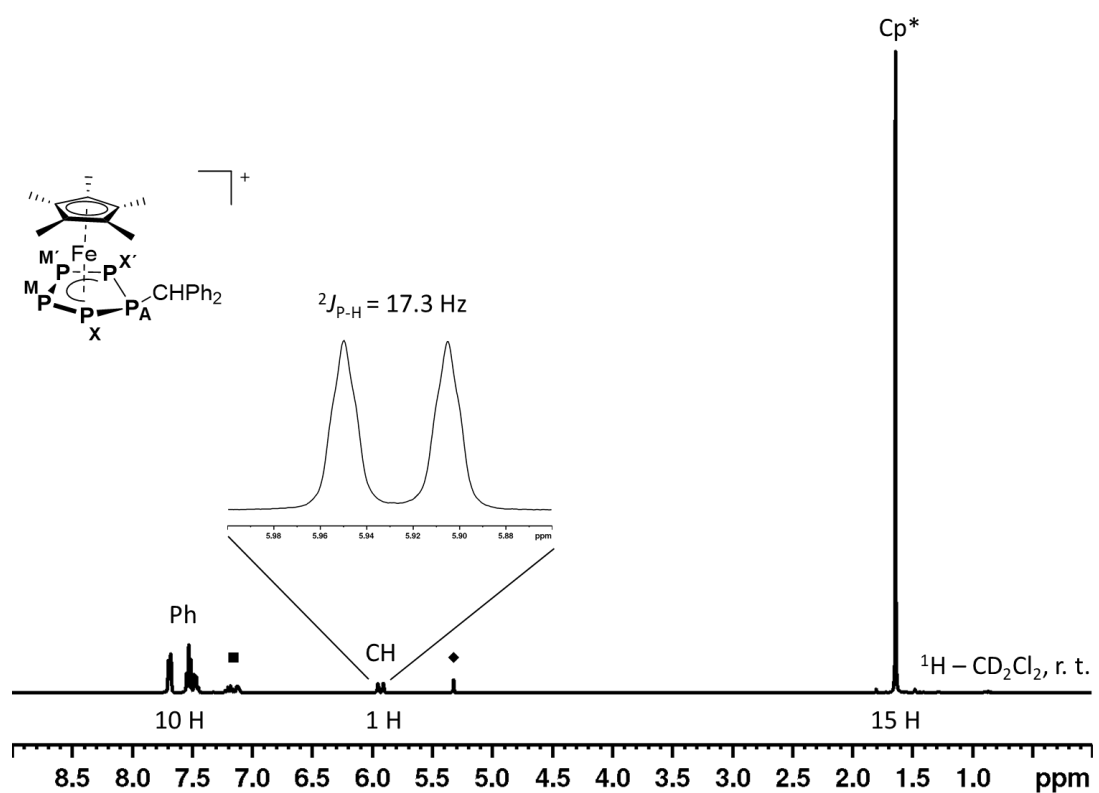


Figure S 22:  $^1\text{H}$  NMR spectrum of **5** in  $\text{CD}_2\text{Cl}_2$  at room temperature;  $\blacklozenge$  marks the residual solvent signal for  $\text{CD}_2\text{Cl}_2$ ,  $\blacksquare$  marks the signal for residual o-DFB.

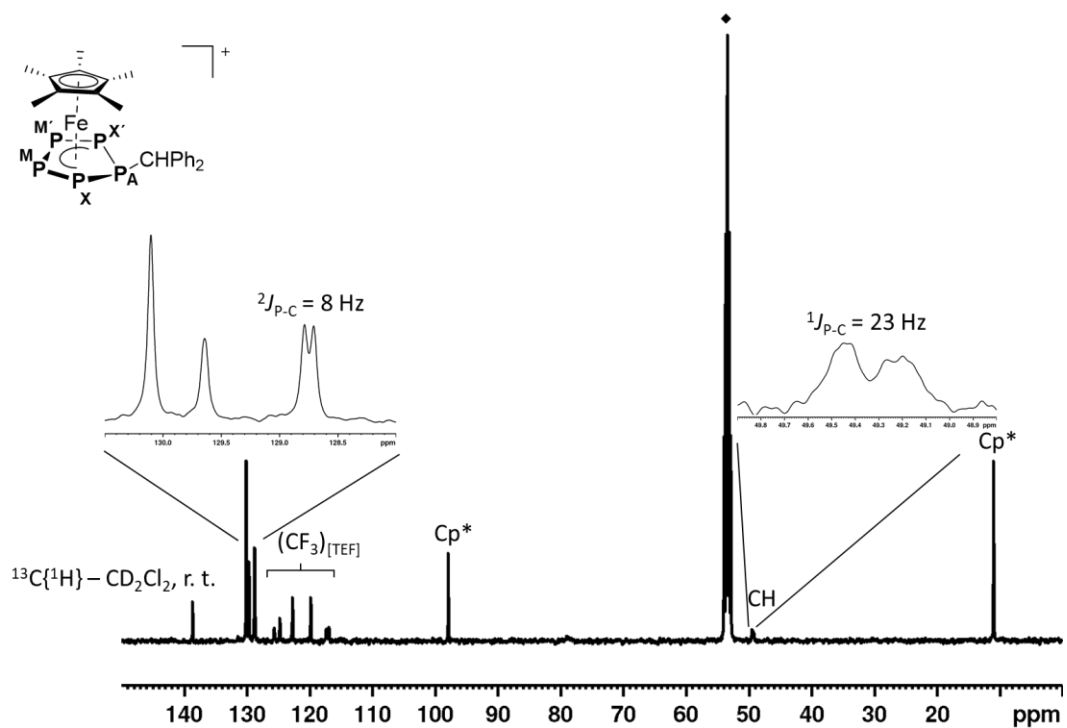


Figure S 23:  $^{13}\text{C}\{^1\text{H}\}$  NMR spectrum of **5** in  $\text{CD}_2\text{Cl}_2$  at room temperature;  $\blacklozenge$  marks the residual solvent signal for  $\text{CD}_2\text{Cl}_2$ .

### 3.5. $[\text{Cp}^*\text{Fe}(\eta^5\text{-P}_5\text{SiHPh}_2)]\text{[B(C}_6\text{F}_5)_4]$ (6)

While **6** is well soluble in *o*-DFB, its  $^{31}\text{P}$  NMR spectrum at room temperature reveals significant dynamic behaviour as indicated by the presence of three broad signals at  $\delta = 76.4, 102.6$  and  $141.1$  ppm. However, even cooling a sample of **6** in  $\text{CD}_2\text{Cl}_2$  to  $-80^\circ\text{C}$  does not resolve this dynamic behaviour and additionally leads to partial degradation by the solvent. The product of this degradation may be formulated as  $[\text{Cp}^*\text{Fe}(\eta^5\text{-P}_5\text{CH}_2\text{Cl})]^+$  due to the similarity of its  $^{31}\text{P}\{\text{H}\}$  NMR spectrum with that of  $[\text{Cp}^*\text{Fe}(\eta^5\text{-P}_5\text{Me})]^+$ .<sup>15</sup> Thus, obtaining a well resolved spectrum of **6** cannot be achieved and no coupling information could be extracted from its  $^{31}\text{P}$  and  $^{31}\text{P}\{\text{H}\}$  spectra. Peak assignment is still possible by comparison of the peak shape with similar compounds reported herein. In contrast, the  $^{29}\text{Si}(\text{DEPT135})$  spectrum of **6** in  $\text{CD}_2\text{Cl}_2$  recorded at  $-30^\circ\text{C}$  shows a doublet of multiplets ( $^1\text{J}_{\text{Si-P}} = 239$  Hz) at  $-20$  ppm manifesting its integrity (although dynamic) in solution.

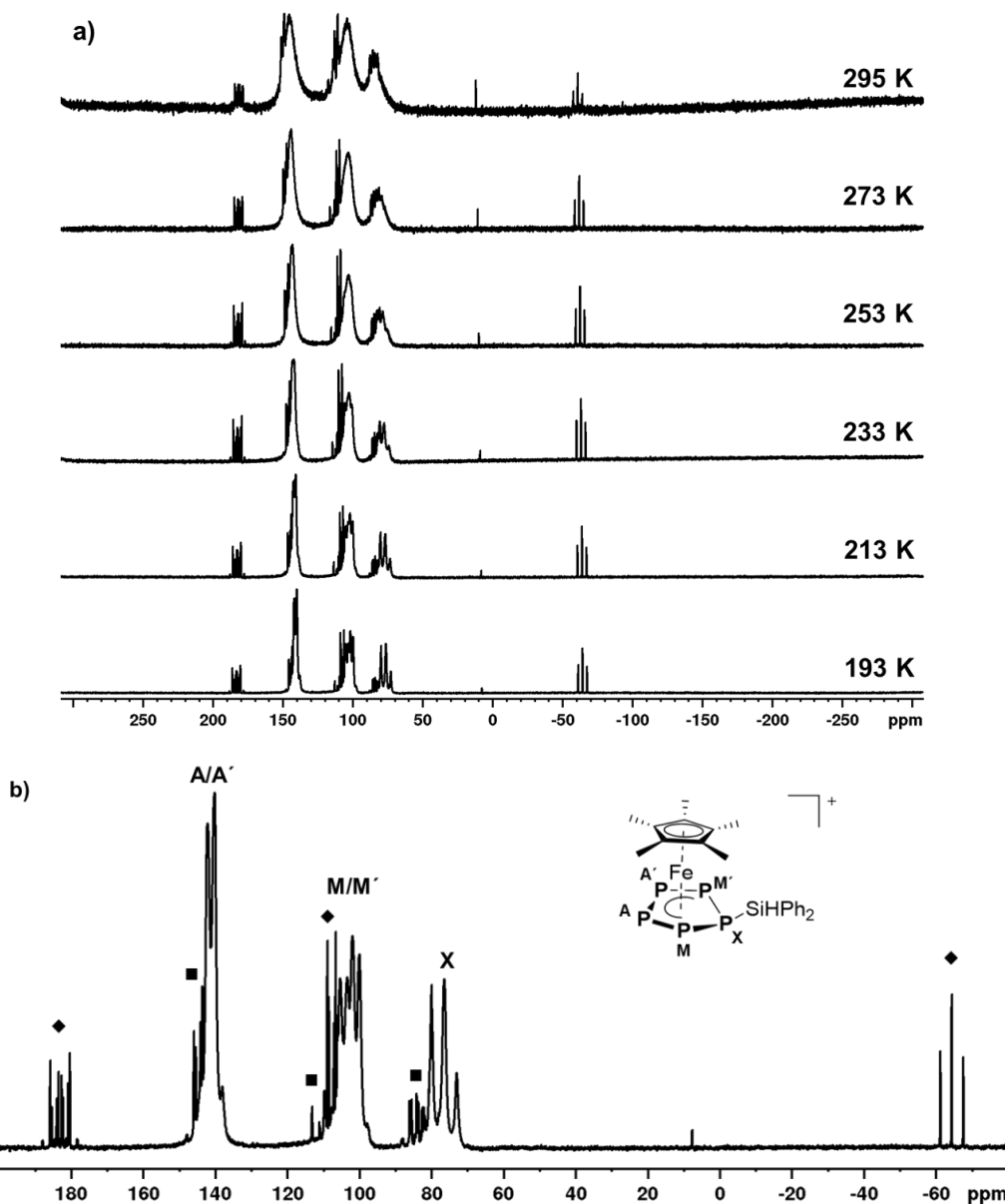


Figure S 24: a)  $^{31}\text{P}\{\text{H}\}$  NMR spectra of **6** in  $\text{CD}_2\text{Cl}_2$  recorded at indicated temperatures, revealing its dynamic behaviour in solution (even at  $-80^\circ\text{C}$ ); b)  $^{31}\text{P}\{\text{H}\}$  NMR spectrum of **6** in  $\text{CD}_2\text{Cl}_2$  at  $-80^\circ\text{C}$  with assignment of the spin system; ♦ marks the signals for  $[\text{Cp}^*\text{Fe}(\eta^5\text{-P}_5\text{H})]^+$ , which is formed in the presence of traces of moisture (< 3 ppm in solvents and on glass surfaces), ■ marks a group of signals, which is assigned to  $[\text{Cp}^*\text{Fe}(\eta^5\text{-P}_5\text{CH}_2\text{Cl})]^+$  arising from degradation of **6** in  $\text{CD}_2\text{Cl}_2$ .

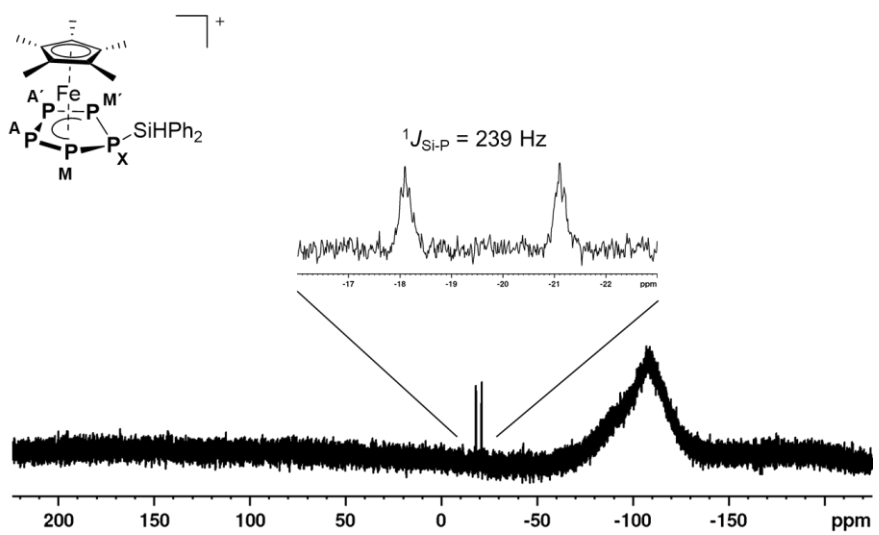


Figure S 25:  $^{29}\text{Si}$ (DEPT135) NMR spectrum of **6** in  $\text{CD}_2\text{Cl}_2$  recorded at  $-30^\circ\text{C}$  with 4096 scans.

### 3.6. $[\text{Cp}^*\text{Fe}(\eta^5\text{-P}_5\text{AsCy}_2)][\text{TEF}]$ (7)

The  $^1\text{H}$  NMR spectrum of **7** in  $\text{CD}_2\text{Cl}_2$  shows a signal at  $\delta = 1.62$  ppm for the  $\text{Cp}^*$  ligand and multiple broad signals in between  $\delta = 1.34\text{-}2.94$  for the Cy groups. The corresponding  $^{31}\text{P}$  NMR spectrum reveals a complex AA'BB'X spin system with slight line broadening. Cooling the sample to 273 K leads to an even better resolved  $^{31}\text{P}$  NMR spectrum (Figure S 26, chemical shifts and coupling constants provided in Table S 9), which agrees with the molecular structure of **7**.

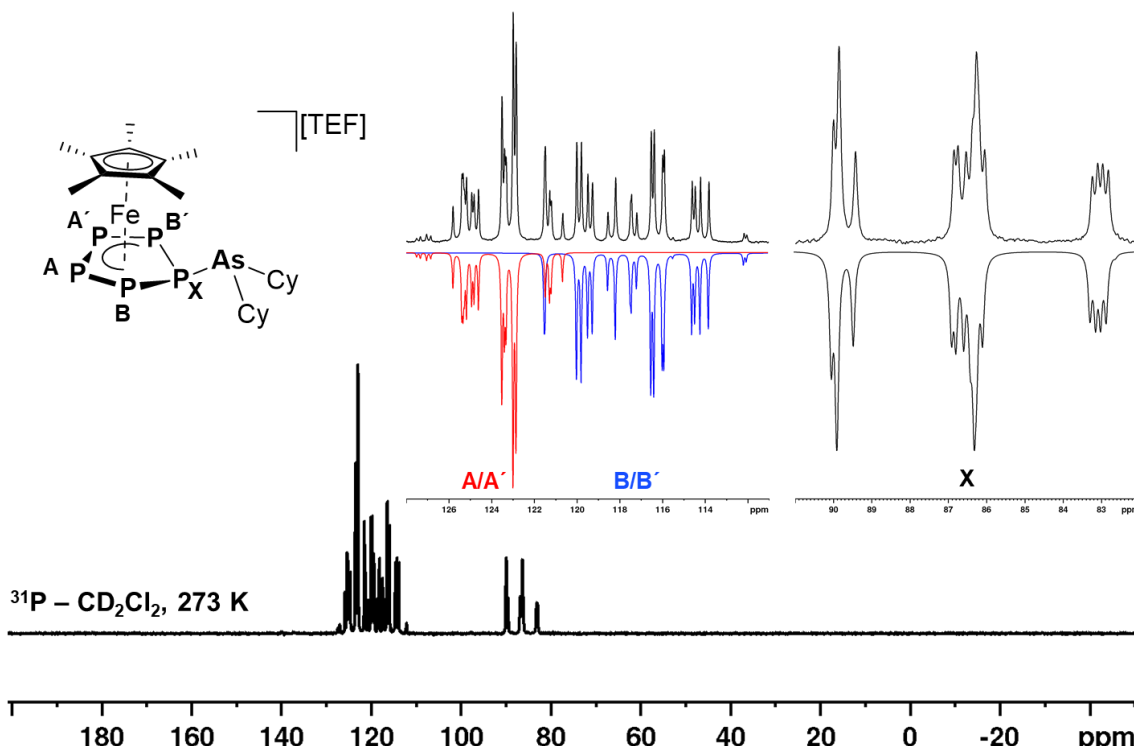


Figure S 26: Experimental (top) and simulated (bottom)  $^{31}\text{P}$  NMR spectrum of **7** in  $\text{CD}_2\text{Cl}_2$  at 273 K and assignment of the spin system (top left).

Table S 9: Coupling constants (left) and chemical shifts (right) of **7** in  $\text{CD}_2\text{Cl}_2$  solution obtained from spectral simulation of the respective  $^{31}\text{P}$  NMR spectrum.

$J$ / Hz		$\delta$ / ppm
$^1J_{\text{PX-PB/B}'}$	576.0/574.5	$\text{P}^{\text{A}/\text{A}'}$ 123.9
$^1J_{\text{PA/A'-PB/B}'}$	432.9/430.0	$\text{P}^{\text{B}/\text{B}'}$ 117.1
$^1J_{\text{PA-PA}'}$	420.1	$\text{P}^{\text{X}}$ 86.6
$^2J_{\text{PA/A'-PB/B}'}$	-52.0/-50.5	
$^2J_{\text{PX-PA/A}'}$	10.2/3.8	
$^2J_{\text{PB-B}'}$	22.2	

### 3.7. [{Cp\*Fe( $\mu$ , $\eta^{5:2}$ -P<sub>5</sub>)}SbICp''] [TEF] (8)

While the <sup>1</sup>H NMR spectrum of **8** in CD<sub>2</sub>Cl<sub>2</sub> recorded at room temperature reveals the signals for the respective Cp\* and Cp'' groups, the respective <sup>31</sup>P NMR spectrum only shows a singlet at  $\delta$  = 164.7 ppm. We thus carried out a VT NMR study (Figure S 27) on **8**, but even at -80°C the signal, now located at  $\delta$  = 172.9 ppm, does not show any splitting. This highlights the extreme dynamic behaviour of **8** in solution.

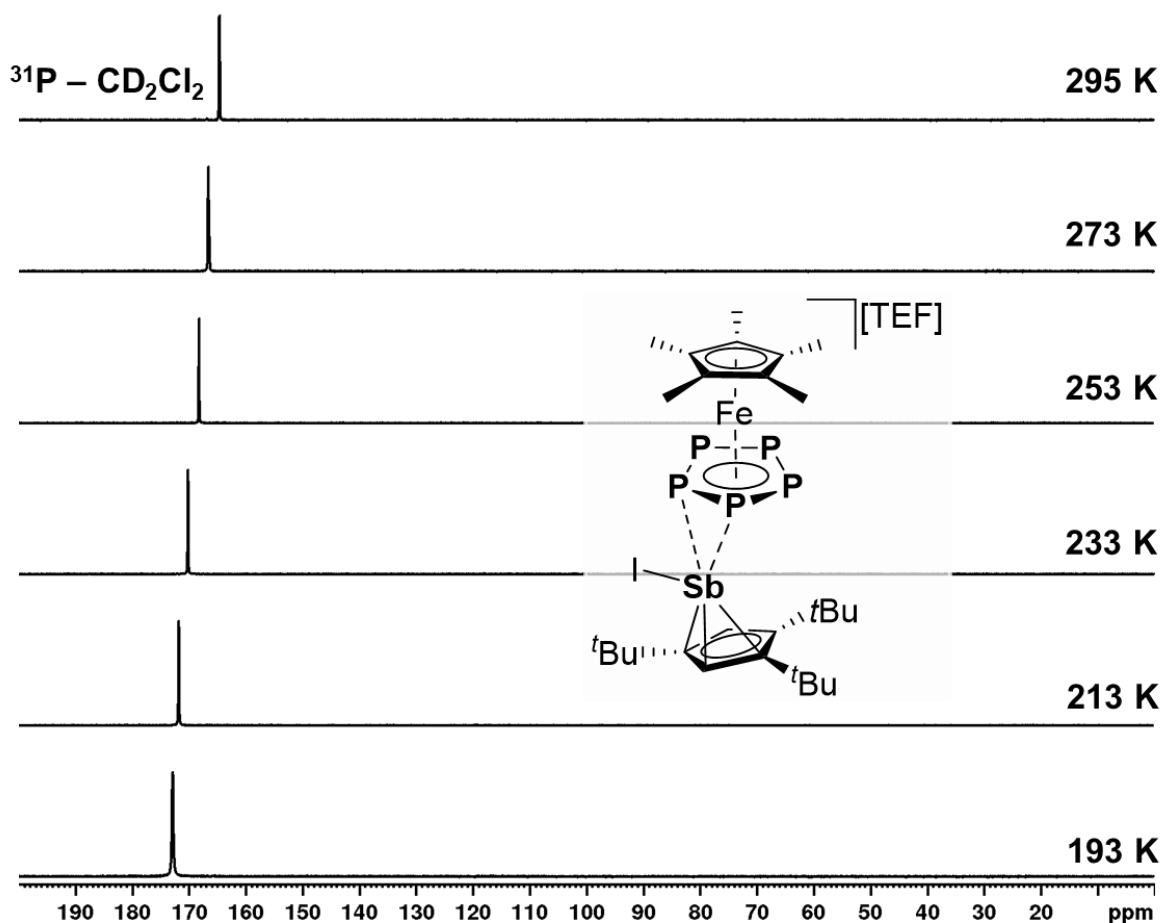


Figure S 27: <sup>31</sup>P NMR spectra of **8** in CD<sub>2</sub>Cl<sub>2</sub> at specified temperatures.

### 3.8. $[\text{Cp}^*\text{Fe}(\eta^5\text{-P}_5\text{SePh})]\text{[TEF]} (9)$

The  $^1\text{H}$  NMR spectrum of **9** in  $\text{CD}_2\text{Cl}_2$  at room temperature shows the expected signals for the  $\text{Cp}^*$  ligand and the Ph group at  $\delta = 1.75$  and 7.47-7.90 ppm, respectively. The corresponding  $^{31}\text{P}$  NMR spectrum (Figure S 28) reveals an AA'MM'X spin system (chemical shifts and coupling constants provided in Table S 10), in which the  $\text{P}^X$  signal has additional  $^{77}\text{Se}$  satellites with a  $^1\text{J}_{\text{P-Se}} = 418$  Hz coupling constant. This coupling constant is corroborated by the  $^{77}\text{Se}\{^1\text{H}\}$  NMR spectrum (Figure S 29) of **9** in  $\text{CD}_2\text{Cl}_2$  solution, which shows a doublet at  $\delta = 287.3$  ppm.

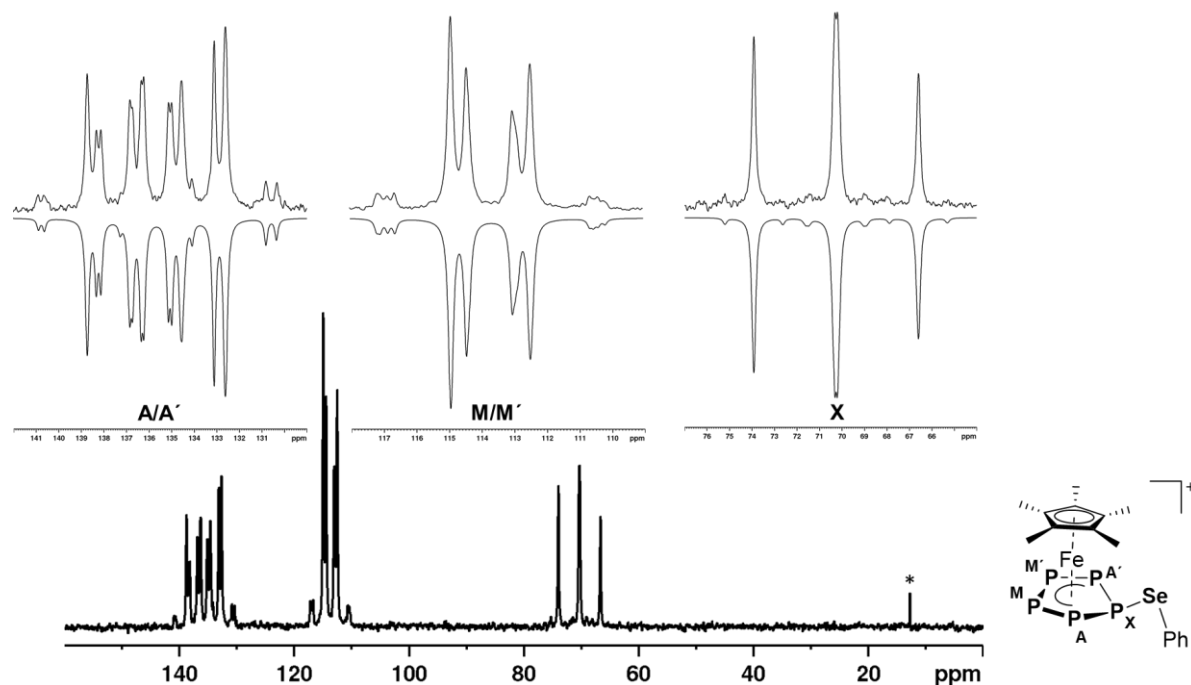


Figure S 28: Experimental (top) and simulated (bottom)  $^{31}\text{P}$  NMR spectrum of **9** in  $\text{CD}_2\text{Cl}_2$  at room temperature and assignment of the spin system (right); \* marks the signal for trace impurities of an unidentified species.

Table S 10: Coupling constants (left) and chemical shifts (right) of **9** in  $\text{CD}_2\text{Cl}_2$  solution obtained from spectral simulation of the respective  $^{31}\text{P}$  NMR spectrum.

$J$ / Hz	$\delta$ / ppm
$^1\text{J}_{\text{PA/A}'\text{-PX}}$	596.9/595.4
$^1\text{J}_{\text{PA/A}'\text{-PM/M}'}$	448.4/441.1
$^1\text{J}_{\text{PM-PM}'}$	413.3
$^2\text{J}_{\text{PA/A}'\text{-PM'/M}}$	-54.2/-48.3
$^2\text{J}_{\text{PM/M}'\text{-PX}}$	7.8/2.4
$^2\text{J}_{\text{PA-A}'}$	37.3
$^1\text{J}_{\text{PX-Se}}$	418

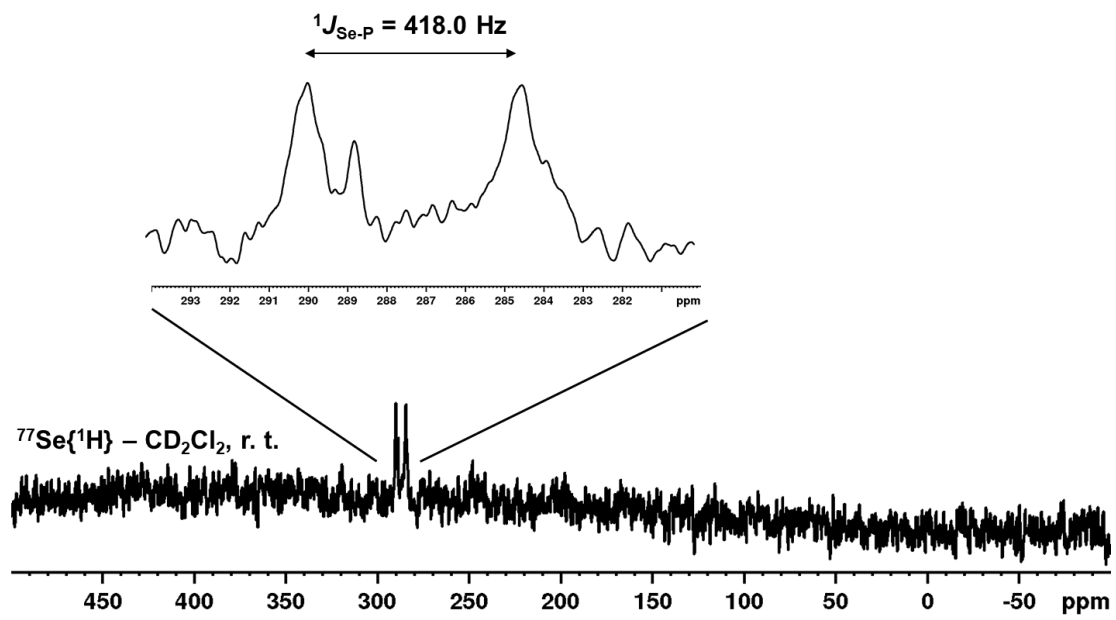


Figure S 29:  ${}^{77}\text{Se}\{{}^1\text{H}\}$  NMR spectrum of **9** in  $\text{CD}_2\text{Cl}_2$  recorded at room temperature with 11000 scans and a dwell time of 6.6 s.

### 3.9. $[\text{Cp}^*\text{Fe}(\eta^5\text{-P}_5\text{TeMes})]\text{[TEF]} (10)$

While **10** is well soluble in *o*-DFB, its  $^{31}\text{P}$  NMR spectrum at room temperature reveals significant dynamic behaviour as indicated by the presence of one extremely broadened signal at  $\delta = 126.3$  ppm. Cooling a sample of **10** in  $\text{CD}_2\text{Cl}_2$  to  $-80^\circ\text{C}$  leads to splitting into three signals located at  $\delta = 10.0, 124.9$  and  $139.3$  ppm but also to partial degradation. Thus, obtaining a well resolved spectrum of **10** cannot be achieved and no coupling information could be extracted from its  $^{31}\text{P}$  and  $^{31}\text{P}\{^1\text{H}\}$  spectra.

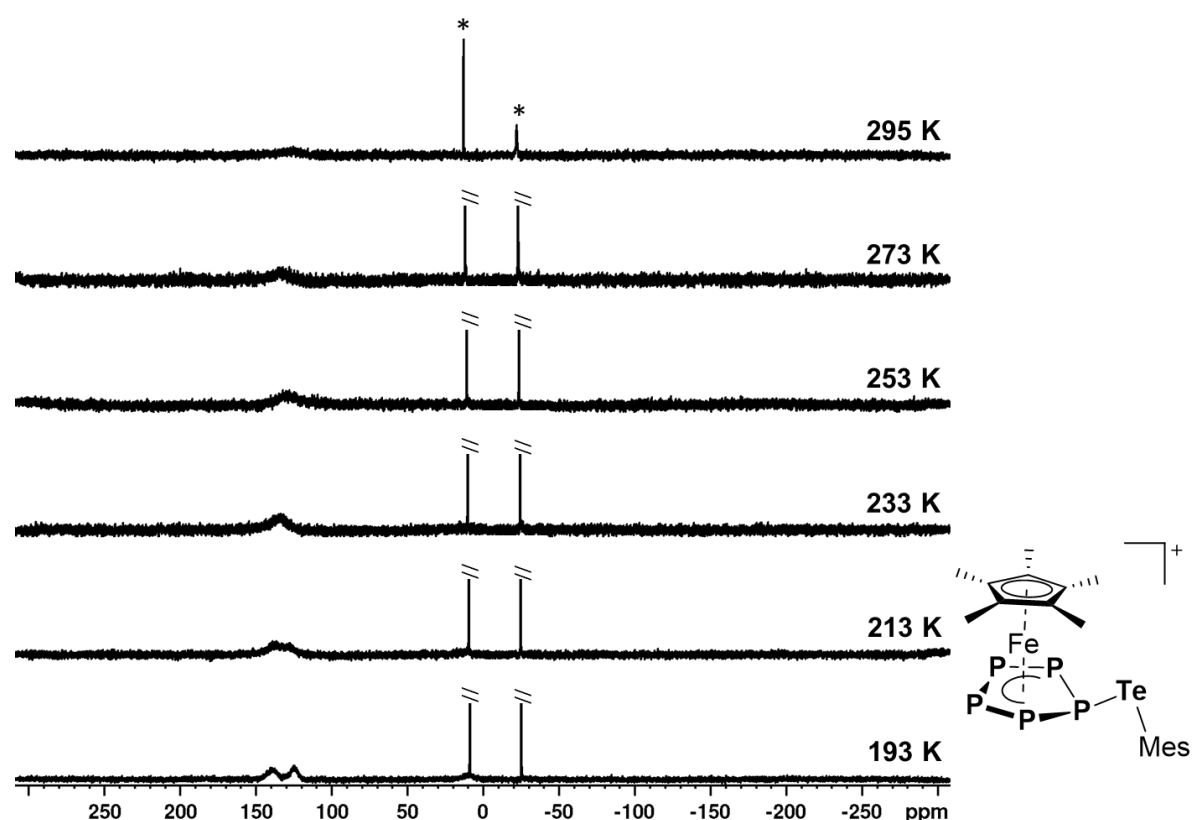


Figure S 30:  $^{31}\text{P}\{^1\text{H}\}$  NMR spectra of **10** in  $\text{CD}_2\text{Cl}_2$  recorded at specified temperatures \* marks the signals for trace impurities of two unidentified species arising from degradation of **10**.

### 3.10. $[\text{Cp}^*\text{Fe}(\eta^5\text{-P}_5\text{Cl})]\text{[TEF]} (11)$

As compound **11** is well soluble in  $\text{CD}_2\text{Cl}_2$ , its NMR spectra can easily be recorded. Its  $^1\text{H}$  NMR spectrum recorded at room temperature only reveals one singlet for the  $\text{Cp}^*$  ligand at  $\delta = 1.73$  ppm. The respective  $^{31}\text{P}$  NMR spectrum (Figure S 31) shows an AA'MXX' spin system (chemical shifts and coupling constants provided in Table S 11), manifesting the structure of **11** in solution.

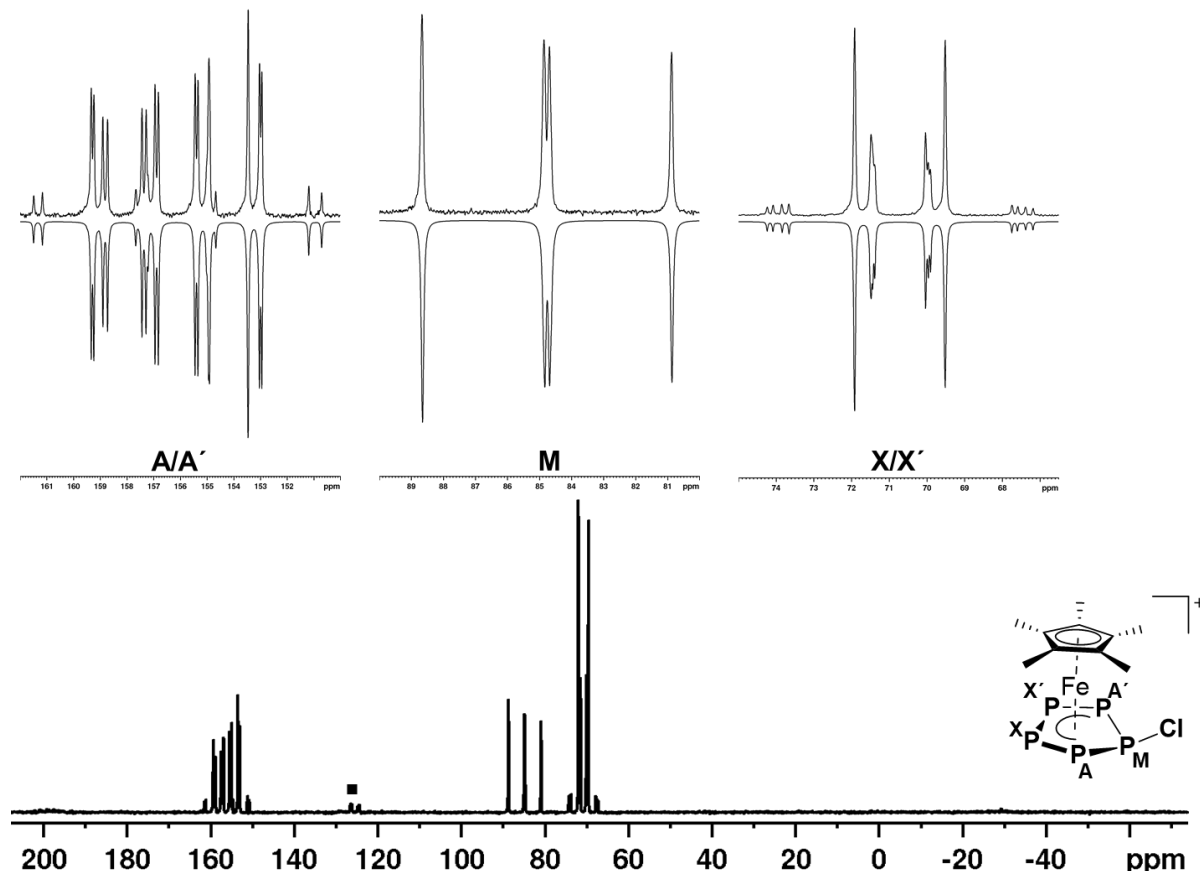


Figure S 31: Experimental (top) and simulated (bottom)  $^{31}\text{P}$  NMR spectrum of **11** in  $\text{CD}_2\text{Cl}_2$  at room temperature and assignment of the spin system (right); ■ marks a signal for trace impurities of  $[(\text{Cp}^*\text{Fe})_2(\mu,\eta^{5,5}\text{-P}_{10})]^+$ .

Table S 11: Coupling constants (left) and chemical shifts (right) of **11** in  $\text{CD}_2\text{Cl}_2$  solution obtained from spectral simulation of the respective  $^{31}\text{P}$  NMR spectrum.

$J/\text{Hz}$		$\delta/\text{ppm}$
$^1J_{\text{PA/A}'\text{-PM}}$	637.3/626.9	$\text{P}^{\text{A/A}'}$ 156.6
$^1J_{\text{PA/A}'\text{-PX/X}'}$	461.8/426.0	$\text{P}^{\text{M}}$ 84.9
$^1J_{\text{PX-PX}'}$	406.2	$\text{P}^{\text{X/X}'}$ 70.7
$^2J_{\text{PA/A}'\text{-PX/X}}$	-71.2/-37.6	
$^2J_{\text{PM-PX/X}'}$	6.1/2.0	
$^2J_{\text{PA-A}'}$	41.7	

### 3.11. $[\text{Cp}^*\text{Fe}(\eta^5\text{-P}_5\text{Br})]\text{[TEF]} (12)$

Compound **12** is well soluble in  $\text{CD}_2\text{Cl}_2$ , its NMR spectra can easily be recorded. Its  $^1\text{H}$  NMR spectrum recorded at room temperature only reveals one singlet for the  $\text{Cp}^*$  ligand at  $\delta = 1.73$  ppm. The respective  $^{31}\text{P}$  NMR spectrum (Figure S 32) shows an AA'MM'X spin system (chemical shifts and coupling constants provided in Table S 12), manifesting the structure of **12** in solution.

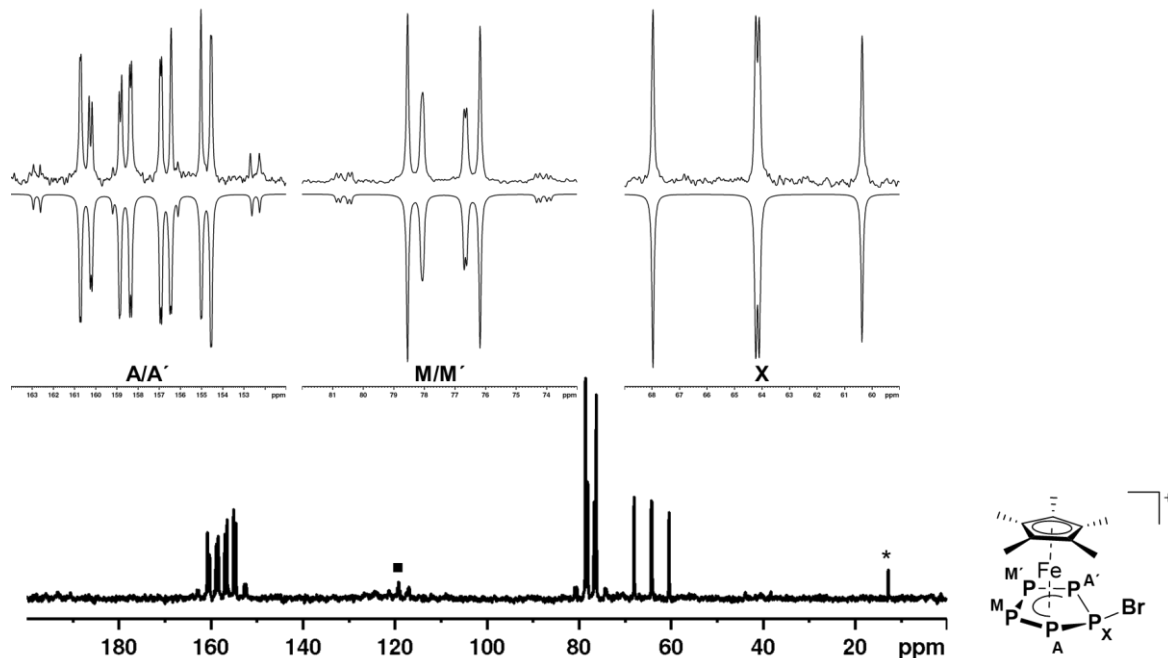


Figure S 32: Experimental (top) and simulated (bottom)  $^{31}\text{P}$  NMR spectrum of **12** in  $\text{CD}_2\text{Cl}_2$  at room temperature and assignment of the spin system (right); ■ marks a signal for trace impurities of  $[\{\text{Cp}^*\text{Fe}\}_2(\mu,\eta^{5:5}\text{-P}_{10})]^2+$ , and \* marks the signal for trace impurities of an unidentified species.

Table S 12: Coupling constants (left) and chemical shifts (right) of **12** in  $\text{CD}_2\text{Cl}_2$  solution obtained from spectral simulation of the respective  $^{31}\text{P}$  NMR spectrum.

$J/\text{Hz}$		$\delta/\text{ppm}$	
$^1J_{\text{PA}/\text{A}'\text{-PX}}$	616.4/615.2	$\text{P}^{\text{A}/\text{A}'}$	135.5
$^1J_{\text{PA}/\text{A}'\text{-PM/M}'}$	439.0/436.5	$\text{P}^{\text{M}/\text{M}'}$	113.8
$^1J_{\text{PM-PM}'}$	415.6	$\text{P}^{\text{X}}$	70.4
$^2J_{\text{PA}/\text{A}'\text{-PM'/M}}$	-58.0/-49.4		
$^2J_{\text{PM/M}'\text{-PX}}$	-1.8/-1.4		
$^2J_{\text{PA-A}'}$	34.4		

### 3.12. $[\text{Cp}^*\text{Fe}(\eta^5\text{-P}_5\text{I})][\text{TEF}]$ (13)

As compound **13** is well soluble in  $\text{CD}_2\text{Cl}_2$ , its NMR spectra can easily be recorded. Its  $^1\text{H}$  NMR spectrum recorded at room temperature only reveals one singlet for the  $\text{Cp}^*$  ligand at  $\delta = 1.67$  ppm. The respective  $^{31}\text{P}$  NMR spectrum however only shows a broad signal at room temperature. We thus carried out a VT NMR study (Figure S 33) on **13**, which revealed splitting of the signal upon cooling. However, the dynamic behaviour of **13** in solution is manifested in the persistent broadening of the observed signals, even at -80 °C. Assignment of the signals to certain P Atoms in **13** (Figure S 33, bottom right) has been carried out by comparison with the spectra of its lighter homologs **11** and **12**.

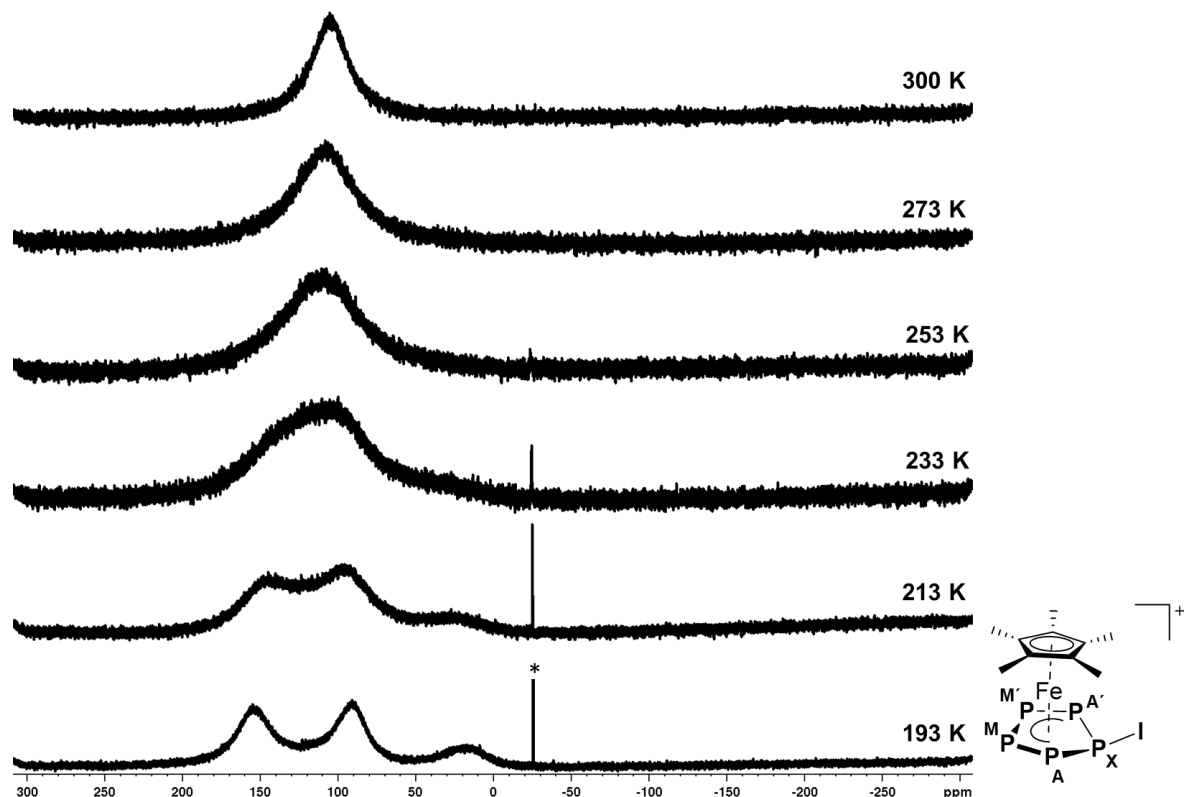


Figure S 33:  $^{31}\text{P}\{^1\text{H}\}$  NMR spectra of **13** in  $\text{CD}_2\text{Cl}_2$  recorded at specified temperatures and assignment of the spin system (bottom right); \* marks a signal for trace impurities of an unidentified species.

### 3.13. [{Cp'''}Ta(CO)<sub>2</sub>}<sub>2</sub>{μ,η<sup>4:4</sup>-((P<sub>4</sub>)<sub>2</sub>BBr<sub>2</sub>)}][TEF] (15)

As compound **15** is well soluble in CD<sub>2</sub>Cl<sub>2</sub>, its NMR spectra can easily be recorded. Its <sup>1</sup>H NMR spectrum recorded at room temperature reveals four signals at  $\delta$  = 1.12, 1.56, 6.33 and 6.34 ppm in agreement with the presence of two chemically equivalent (on the NMR time scale) Cp''' ligands. The <sup>31</sup>P NMR spectrum (Figure S 34) shows a complex A<sub>2</sub>A'₂MM'XX'Z spin system (chemical shift and coupling constants provided in Table S 13) and the <sup>11</sup>B{<sup>1</sup>H} NMR spectrum (Figure S 35) corroborates the <sup>1</sup>J<sub>B-PM/M'</sub> = 61 Hz coupling constant.

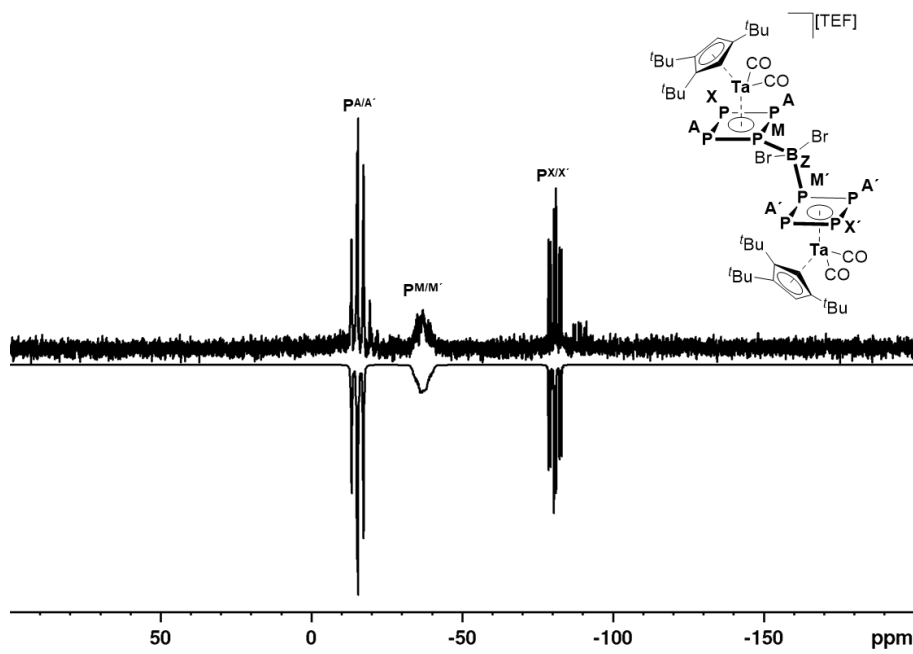


Figure S 34: Experimental (top) and simulated (bottom) <sup>31</sup>P NMR spectrum of **15** in CD<sub>2</sub>Cl<sub>2</sub> recorded at room temperature and assignment of the spin system according to the scheme on the right.

Table S 13: Coupling constants (left) and chemical shifts (right) of **15** in CD<sub>2</sub>Cl<sub>2</sub> solution obtained from spectral simulation of the respective <sup>31</sup>P NMR spectrum; Simulation was performed manually and thus coupling constants are provided without decimals.

$J$ / Hz	$\delta$ ppm
<sup>1</sup> J <sub>PA/A'-PM/M'</sub>	350
<sup>1</sup> J <sub>PA/A'-PX/X'</sub>	293
<sup>2</sup> J <sub>PM-PM'</sub>	120
<sup>2</sup> J <sub>PX/X'-PM/M'</sub>	117

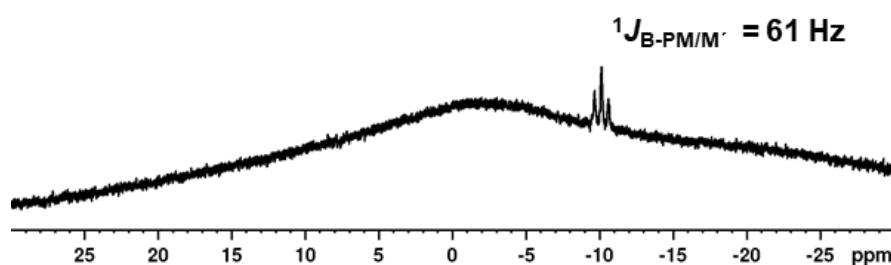


Figure S 35: <sup>11</sup>B{<sup>1</sup>H} NMR spectrum of **15** in CD<sub>2</sub>Cl<sub>2</sub> recorded at room temperature.

### 3.14. Additional Data

When **1** (0.2 mmol, 70 mg, 1 eq.) is reacted with equimolar amounts of  $\text{BBr}_3$  (0.2 mmol, 19  $\mu\text{L}$ , 1 eq.) and  $\text{Ti}[\text{TEF}]$  (0.2 mmol, 234 mg, 1 eq.) in *o*-DFB at room temperature, two products can be observed in the  $^{31}\text{P}\{\text{H}\}$  NMR spectrum (Figure S 36) of the crude reaction mixture. While one of them can clearly be identified as compound **2**, the major product is the protonated species  $[\text{Cp}^*\text{Fe}(\eta^5\text{-P}_5\text{H})]^+$ ,<sup>15</sup> which we hypothesize to be formed from the reaction of excess borinium species  $[\text{BBr}_2]^+$  with the solvent *o*-DFB.

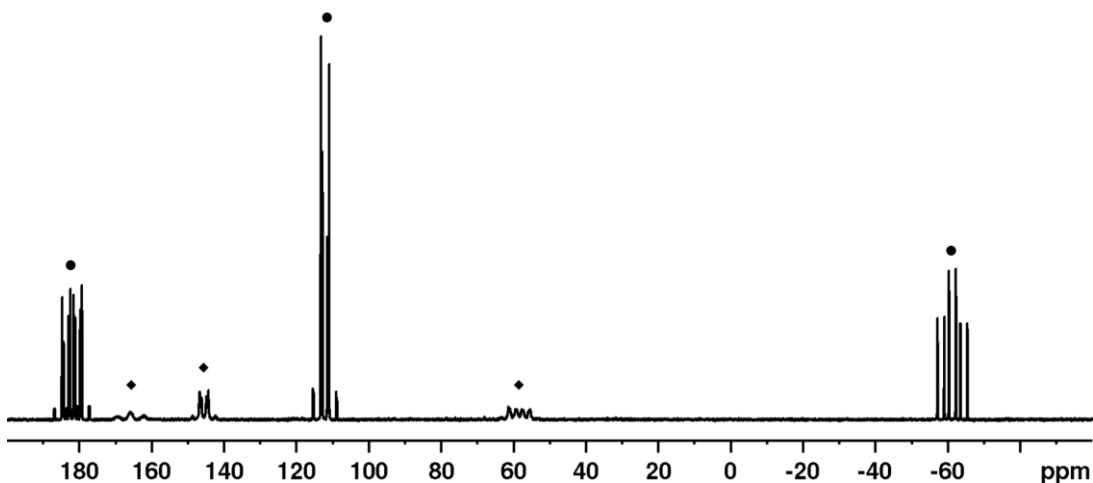


Figure S 36:  $^{31}\text{P}$  NMR spectrum of the crude mixture of **1**,  $\text{BBr}_3$  and  $\text{Ti}[\text{TEF}]$  in *o*-DFB; ♦ marks the signals for compound **2** and ● marks those assigned to the protonated species  $[\text{Cp}^*\text{Fe}(\eta^5\text{-P}_5\text{H})]^+$ .

Attempts to functionalize  $[\text{Cp}^*\text{Fe}(\eta^5\text{-P}_5)]$  (**1**) with *in situ* generated phosphonium ions suffer from the high tendency of phosphinophosphonium ion ( $(\text{R}_2\text{P}-\text{P}(\text{Cl})\text{R}_2)^+$ ) formation upon exposing Chlorophosphanes ( $\text{R}_2\text{PCl}$ , R = Aryl, Alkyl) to Lewis acidic conditions.<sup>16</sup> As this behavior can be attributed to the high (compared to e. g. the respective Chloroarsines) Lewis basicity of most Chlorophosphanes, we thought  $\text{PBr}_3$  could be a suitable phosphonium ion precursor for the functionalization of **1**. Indeed, the desired product  $[\text{Cp}^*\text{Fe}(\eta^5\text{-P}_5\text{PBr}_2)]^+$  can be detected NMR spectroscopically (Figure S 37) in mixtures of **1**,  $\text{PBr}_3$  and  $\text{Ti}[\text{TEF}]$  in  $\text{CD}_2\text{Cl}_2$ , which are cooled to -80 °C (already after ~10min, the reaction seems to be nearly complete). However, this compound appears to be highly unstable in solution and decomposes above -60 °C, prohibiting its isolation and further characterization. When the sample is allowed to warm from -80 °C to room temperature over the course of 6 h, this decomposition process can be monitored (Figure S 38), revealing  $[\text{Cp}^*\text{Fe}(\eta^5\text{-P}_5\text{Br})]\text{[TEF]}$  (**12**) as the major product of this decomposition. However, formation of several other P-containing (and probably ionic) products is visible. Despite various attempts, separation of this product mixture was not possible.

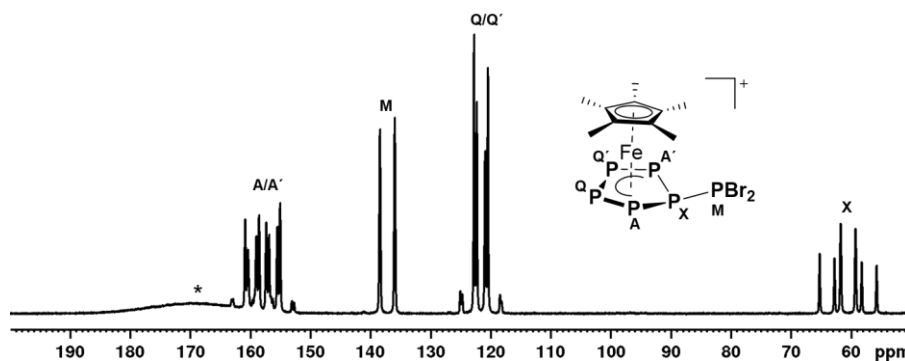


Figure S 37:  $^{31}\text{P}\{^1\text{H}\}$  NMR spectrum of the reaction mixture containing **1**,  $\text{PBr}_3$  and  $\text{Ti}[\text{TEF}]$  (1:1:1) in  $\text{CD}_2\text{Cl}_2$  recorded at 193 K and signal assignment; \* marks the broad signal for **1**, which coordinates to  $\text{Ti}^+$  in solution.

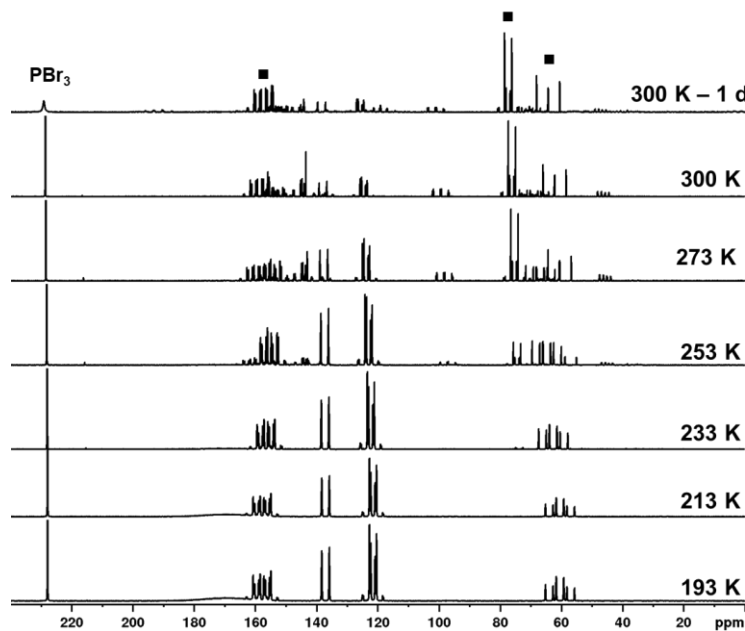


Figure S 38:  $^{31}\text{P}\{^1\text{H}\}$  NMR spectra of the 1:1:1 mixture of **1**,  $\text{PBr}_3$  and  $\text{Ti}[\text{TEF}]$  in  $\text{CD}_2\text{Cl}_2$  recorded at different temperatures and times (right); ■ marks the group of signals assigned to **12**.

Comparison of the  $^{31}\text{P}$  NMR spectra of the obtained pentaphosphole complexes reveals a periodic trend (Figure S 39) according to which, the signal assigned to P1 is shifted upfield with the main group of the central atom of the electrophile. Similarly, the signal assigned to P2/3 is shifted downfield in the same

order. Note that compounds **3**, **6**, **8** and **10** are not included in this consideration, as they do not show well resolved  $^{31}\text{P}$  NMR spectra at room temperature.

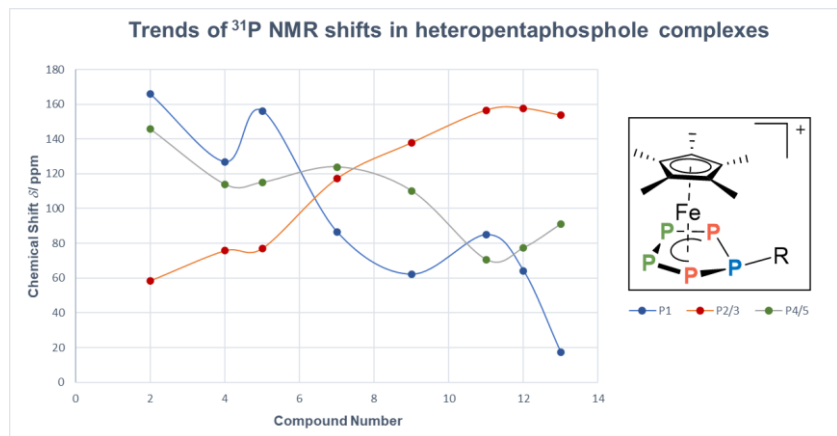


Figure S 39:  $^{31}\text{P}$  Chemical shifts within the pentaphosphole complexes **2**, **4**, **5**, **7**, **9** and **11 – 13** showing a significant upfield shift for P1, while the signal for P2/3 experiences a downfield shift; Spectra of all other pentaphospholes complexes reported herein are not considered as they do not show resolved  $^{31}\text{P}$  NMR spectra at room temperature.

Comparison of the above shown NMR spectroscopic data to structural parameters of the respective compounds reveals a very similar periodic trend for the pyramidalization at the P1 atom (which also represents the folding angle of the envelope cyclo- $\text{P}_5$  structure, Figure S 40). Both, data from X-ray structural analysis (blue) and computational data (red) show an increase of the pyramidalization at the P1 atom, where the computational data slightly overestimates the experimentally derived values. This may suggest a dependency of the  $^{31}\text{P}$  NMR chemical shifts within the studied pentaphosphole complexes on the observed pyramidalization at P1.

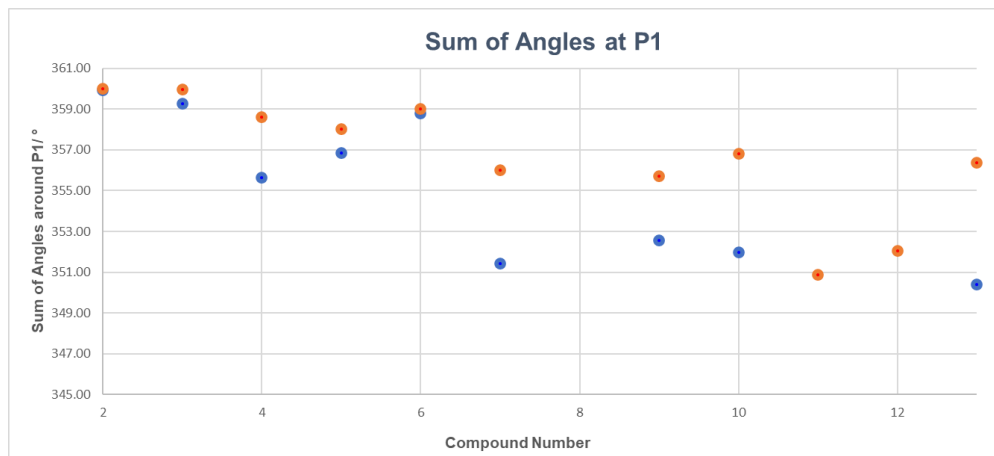


Figure S 40: Summed up  $\alpha(P_2-P_1-E)$ ,  $\alpha(P_5-P_1-E)$  and  $\alpha(P_2-P_1-P_1)$  angles around P1 decreasing with the main group of the central atom of the electrophile determined from Xray crystallographic data (blue) and from the computationally optimized structures (vide infra, red).

## 4. Computational Details

### 4.1. General remarks

DFT calculations were performed using the Gaussian09 software package.<sup>17</sup> Geometry optimizations were performed at the B3LYP<sup>18</sup>/def2-TZVP<sup>19</sup> (or B3LYP<sup>18</sup>/def2-SVP<sup>19</sup> for compounds **14** and **15**) level of theory with PCM solvent correction for CH<sub>2</sub>Cl<sub>2</sub>.<sup>20</sup> Stationary points were verified by analytical frequency calculations. Magnetic shielding tensors were calculated using the PBE0<sup>21</sup> functional and the basis sets aug-pcSseg-1<sup>22</sup> (for P) and def2-TZVPPD<sup>19,23</sup> (all other atoms). Ring critical points were derived using MultiWFN.<sup>24</sup> Charge decomposition analysis (CDA)<sup>25</sup> was also performed utilizing MultiWFN.<sup>24</sup> The basis sets def2-TZVPPD<sup>19,23</sup> and aug-pcSseg-1<sup>22</sup> were generated with the help of the open access “basis set exchange” web page.<sup>26</sup>

### 4.2. NBO Analyses

NBO analysis was performed on the pre-optimized (B3LYP<sup>18</sup>/def2-TZVP,<sup>19</sup> PCM solvent correction for CH<sub>2</sub>Cl<sub>2</sub>)<sup>20</sup> molecular structures of **2 – 15** using the NBO6.0 software package<sup>27</sup> and its implementation in Gaussian09.<sup>17</sup> Wiberg bond indices (WBI, Table S 14) for the respective P1-E and P1-Fe bonds have also been obtained from these calculations. These WBIs suggest covalent P1-E single bonds for most of the obtained pentaphosphole complexes. However, the WBIs for the P1-Ga and P1-Si bonds in **3** and **6**, respectively, suggest weaker and more polar bonds in these cases. The more expressed bond polarity in these cases is also expressed by the orbital contributions (from P1 and the central atom of the electrophile) to the respective bonding NBO. The P1-E bond lengths determined in the solid state are generally well reproduced by our calculations. However, the closest P-Sb contact in **8** is highly overestimated and no orbital interaction between both fragments could be found. Thus, the structure of **8** seems to mostly depend on electrostatic and dispersive interactions, which is also indicated by its highly dynamic behaviour in solution (*vide supra*). Analysing the natural charges within **2 – 13** reveals a clear trend (Figure S 41) for the charge accumulation at the fragment {1} and the respective electrophile fragment {E} upon formation of the pentaphosphole complex. Thus, charge transfer, computed via extended charge decomposition analysis (ECDA),<sup>25</sup> increases, the higher the electronegativity (Allred/Rochow) of the central atom of the electrophile is (Figure S 42). Again, **8** does not follow this trend, which we attribute to its significantly different molecular structure. Furthermore, the charge transfer in **2** and **3** is more expressed, as the positive charge can be distributed across two units of {1}.

*Table S 14: Selected computational and experimental parameters for the pentaphosphole complexes **2 – 7** and **9 – 13**:<sup>a)</sup> As **2** and **3** are dinuclear complexes the average of the actual values is provided for clarity; <sup>b)</sup> The charge transfer from fragment {1} to the respective fragments {E} is obtained by ECDA; <sup>c)</sup> The cations in **2** and **3** were dissected into two fragments (Fragment 1 = 2\*{1}, Fragment 2 = {EX<sub>2</sub>}<sup>+</sup>) for ECDA and the value in brackets is simply the charge transfer per {1} unit.*

Compound	WBI (P1-E)	Orbital contribution P1-E to σ(P1-E) NBO	d(P1-E)/ Å		Σcharge		Charge Transfer {1}→{E} <sup>b)</sup>
			Exp.	Theo.	{1}	{E}	
<b>2</b>	0.89 <sup>a)</sup>	57/43 <sup>a)</sup>	1.985(7) <sup>a)</sup>	2.01 <sup>a)</sup>	0.79 <sup>a)</sup>	-0.58 <sup>a)</sup>	1.13(0.57) <sup>c)</sup>
<b>3</b>	0.58 <sup>a)</sup>	79/21 <sup>a)</sup>	2.399(1) <sup>a)</sup>	2.46 <sup>a)</sup>	0.43 <sup>a)</sup>	0.14 <sup>a)</sup>	1.11(0.56) <sup>c)</sup>
<b>4</b>	0.92	45/55	1.853(4)	1.86	1.09	-0.09	0.85
<b>5</b>	0.88	45/55	1.866(4)	1.89	1.09	-0.09	0.84
<b>6</b>	0.72	72/28	2.3053(8)	2.35	0.57	0.43	0.68
<b>7</b>	0.82	67/33	2.348(1)	2.38	0.63	0.37	0.63
<b>8</b>	-	-	3.236(2)	4.53	0.01	0.99	0.02
<b>9</b>	0.98	53/47	2.2234(7)	2.25	0.84	0.16	0.83
<b>10</b>	0.92	62/38	2.438(2)	2.48	0.67	0.33	0.74
<b>11</b>	0.96	36/64	-	2.03	1.17	-0.17	1.09
<b>12</b>	0.98	41/59	-	2.21	1.06	-0.06	1.05
<b>13</b>	0.99	51/49	2.385(1)	2.42	0.89	0.11	0.94

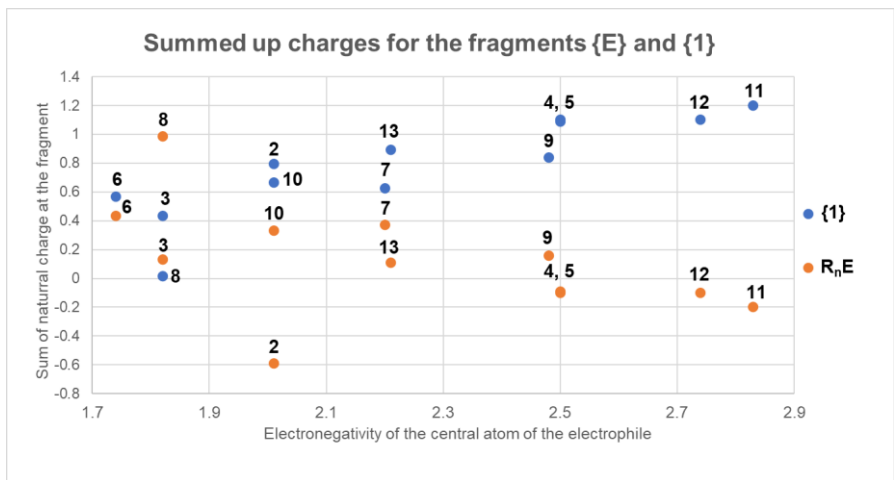


Figure S 41: Natural charge accumulation at  $\{1\}$  and the employed electrophile  $\{E\}$  against the electronegativity of the central atom of the electrophile.

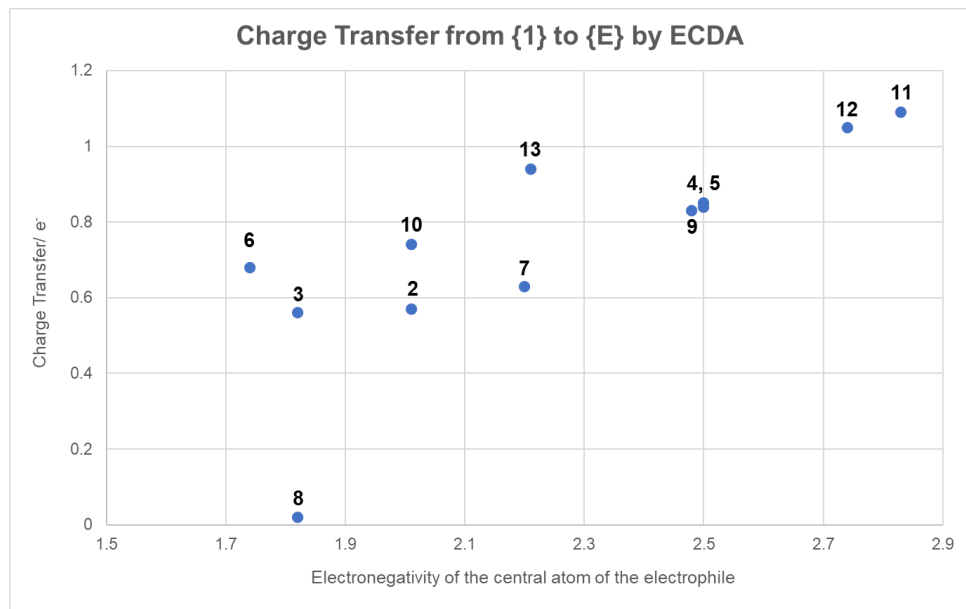


Figure S 42: Charge transfer from  $\{1\}$  to the respective electrophile  $\{E\}$  within in cations **2 – 13**, computed via ECDA of their optimized geometries (vide supra, against the electronegativity of the central atom of the electrophile).

### 4.3. NICS Values

NICS<sup>28</sup> values (Table S 15) were obtained on the ligand geometries from the optimized structures of the cationic pentaphosphole complexes as well as **1**, **14** and **15**. The computed values derived for the (*cyclo-P<sub>5</sub>*)<sup>-</sup> ligand in **1** and the parent pentaphosphole ligand compare well with those previously calculated on a different level of theory.<sup>16</sup> Ring critical points and the points above and below the ring plane, respectively, were derived using MultiWFN.<sup>24</sup> Magnetic shielding tensors were calculated using the correlation functional PBE0<sup>21</sup> and the basis sets aug-pcSseg-1<sup>22</sup> (for P atoms) and def2-TZVPPD<sup>19,23</sup> (for all other atoms: C, H, B, Ga, Si, As, Se, Te, Cl, Br, I; in case of **15**, the aug-pcSseg-1 basis set was used for B and Br). The negative of the eigenvalue (z) of the magnetic shielding tensor at the respective position (RCP (0), one angstrom above (+1) and one angstrom below (-1))<sup>24</sup> represents the corresponding NICS value.<sup>28</sup>

*Table S 15: NICS values for compounds **2 – 7** and **9 – 15** obtained on the PBE1/aug-pcSseg-1/def2-TZVPPD level of theory; NICS values of the ligand geometries in **1** and [Cp\*Fe(*η*<sup>5</sup>-P<sub>5</sub>H)]<sup>+</sup> were recalculated for better comparison; for **15**, the NICS values for both P<sub>4</sub>-rings are listed, as they are chemically distinct within the solid state structure of this compound.*

Compound	NICS(0) <sub>zz</sub>	NICS(1) <sub>zz</sub>	NICS(-1) <sub>zz</sub>
<b>1</b>	-32.5205	-40.5356	-40.5356
<b>2</b>	-19.48	-31.19	-30.47
<b>3</b>	-24.23	-34.73	-34.28
<b>4</b>	-21.31	-33.67	-32.84
<b>5</b>	-20.26	-32.05	-31.22
<b>6</b>	-24.11	-34.66	-34.33
<b>7</b>	-22.91	-34.03	-33.42
<b>9</b>	-24.31	-33.46	-32.62
<b>10</b>	-26.17	-34.92	-34.02
<b>11</b>	-22.47	-31.05	-30.89
<b>12</b>	-23.28	-31.79	-31.66
<b>13</b>	-26.25	-34.26	-34.20
<b>14</b>	-22.37	-3.27	-3.47
<b>15</b>	-29.06/-29.30	-9.53/-10.75	-9.73/-9.61
[Cp*Fe( <i>η</i> <sup>5</sup> -P <sub>5</sub> H)] <sup>+</sup>	-21.6272	-32.1365	-31.2407

To evaluate possible correlation between the calculated NICS(1/-1)<sub>zz</sub> values and the pyramidalization at P1, the former values are plotted against the sum of the respective P2-P1-R, P5-P1-R and P2-P1-P5 bond angles at P1 (Figure S 43). While a general trend of decreasing NICS(1/-1)<sub>zz</sub> values (thus increasing aromaticity) for increasing planarization of P1 can be observed within this plot, the presence of two outliers, namely compounds **2** and **5**, suggests a more complicated electronic situation for the pentaphosphole complexes in question.

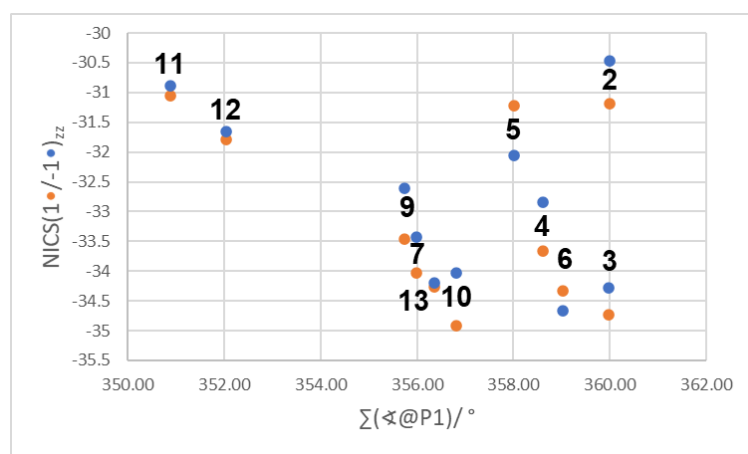


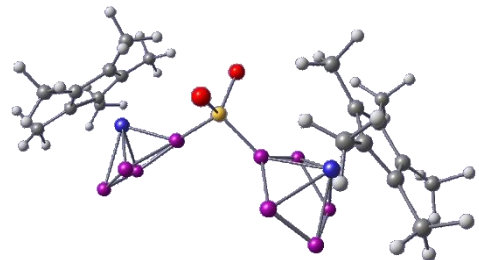
*Figure S 43: Plot of the calculated NICS(1/-1)<sub>zz</sub> for compounds **2 – 7** and **9 – 13** against the sum of the bond angles at P1 of the respective compound; Labelling according to color code and compound number.*

#### 4.4. Optimized Geometries

[2]<sup>+</sup>

B3LYP/def2TZVP: Energies/H = -11894.674338, Enthalpies/H = -11894.673394, Free Energies/H = -11894.802066, ZPVE/ kJ/mol = 1241.735

Symbol	X	Y	Z
Br	0.0667610	1.8324550	1.6797950
Br	-0.0730920	1.8412310	-1.7100220
Fe	3.8926080	-0.3980390	-0.0156470
Fe	-3.8904920	-0.3994770	0.0197000
P	1.5684480	-0.4961750	-0.0970090
P	-1.5660080	-0.5013370	0.0488110
P	-2.4517260	-1.1063740	1.8704230
P	-2.4184870	-1.3052410	-1.7106870
P	2.3828040	-1.3587820	1.6519830
P	-3.8549720	-2.6434570	-0.9207760
P	-3.8777420	-2.5216000	1.2061960
P	2.4931830	-1.0397500	-1.9188070
P	3.8352680	-2.6720830	0.8488390
P	3.9023000	-2.4799920	-1.2720460
C	4.6981500	1.1304370	1.2140870
C	-4.3186080	1.6853940	0.0715130
C	-4.7589400	1.1277390	-1.1691670
C	-4.9446210	1.3729820	2.5784240
H	-5.1545690	0.5162150	3.2167830
H	-5.6891000	2.1423510	2.8048030
H	-3.9685330	1.7695150	2.8528160
C	-5.0160420	1.0219390	1.1275480
C	-3.4264920	2.8722010	0.2299270
H	-2.8742780	2.8470930	1.1667380
H	-4.0374630	3.7804720	0.2306380
H	-2.7103340	2.9583370	-0.5841540
C	-5.8993360	0.0632120	0.5401940



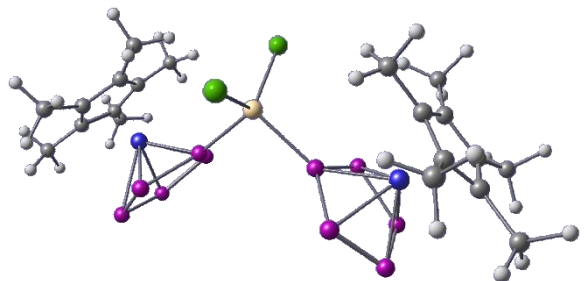
C	5.9304020	0.0565140	-0.4241100
C	5.0851050	1.0155550	-1.0638830
C	-4.3747340	1.6111570	-2.5300020
H	-3.3502090	1.9783450	-2.5566260
H	-5.0305960	2.4367910	-2.8227420
H	-4.4747360	0.8304230	-3.2820960
C	5.6910280	0.1277580	0.9846290
C	-5.7400160	0.1287750	-0.8802690
C	-6.9213220	-0.7471090	1.2693310
H	-7.1486610	-1.6790260	0.7547090
H	-7.8512270	-0.1745860	1.3412440
H	-6.6047030	-0.9881090	2.2825430
C	6.4526500	-0.6053380	2.0406210
H	5.8544790	-0.7710660	2.9351630
H	7.3254210	-0.0137750	2.3336500
H	6.8119590	-1.5710530	1.6899590
C	4.3291290	1.6834910	-0.0520120
C	-6.5621060	-0.6034620	-1.8905870
H	-6.0112380	-0.7799480	-2.8130750
H	-7.4427840	-0.0047130	-2.1426000
H	-6.9127160	-1.5634120	-1.5161160
C	4.2395840	1.6197560	2.5493840
H	3.2148690	1.9854480	2.5175950
H	4.8777090	2.4474530	2.8737440
H	4.2989690	0.8424160	3.3092390
B	-0.0006470	0.7556230	-0.0182980
C	6.9887380	-0.7603170	-1.0914240
H	7.1949290	-1.6830870	-0.5520240
H	7.9190430	-0.1850580	-1.1274560
H	6.7217740	-1.0180150	-2.1147680
C	3.4445050	2.8668820	-0.2690500
H	4.0542100	3.7759170	-0.2626190

H	2.6958980	2.9673260	0.5136130
H	2.9304990	2.8230260	-1.2270470
C	5.1004740	1.3631320	-2.5171040
H	4.1426080	1.7580570	-2.8512790
H	5.3508930	0.5055060	-3.1395180
H	5.8564020	2.1331310	-2.6992240

**[3]<sup>+</sup>**

B3LYP/def2TZVP: Energies/H = -9242.030969, Enthalpies/H = -9242.030024, Free Energies/H = -9242.164203, ZPVE/ kJ/mol = 1233.115

Symbol	X	Y	Z
Ga	-0.0032500	-0.8622180	-0.0374390
Fe	-4.1824360	0.7588690	-0.0284490
Fe	4.1879380	0.7573810	0.0016060
P	1.8432860	0.7632060	-0.0500600
P	-1.8440310	0.7567690	-0.2167960
P	2.7518600	1.4614330	-1.8313740
P	-2.5828960	1.8502430	1.4393890
P	2.6784970	1.5494770	1.7315320
P	-2.8633560	1.1201530	-2.0387000
P	4.1235860	2.9087460	-1.1211240
P	-4.0376920	3.1104300	0.5575600
P	-4.2039720	2.6740670	-1.5198520
P	4.0784970	2.9628380	1.0065550
C	-6.2494280	0.3132060	-0.2566830
C	-5.4653430	-0.7216330	-0.8558550
C	4.6538660	-1.3181060	-0.0545890
C	-4.9270800	-0.6282650	1.3922210
C	6.1931520	0.3336320	-0.5555920
C	5.3172050	-0.6429970	-1.1253620
C	-4.6518110	-1.3053020	0.1630880
C	5.1100880	-0.7534550	1.1765550
C	-7.3320420	1.0934970	-0.9292030
H	-7.1312810	1.2422740	-1.9887380
H	-7.4763130	2.0707510	-0.4712660
H	-8.2770820	0.5480620	-0.8454400
C	-5.9166200	0.3705460	1.1330870
C	5.2243820	-0.9980250	-2.5741830
H	4.2419370	-1.3876780	-2.8360960



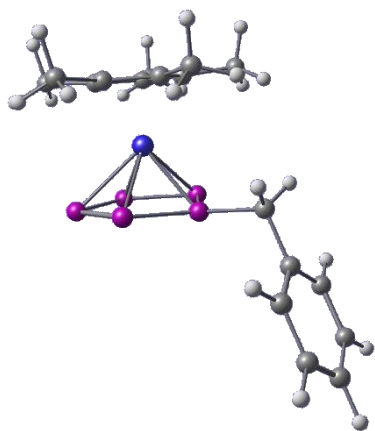
H	5.9603270	-1.7732350	-2.8082220
H	5.4321110	-0.1440360	-3.2168700
C	3.7708440	-2.5140530	-0.1938330
H	3.0724110	-2.6076380	0.6356830
H	4.3877930	-3.4181090	-0.2036870
H	3.2025250	-2.4980830	-1.1214920
C	6.0650780	0.2645970	0.8673420
C	-6.5904660	1.2204010	2.1607710
H	-6.9634940	2.1521980	1.7395650
H	-5.9260770	1.4646770	2.9880690
H	-7.4464230	0.6787350	2.5746760
C	7.1793420	1.1706570	-1.3035730
H	6.8428110	1.3929880	-2.3145830
H	8.1279210	0.6306970	-1.3818460
H	7.3788220	2.1141920	-0.7986400
C	6.8862780	1.0193040	1.8616710
H	7.2364900	1.9703440	1.4647020
H	7.7671460	0.4278310	2.1295700
H	6.3333160	1.2187320	2.7782540
C	-4.3885490	-1.0008930	2.7354860
H	-3.3674040	-1.3746750	2.6772640
H	-5.0062010	-1.7935090	3.1688110
H	-4.4024750	-0.1599930	3.4267740
C	-5.5882400	-1.2081840	-2.2634700
H	-6.3774000	-1.9642750	-2.3185000
H	-4.6677600	-1.6692650	-2.6171660
H	-5.8545730	-0.4080430	-2.9522840
C	4.7651410	-1.2433480	2.5454910
H	4.8682420	-0.4604700	3.2951020
H	5.4425780	-2.0566110	2.8233770
H	3.7487280	-1.6306080	2.5964810
C	-3.7901650	-2.5144940	0.0014080

H	-3.3104580	-2.5515940	-0.9751700
H	-4.4070770	-3.4134830	0.0966610
H	-3.0170250	-2.5691230	0.7652500
I	-0.0042570	-2.2705500	-2.1630990
I	-0.0184770	-2.0635580	2.2129600

**[4]<sup>+</sup>**

B3LYP/def2TZVP: Energies/H = -3631.534317, Enthalpies/H = -3631.533373, Free Energies/H = -3631.616864, ZPVE/ kJ/mol = 925.420

Symbol	X	Y	Z
Fe	1.1938160	-0.1232520	-0.0173070
P	-1.1207140	-0.2411500	0.0488410
P	-0.1861600	-1.1767020	1.6905910
P	-0.3232960	-0.5794790	-1.8710540
P	1.1665180	-2.4511880	0.6757060
P	1.0873860	-2.0958100	-1.4308700
C	2.8701610	0.5045910	1.1271760
C	3.2808370	0.2474060	-0.2174250
C	2.5486500	1.1242060	-1.0761020
C	1.6891620	1.9278780	-0.2623450
C	1.8891610	1.5456570	1.1002490
C	4.3725740	-0.6816570	-0.6377390
C	2.7483480	1.2715880	-2.5492270
C	0.8573640	3.0696960	-0.7511710
C	3.4587900	-0.1073530	2.3563800
C	1.2995980	2.2090820	2.3023270
H	4.4660670	-1.5316320	0.0361950
H	4.2175420	-1.0625670	-1.6458440
H	3.0235300	0.3291550	-3.0206020
H	2.7477830	-0.1307150	3.1809990
H	0.3759820	2.8499800	-1.7035480
H	3.8080340	-1.1230920	2.1792070
H	5.3274460	-0.1476830	-0.6291270
H	1.1731240	1.5132420	3.1302410
H	4.3187230	0.4856820	2.6815200
H	3.5592510	1.9818080	-2.7366520
H	0.3348520	2.6662150	2.0906010
H	1.8577260	1.6536590	-3.0455240

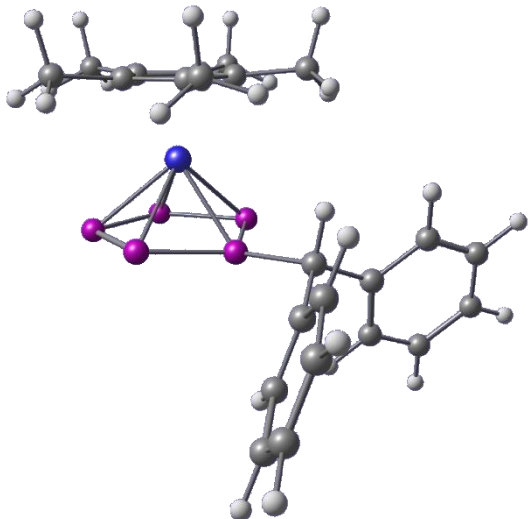


H	1.9695960	3.0041480	2.6427200
H	0.0900740	3.3547310	-0.0341070
H	1.4968660	3.9436460	-0.9059120
C	-2.3503340	1.1242870	0.3085160
H	-2.1068940	1.8975960	-0.4192260
C	-3.7687880	0.6354930	0.1569960
C	-4.3959120	0.6636310	-1.0893490
C	-4.4699880	0.1484480	1.2610910
C	-5.7048800	0.2174450	-1.2277640
H	-3.8620970	1.0416260	-1.9531840
C	-5.7789610	-0.2975200	1.1220780
H	-3.9942770	0.1247420	2.2342890
C	-6.3988360	-0.2651160	-0.1228450
H	-6.1833460	0.2498530	-2.1981170
H	-6.3149770	-0.6666640	1.9869560
H	-7.4188210	-0.6107110	-0.2307740
H	-2.1630770	1.5198870	1.3065890

[5]<sup>+</sup>

B3LYP/def2TZVP: Energies/H = -3862.572624, Enthalpies/H = -3862.571680, Free Energies/H = -3862.665852, ZPVE/ kJ/mol = 1137.939

Symbol	X	Y	Z
Fe	1.6880580	0.0174600	-0.1262580
P	-0.5765820	0.0358180	-0.7257040
P	0.4318820	-1.7579410	-1.2029240
P	0.4350400	1.8523250	-1.1027350
P	2.0718720	-0.9911510	-2.3012280
P	2.0726870	1.1447500	-2.2437180
C	2.9406270	-1.1936760	1.0894420
C	3.6862350	-0.0746500	0.6051250
C	3.0522170	1.1148850	1.0790140
C	1.9186010	0.7323120	1.8619460
C	1.8492850	-0.6957200	1.8682790
C	4.9724030	-0.1373360	-0.1517750
C	3.5600010	2.5085470	0.9042730
C	1.0614620	1.6686440	2.6504410
C	3.3108650	-2.6314820	0.9233940
C	0.9056850	-1.5353490	2.6677970
H	5.0438670	-1.0365880	-0.7609220
H	5.1054000	0.7258200	-0.8020560
H	4.0870910	2.6362730	-0.0396500
H	2.4418600	-3.2846330	0.9865610
H	0.8561870	2.5910890	2.1090540
H	3.8090950	-2.8185520	-0.0267660
H	5.8079390	-0.1498920	0.5543660
H	0.6236450	-2.4489090	2.1461940
H	4.0009670	-2.9237750	1.7203680
H	4.2632570	2.7425030	1.7091020
H	-0.0025850	-0.9959050	2.9285530
H	2.7569770	3.2427730	0.9483230

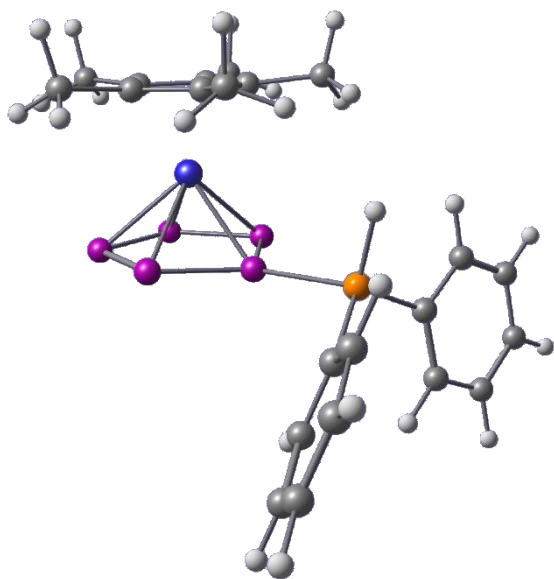


H	1.3863030	-1.8296810	3.6053490
H	0.1111330	1.2178670	2.9288360
H	1.5765420	1.9401260	3.5764000
C	-2.0917130	0.0001070	0.4028620
H	-1.6819080	-0.0011810	1.4105520
C	-2.8574440	-1.3016570	0.2186590
C	-3.4025700	-1.6918560	-1.0066500
C	-3.0483970	-2.1234540	1.3306190
C	-4.1245620	-2.8736960	-1.1131090
H	-3.2673000	-1.0814440	-1.8894620
C	-3.7746250	-3.3045000	1.2253130
H	-2.6339980	-1.8362500	2.2890750
C	-4.3142310	-3.6835480	0.0022260
H	-4.5393220	-3.1616500	-2.0704710
H	-3.9160480	-3.9261430	2.1000130
H	-4.8777830	-4.6035500	-0.0833060
C	-2.9112780	1.2715490	0.2418940
C	-3.2312050	2.0022060	1.3879190
C	-3.3883030	1.7164690	-0.9931010
C	-4.0198050	3.1441560	1.3047810
H	-2.8712340	1.6729920	2.3549760
C	-4.1737430	2.8592350	-1.0765470
H	-3.1466000	1.1828010	-1.9029370
C	-4.4938270	3.5760660	0.0718490
H	-4.2605090	3.6951340	2.2048220
H	-4.5343590	3.1900810	-2.0419460
H	-5.1056760	4.4662300	0.0044090

**[6]<sup>+</sup>**

B3LYP/def2TZVP: Energies/H = -4114.014234, Enthalpies/H = -4114.013290, Free Energies/H = -4114.013290, ZPVE/ kJ/mol = 1115.353

Symbol	X	Y	Z
Fe	1.9051020	0.0370700	-0.1471990
P	-0.3945050	0.0369380	-0.6637860
P	0.6400010	-1.7209090	-1.2313700
P	0.6099340	1.8526100	-1.0908200
P	2.2653110	-0.9391190	-2.3409610
P	2.2459460	1.1891080	-2.2595570
C	3.2709650	-1.1397640	0.9769460
C	3.9127860	0.0654320	0.5555910
C	3.1918340	1.1663800	1.1138690
C	2.1058870	0.6420010	1.8811730
C	2.1551750	-0.7849910	1.7966860
C	5.1866760	0.1540860	-0.2193390
C	3.5834310	2.6045620	1.0164080
C	1.1831350	1.4485310	2.7365340
C	3.7570680	-2.5282850	0.7175200
C	1.2969670	-1.7503590	2.5483720
H	5.3087360	-0.6862790	-0.9007150
H	5.2483100	1.0733590	-0.7994040
H	4.0906420	2.8244520	0.0782820
H	2.9453000	-3.2538480	0.7353950
H	0.9606100	2.4184030	2.2940460
H	4.2659830	-2.6112130	-0.2414600
H	6.0342400	0.1434130	0.4724290
H	1.0728340	-2.6418440	1.9638650
H	4.4712870	-2.8150650	1.4952330
H	4.2733430	2.8500310	1.8292270
H	0.3564880	-1.3024380	2.8619100
H	2.7248490	3.2685430	1.1033930

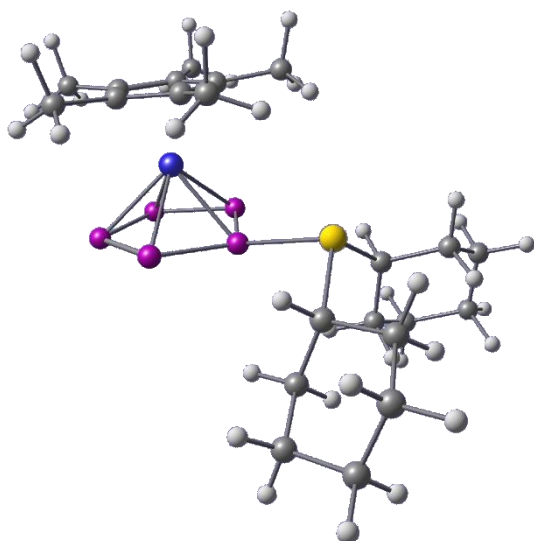


H	1.8218150	-2.0755980	3.4513290
H	0.2421580	0.9353090	2.9225260
H	1.6535540	1.6318080	3.7070860
C	-3.1491680	-1.6422780	0.2985780
C	-4.1022360	-1.7620380	-0.7222600
C	-2.8383250	-2.7780180	1.0606920
C	-4.7225390	-2.9795390	-0.9738110
H	-4.3758110	-0.9024930	-1.3208320
C	-3.4591520	-3.9953050	0.8087370
H	-2.1127370	-2.7147790	1.8628400
C	-4.4007570	-4.0972340	-0.2100150
H	-5.4596210	-3.0549220	-1.7629460
H	-3.2117300	-4.8612430	1.4093260
H	-4.8865660	-5.0446930	-0.4055890
C	-3.2211450	1.5471190	0.3316600
C	-3.5736190	2.3707440	1.4109460
C	-3.6045040	1.9381450	-0.9597400
C	-4.2955000	3.5412810	1.2067350
H	-3.2859480	2.0993370	2.4196260
C	-4.3243040	3.1082220	-1.1628360
H	-3.3380880	1.3370990	-1.8207640
C	-4.6721020	3.9101580	-0.0796460
H	-4.5610340	4.1642550	2.0511800
H	-4.6124450	3.3955430	-2.1658820
H	-5.2327730	4.8222540	-0.2396550
Si	-2.3081580	-0.0312640	0.6963710
H	-1.7955580	-0.0380600	2.0781410

[7]<sup>+</sup>

B3LYP/def2TZVP: Energies/H = -6066.908076, Enthalpies/H = -6066.907131, Free Energies/H = -6067.010590, ZPVE/ kJ/mol = 1455.621

Symbol	X	Y	Z
Fe	-2.2944020	-0.0014260	-0.1511160
P	0.0102680	-0.0303850	-0.7092890
P	-1.0227400	1.7520850	-1.2069470
P	-1.0441590	-1.8248820	-1.1086060
P	-2.6602400	1.0062860	-2.3273520
P	-2.6735910	-1.1240750	-2.2687050
C	-3.6080970	1.1865110	1.0224630
C	-4.2870840	0.0037390	0.5954550
C	-3.5799060	-1.1229030	1.1181190
C	-2.4648870	-0.6368630	1.8698150
C	-2.4821860	0.7914240	1.8105840
C	-5.5781590	-0.0434750	-0.1547190
C	-4.0056510	-2.5502570	1.0053620
C	-1.5389060	-1.4731530	2.6923800
C	-4.0670890	2.5894220	0.7930850
C	-1.5754880	1.7144420	2.5581720
H	-5.6926420	0.8078310	-0.8237350
H	-5.6730740	-0.9538420	-0.7442840
H	-4.5284080	-2.7461370	0.0704150
H	-3.2380730	3.2953170	0.7967500
H	-1.3772860	-2.4559710	2.2517430
H	-4.5985610	2.6953190	-0.1512600
H	-6.4118050	-0.0209230	0.5534520
H	-1.4475840	2.6655970	2.0434730
H	-4.7534720	2.8841570	1.5924290
H	-4.6908550	-2.7922800	1.8231500
H	-0.5911680	1.2784960	2.7200180
H	-3.1606990	-3.2336940	1.0729670



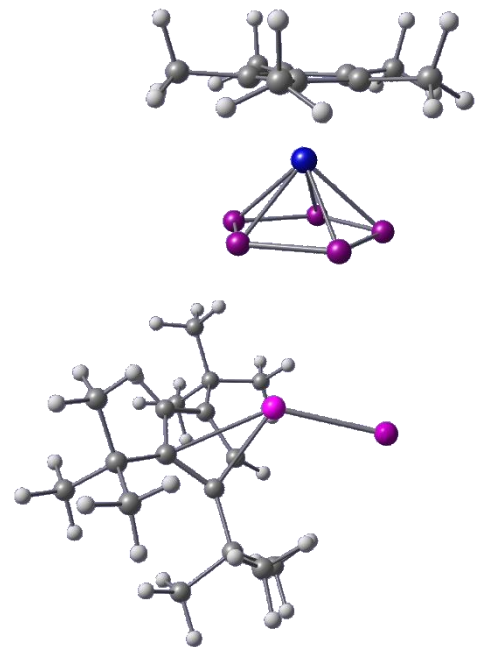
H	-2.0048480	1.9295450	3.5412600
H	-0.5697330	-0.9967040	2.8293170
H	-1.9723400	-1.6266480	3.6851500
C	2.7162000	-1.6671020	0.3257020
C	3.0444390	-1.9204930	-1.1477410
C	3.9666570	-1.8211390	1.2090810
H	1.9842450	-2.4150470	0.6501750
C	3.6568200	-3.3178040	-1.3239490
H	3.7563820	-1.1753640	-1.5057290
H	2.1527520	-1.8311110	-1.7712260
C	4.5900640	-3.2121210	1.0241490
H	4.7049780	-1.0600880	0.9378040
H	3.7203420	-1.6636170	2.2624290
C	4.8963140	-3.5064060	-0.4459510
H	3.9090390	-3.4728920	-2.3759310
H	2.9081240	-4.0747420	-1.0658040
H	5.4996720	-3.2837450	1.6255100
H	3.8971810	-3.9670610	1.4111350
H	5.2823040	-4.5231610	-0.5520080
H	5.6888460	-2.8332800	-0.7916070
C	2.7137460	1.6524020	0.1619440
C	3.6978250	2.1400130	1.2394570
C	3.3820910	1.5913980	-1.2124840
H	1.8873590	2.3705240	0.1176990
C	4.2871710	3.5051680	0.8563060
H	4.5118660	1.4166080	1.3510510
H	3.2024040	2.2104870	2.2108620
C	3.9530410	2.9661560	-1.5913100
H	4.2006710	0.8678920	-1.1930490
H	2.6787140	1.2574240	-1.9778900
C	4.9303530	3.4801560	-0.5318840
H	5.0175100	3.8091190	1.6102370

H	3.4878260	4.2541200	0.8733340
H	4.4465620	2.8990700	-2.5640690
H	3.1290320	3.6790280	-1.7054020
H	5.2842790	4.4789840	-0.7986230
H	5.8131880	2.8313480	-0.5110320
As	1.7628800	0.0228000	0.8939270

**[8]<sup>+</sup>**

B3LYP/def2TZVP: Energies/H = -4563.845732, Enthalpies/H = -4563.844788, Free Energies/H = -4563.976174, ZPVE/ kJ/mol = 1716.721

Fe	-3.947394000	-0.130964000	0.099206000
Sb	1.979679000	0.454908000	0.025960000
I	2.064682000	3.217810000	0.267696000
P	-2.540770000	0.721371000	1.853883000
P	-2.154268000	-1.270204000	1.216645000
P	-2.726821000	1.941046000	0.123575000
P	-2.448421000	0.706996000	-1.584497000
P	-2.099663000	-1.279855000	-0.909982000
C	-5.618481000	-0.802548000	1.220758000
C	-5.857237000	0.526094000	0.751747000
C	-5.556730000	-0.838638000	-1.090411000
C	-5.818502000	0.503861000	-0.676338000
C	-5.433425000	-1.646246000	0.082221000
C	-6.110126000	1.659155000	-1.578748000
H	-5.622749000	1.548770000	-2.546314000
H	-5.784611000	2.603980000	-1.145338000
H	-7.187419000	1.730337000	-1.757017000
C	-6.198373000	1.708123000	1.600436000
H	-5.892771000	2.643246000	1.132951000
H	-5.726533000	1.652838000	2.580603000
H	-7.280503000	1.754364000	1.756402000
C	-5.664002000	-1.249840000	2.646175000
H	-5.335447000	-0.465330000	3.326539000
H	-5.037836000	-2.124849000	2.815154000
H	-6.688803000	-1.518143000	2.920332000
C	-5.529579000	-1.330310000	-2.501764000
H	-4.910837000	-2.220261000	-2.608256000
H	-5.150299000	-0.573454000	-3.187353000
H	-6.542119000	-1.591018000	-2.824581000



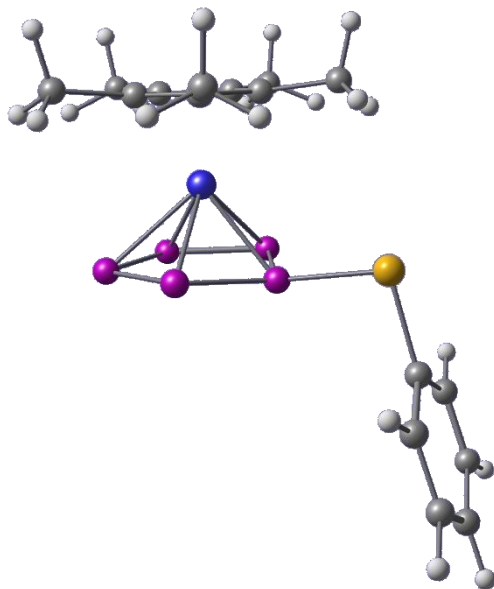
C	-5.249614000	-3.129382000	0.110618000
H	-4.731654000	-3.454999000	1.011795000
H	-4.681657000	-3.482767000	-0.749036000
H	-6.223920000	-3.627154000	0.090791000
C	3.998453000	-0.050063000	-0.962266000
H	4.520207000	0.808747000	-1.346329000
C	3.454818000	-1.878788000	0.378952000
C	3.240095000	-0.969917000	-1.762975000
C	2.995013000	0.574496000	-3.742567000
H	2.184734000	1.147192000	-3.286474000
H	3.936211000	1.084033000	-3.533583000
H	2.846544000	0.594005000	-4.822524000
C	2.923622000	-2.048948000	-0.909959000
H	2.319798000	-2.886623000	-1.210332000
C	4.174459000	-0.584032000	0.378354000
C	5.221217000	0.040137000	1.331470000
C	2.999125000	-0.881309000	-3.253360000
C	1.885528000	-3.669340000	1.231158000
H	1.776406000	-4.156939000	0.264008000
H	1.768076000	-4.441982000	1.991359000
H	1.070798000	-2.953959000	1.353916000
C	1.677281000	-1.558258000	-3.650528000
H	1.651574000	-2.609629000	-3.362831000
H	0.821178000	-1.056120000	-3.196765000
H	1.558381000	-1.512640000	-4.733770000
C	4.177446000	-1.637033000	-3.923367000
H	4.056520000	-1.595877000	-5.006896000
H	5.137225000	-1.184728000	-3.669809000
H	4.199116000	-2.684601000	-3.620862000
C	5.916614000	1.239914000	0.653928000
H	5.218092000	2.037772000	0.399830000
H	6.640517000	1.657327000	1.353757000

H	6.460275000	0.945533000	-0.244526000
C	3.266644000	-2.997679000	1.416866000
C	4.626026000	0.566974000	2.652714000
H	4.064196000	-0.180070000	3.201163000
H	5.435627000	0.916342000	3.295367000
H	3.969156000	1.418865000	2.466626000
C	6.324665000	-1.004774000	1.608658000
H	6.742783000	-1.389472000	0.677007000
H	7.131363000	-0.525314000	2.164808000
H	5.974256000	-1.845335000	2.199393000
C	3.340815000	-2.570577000	2.889133000
H	2.592890000	-1.812813000	3.126645000
H	3.130785000	-3.441179000	3.511430000
H	4.318889000	-2.202385000	3.181672000
C	4.350981000	-4.070182000	1.136929000
H	5.359261000	-3.680664000	1.265478000
H	4.217596000	-4.901353000	1.831480000
H	4.263901000	-4.458499000	0.121538000

**[9]<sup>+</sup>**

B3LYP/def2TZVP: Energies/H = -3658.406358, Enthalpies/H = -3658.405413, Free Energies/H = -3658.481294, ZPVE/ kJ/mol = 612.879

Symbol	X	Y	Z
Fe	1.5155710	-0.2184240	-0.0087880
P	-0.8186570	-0.4260130	-0.0163240
P	0.1383470	-1.0681000	1.7746470
P	0.1374190	-0.9560060	-1.8428580
P	1.5388320	-2.4396470	0.9960810
P	1.5404160	-2.3706580	-1.1491680
C	2.6795780	1.0510670	1.2438700
C	3.5448080	0.2346710	0.4502790
C	3.2837990	0.5235260	-0.9253820
C	2.2547180	1.5165520	-0.9820510
C	1.8854290	1.8448550	0.3596900
C	4.6294850	-0.6521460	0.9686540
C	4.0521170	-0.0051420	-2.0920650
C	1.7631980	2.2008570	-2.2161080
C	2.7091930	1.1704270	2.7328190
C	0.9660500	2.9471210	0.7739030
H	4.3917080	-1.0530600	1.9522650
H	4.8299530	-1.4876930	0.3002400
H	4.4627450	-0.9941220	-1.8971690
H	1.7476290	1.4842250	3.1354640
H	1.8467690	1.5650140	-3.0959100
H	2.9938100	0.2367240	3.2154550
H	5.5543570	-0.0749130	1.0619350
H	0.4266740	2.7133920	1.6904530
H	3.4475270	1.9254570	3.0194470
H	4.8905310	0.6649290	-2.3047590
H	0.2429190	3.1905260	-0.0021270
H	3.4422970	-0.0618690	-2.9922800

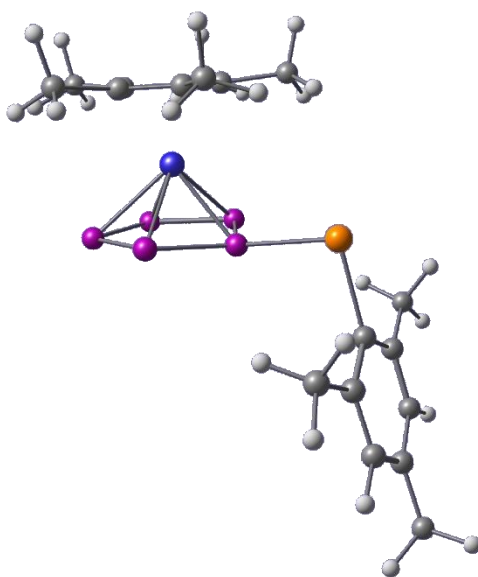


H	1.5528400	3.8511980	0.9630060
H	0.7251990	2.5157660	-2.1213990
H	2.3639500	3.0967560	-2.3992660
C	-3.8857370	0.3470040	0.0152140
C	-4.5384950	0.1431390	-1.1981440
C	-4.4475260	-0.0869920	1.2136130
C	-5.7671560	-0.5085130	-1.2072880
H	-4.0969050	0.4876530	-2.1232120
C	-5.6745390	-0.7404660	1.1916520
H	-3.9370920	0.0826630	2.1517660
C	-6.3329590	-0.9509520	-0.0159150
H	-6.2797420	-0.6693390	-2.1467560
H	-6.1153630	-1.0811970	2.1194480
H	-7.2888510	-1.4583390	-0.0280730
Se	-2.2171450	1.3365170	0.0417010

**[10]<sup>+</sup>**

B3LYP/def2TZVP: Energies/H = -3978.258935, Enthalpies/H = -3978.257990, Free Energies/H = -3978.359390, ZPVE/ kJ/mol = 1065.305

Symbol	X	Y	Z
Fe	2.1688790	-0.3178170	-0.0363820
P	-0.1812110	-0.4462170	-0.0937990
P	0.7326150	-1.3057140	1.6277440
P	0.7945370	-0.8605680	-1.9418070
P	2.1322800	-2.6213800	0.7554610
P	2.1696900	-2.3551550	-1.3692430
C	3.6267360	0.5138020	1.2730440
C	4.2698870	0.0155350	0.0980440
C	3.7396990	0.7204690	-1.0261950
C	2.7706390	1.6562940	-0.5469960
C	2.7009350	1.5282350	0.8761600
C	5.3921940	-0.9694830	0.0648020
C	4.2090430	0.5963640	-2.4388700
C	2.0745990	2.6795520	-1.3844750
C	3.9590520	0.1331230	2.6785910
C	1.9207140	2.3944500	1.8108440
H	5.3298120	-1.6873910	0.8809120
H	5.4231570	-1.5219330	-0.8728230
H	4.5512600	-0.4113780	-2.6689570
H	3.1156060	0.2811370	3.3510670
H	1.8014580	2.2884000	-2.3636140
H	4.2779780	-0.9051950	2.7541910
H	6.3432810	-0.4381380	0.1653640
H	1.5664150	1.8416560	2.6798190
H	4.7813660	0.7577460	3.0398460
H	5.0504150	1.2760960	-2.6031740
H	1.0617510	2.8552840	1.3273480
H	3.4299080	0.8622960	-3.1515870

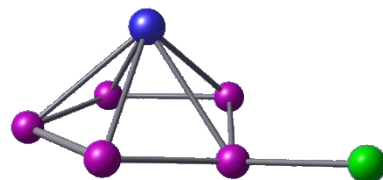
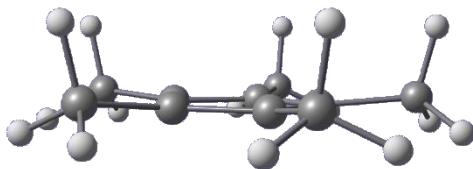


H	2.5603470	3.2034410	2.1758490
H	1.1728560	3.0589760	-0.9081610
H	2.7413790	3.5315200	-1.5463550
C	-3.5438310	0.3287330	0.0360350
C	-4.1831530	0.1491800	-1.2054010
C	-4.1001120	-0.1698640	1.2282130
C	-5.3890060	-0.5497040	-1.2219730
C	-5.3080970	-0.8623800	1.1452370
C	-5.9680990	-1.0623130	-0.0636020
H	-5.8890550	-0.6968910	-2.1722280
H	-5.7434660	-1.2551510	2.0565460
Te	-1.7325510	1.4716740	0.1268920
C	-3.4649770	0.0007680	2.5843530
H	-2.4860160	-0.4794940	2.6365720
H	-3.3188470	1.0534880	2.8318900
H	-4.0954490	-0.4420160	3.3540640
C	-3.6377640	0.6670730	-2.5115590
H	-3.4820800	1.7467630	-2.4858310
H	-2.6775650	0.2103910	-2.7584600
H	-4.3307070	0.4458860	-3.3220840
C	-7.2850140	-1.7868460	-0.1175620
H	-8.1151460	-1.0747020	-0.1205490
H	-7.3704540	-2.3867660	-1.0243970
H	-7.4157480	-2.4402840	0.7448350

[11]<sup>+</sup>

B3LYP/def2TZVP: Energies/H = -3820.828078, Enthalpies/H = -3820.827134, Free Energies/H = -3820.902382, ZPVE/ kJ/mol = 613.509

Symbol	X	Y	Z
Fe	-0.2265480	-0.1485790	0.0000400
P	2.0971580	-0.5895230	-0.0005900
P	1.0664590	-0.9689980	-1.8247800
P	1.0669590	-0.9716320	1.8234020
P	-0.3743200	-2.3246800	-1.0779350
P	-0.3739980	-2.3262500	1.0750260
C	-1.6244260	0.9662670	-1.1553320
C	-2.2766290	0.4311680	-0.0017910
C	-1.6275880	0.9618790	1.1555630
C	-0.5693180	1.8216540	0.7173720
C	-0.5673810	1.8243500	-0.7110410
C	-3.4993740	-0.4271230	-0.0051690
C	-2.0643310	0.7655940	2.5702370
C	0.2790200	2.6817160	1.5959350
C	-2.0573840	0.7758620	-2.5719490
C	0.2824290	2.6880580	-1.5846230
H	-3.5493250	-1.0625820	-0.8876770
H	-3.5530810	-1.0641310	0.8759830
H	-2.5379260	-0.2026050	2.7235050
H	-1.2272860	0.8672370	-3.2709260
H	0.4333580	2.2392450	2.5784960
H	-2.5329390	-0.1906030	-2.7298880
H	-4.3890340	0.2093040	-0.0064770
H	0.4498930	2.2433560	-2.5640780
H	-2.7885060	1.5474490	-2.8305940
H	-2.7981350	1.5344540	2.8293880
H	1.2503370	2.8994530	-1.1344750
H	-1.2364960	0.8565490	3.2719480

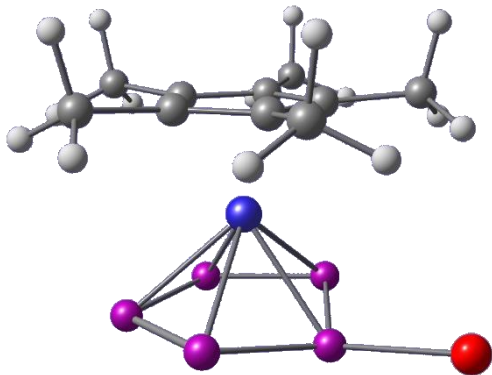


H	-0.2217950	3.6460570	-1.7423530
H	1.2530880	2.8830490	1.1544720
H	-0.2185070	3.6445420	1.7451510
Cl	3.3925070	0.9759980	0.0002610

**[12]<sup>+</sup>**

B3LYP/def2TZVP: Energies/H = -5934.784939, Enthalpies/H = -5934.783995, Free Energies/H = -5934.858303, ZPVE/ kJ/mol = 613.138

Symbol	X	Y	Z
Fe	-0.5751750	-0.1361500	0.0012240
P	1.6307580	-1.0021170	-0.0061200
P	0.5426040	-1.1813000	-1.8271720
P	0.5497140	-1.2010980	1.8168380
P	-1.1266840	-2.2448730	-1.0829130
P	-1.1230920	-2.2554310	1.0677370
C	-1.6819060	1.2508340	-1.1737540
C	-2.4876030	0.7980130	-0.0836640
C	-1.8280990	1.1609110	1.1311220
C	-0.6114560	1.8359690	0.7922990
C	-0.5219560	1.8922000	-0.6331450
C	-3.8405070	0.1749910	-0.1951940
C	-2.3795100	0.9848690	2.5077480
C	0.3213350	2.4952020	1.7553370
C	-2.0540750	1.1893400	-2.6187780
C	0.5162240	2.6207350	-1.4217170
H	-3.9455250	-0.4118460	-1.1061040
H	-4.0645160	-0.4696090	0.6529200
H	-3.0134710	0.1030350	2.5837010
H	-1.1795790	1.2093670	-3.2673170
H	0.3266250	2.0010780	2.7253420
H	-2.6363610	0.3000760	-2.8551140
H	-4.6003070	0.9616410	-0.2206310
H	0.6936590	2.1591330	-2.3919310
H	-2.6678670	2.0594030	-2.8698580
H	-2.9919770	1.8542050	2.7643800
H	1.4651810	2.6791570	-0.8931590
H	-1.5944640	0.9065670	3.2580230

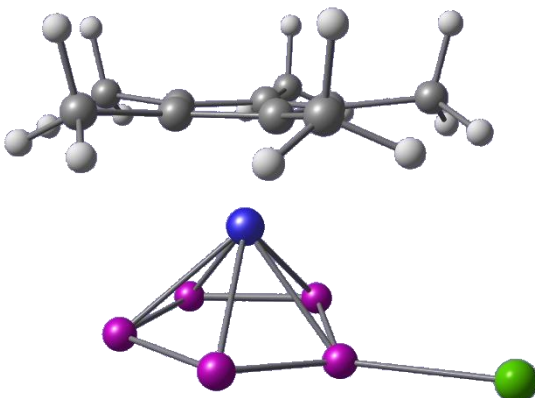


H	0.1774770	3.6449730	-1.6032070
H	1.3431710	2.5238530	1.3814590
H	0.0024740	3.5292690	1.9161440
Br	3.3698810	0.3526720	0.0001850

**[13]<sup>+</sup>**

B3LYP/def2TZVP: Energies/H = -3658.406358, Enthalpies/H = -3658.405413, Free Energies/H = -3658.481294, ZPVE/ kJ/mol = 612.879

Symbol	X	Y	Z
Fe	0.8989940	-0.1248060	0.0001740
P	-1.2617830	-1.0356970	0.0025800
P	-0.1904870	-1.2636370	1.8228410
P	-0.1936720	-1.2648490	-1.8188450
P	1.5440580	-2.2105720	1.0740480
P	1.5425150	-2.2112310	-1.0716410
C	1.8932350	1.3287030	1.1979380
C	2.7810840	0.8578870	0.1810250
C	2.1978710	1.1630940	-1.0877630
C	0.9491670	1.8219050	-0.8558860
C	0.7615170	1.9248300	0.5579810
C	4.1391080	0.2756820	0.4009400
C	2.8432590	0.9581380	-2.4188680
C	0.0800030	2.4348830	-1.9050670
C	2.1680700	1.3278970	2.6660200
C	-0.3381330	2.6624680	1.2481430
H	4.2076360	-0.2538600	1.3494800
H	4.4220380	-0.4121860	-0.3942070
H	3.5076260	0.0958620	-2.4231510
H	1.2518950	1.3122140	3.2541470
H	0.1226500	1.8866010	-2.8447730
H	2.7829270	0.4813500	2.9673650
H	4.8792390	1.0811150	0.4181470
H	-0.5659070	2.2386620	2.2250360
H	2.7122470	2.2391790	2.9312740
H	3.4435730	1.8381920	-2.6678100
H	-1.2533040	2.6780000	0.6602260
H	2.1099810	0.8281150	-3.2132380

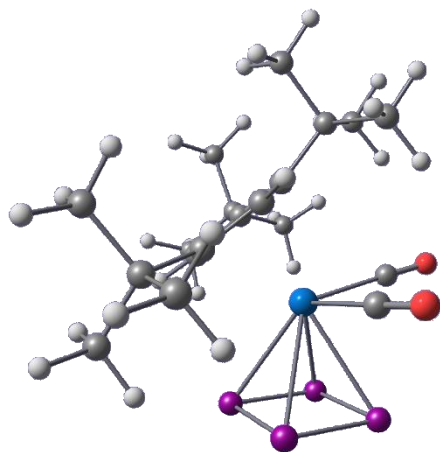


H	-0.0317950	3.7010350	1.4051420
H	-0.9605510	2.4970890	-1.5922910
H	0.4231090	3.4543730	-2.1053570
I	-3.3374670	0.2044540	-0.0003030

## 14

B3LYP/def2SVP: Energies/H = -2312.831455, Enthalpies/H = -2312.830511, Free Energies/H = -2312.924899, ZPVE/ kJ/mol = 1164.342

Ta	0.577394000	-0.290233000	-0.226926000
P	2.738341000	-1.833228000	-0.881675000
P	1.752908000	-2.403754000	1.020978000
P	3.236452000	0.161214000	-0.049693000
P	2.260494000	-0.430286000	1.826807000
O	-0.621992000	-3.004082000	-1.558715000
O	1.476547000	0.704602000	-3.191682000
C	-0.197535000	-2.044343000	-1.083159000
C	-1.017844000	1.496527000	-0.784256000
H	-1.026748000	1.987648000	-1.753089000
C	-0.612623000	1.062016000	1.394652000
H	-0.252127000	1.156546000	2.411771000
C	-1.573810000	0.079464000	0.962072000
C	0.444373000	3.300833000	0.458718000
C	1.175448000	0.338094000	-2.143731000
C	-0.276749000	1.956227000	0.336974000
C	-2.268536000	-0.836610000	2.005121000
C	-1.843625000	0.373965000	-0.447924000
C	1.487940000	3.290111000	1.589940000
H	1.041929000	3.034759000	2.563272000
H	1.941694000	4.288698000	1.688159000
H	2.297887000	2.574036000	1.383964000
C	-2.969939000	-0.002446000	-1.454033000
C	-3.720225000	-0.338536000	2.213776000
H	-3.733330000	0.727849000	2.489189000
H	-4.195088000	-0.904414000	3.031162000
H	-4.344855000	-0.463161000	1.320713000
C	1.132952000	3.703659000	-0.858141000
H	1.934414000	2.997693000	-1.121201000

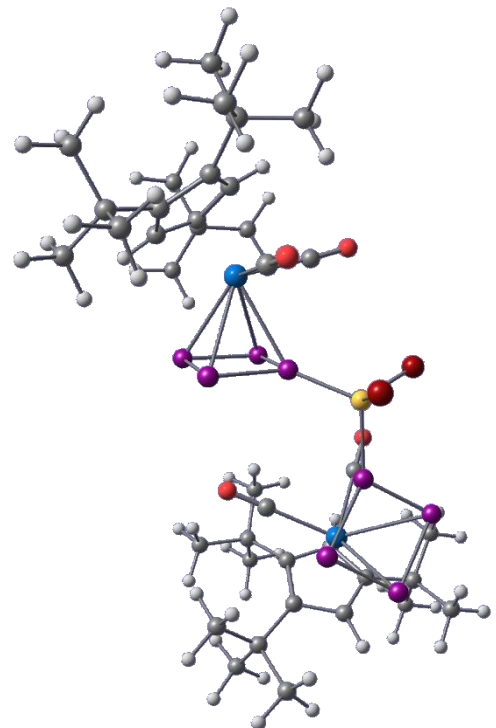


H	1.582353000	4.703438000	-0.752589000
H	0.424142000	3.752596000	-1.699224000
C	-4.052365000	1.101256000	-1.300714000
H	-4.465569000	1.124269000	-0.281804000
H	-4.882921000	0.911962000	-1.999489000
H	-3.643747000	2.098951000	-1.521597000
C	-2.450570000	0.037965000	-2.912021000
H	-2.041144000	1.016220000	-3.199682000
H	-3.286651000	-0.169693000	-3.596975000
H	-1.677277000	-0.723594000	-3.091715000
C	-1.565234000	-0.720177000	3.378514000
H	-0.499826000	-0.990103000	3.324254000
H	-2.045478000	-1.413893000	4.084978000
H	-1.646702000	0.289208000	3.808433000
C	-2.255066000	-2.337196000	1.644921000
H	-2.696493000	-2.554393000	0.668574000
H	-2.826095000	-2.900853000	2.399899000
H	-1.225110000	-2.722409000	1.642982000
C	-0.647609000	4.348363000	0.797726000
H	-1.407754000	4.403471000	0.002834000
H	-0.195398000	5.347213000	0.907995000
H	-1.159119000	4.099201000	1.740681000
C	-3.658534000	-1.367669000	-1.276112000
H	-2.966048000	-2.209366000	-1.400763000
H	-4.432602000	-1.468589000	-2.052451000
H	-4.164166000	-1.468635000	-0.309716000

**[15]<sup>+</sup>**

B3LYP/def2SVP: Energies/H = -9798.557610, Enthalpies/H = -9798.556666, Free Energies/H  
= -9798.733683, ZPVE/ kJ/mol = 2349.701

Ta	3.870701000	-0.158907000	-0.080086000
Ta	-3.670091000	0.266379000	0.075639000
Br	-0.747014000	-3.622675000	-1.247428000
Br	-0.050137000	-2.722825000	1.960431000
P	1.863380000	-1.876914000	-0.432854000
P	-1.161017000	-0.582493000	-0.228570000
P	2.896458000	-1.538017000	-2.316371000
P	-1.890939000	0.288143000	-2.079599000
P	3.512136000	-2.810825000	0.623164000
P	4.608457000	-2.409658000	-1.250752000
P	-1.238204000	1.220359000	0.982363000
P	-2.040267000	2.118687000	-0.865166000
O	2.310014000	0.012470000	2.779398000
O	1.607889000	1.740601000	-1.449645000
O	-4.133121000	-2.562400000	-1.475595000
O	-3.218384000	-1.317065000	2.891677000
C	2.845446000	-0.066553000	1.770672000
C	4.936251000	2.118192000	0.147104000
C	-5.210321000	2.110895000	-0.174254000
H	-4.903663000	3.036075000	-0.647428000
C	6.235442000	0.260337000	-0.354202000
H	6.868757000	-0.434375000	-0.892918000
C	-3.350938000	-0.770192000	1.895636000
C	4.385670000	3.559484000	0.351715000
C	6.021993000	0.225131000	1.054336000
C	-6.183266000	0.029808000	0.163773000
C	-6.249613000	1.177032000	-2.355372000
C	5.595146000	1.405292000	-0.951151000
C	-5.843311000	1.016154000	-0.866212000



C	5.194906000	1.347801000	1.330323000
H	4.887348000	1.646632000	2.328426000
C	5.903733000	1.780929000	-2.425090000
C	2.405711000	1.072404000	-0.966062000
C	-3.965507000	-1.568021000	-0.932557000
C	-5.144843000	1.866821000	1.228462000
C	-5.842073000	-0.002210000	-3.262500000
H	-4.747295000	-0.071147000	-3.343110000
H	-6.240663000	0.163078000	-4.275589000
H	-6.218926000	-0.967847000	-2.916324000
C	7.235064000	-1.965280000	1.501530000
H	7.870555000	-1.840744000	0.611837000
H	6.379692000	-2.601872000	1.227831000
H	7.825288000	-2.512799000	2.252091000
C	-5.711048000	0.575490000	1.404621000
H	-5.868518000	0.105495000	2.371163000
C	3.266167000	3.577619000	1.420484000
H	2.386801000	2.998380000	1.101741000
H	2.937840000	4.615672000	1.578772000
H	3.592570000	3.197361000	2.398219000
C	6.779159000	-0.616095000	2.084239000
C	-7.160092000	-1.179092000	0.256559000
C	-4.855038000	2.885157000	2.333859000
C	-5.589330000	2.437394000	-2.963222000
H	-5.936609000	3.366691000	-2.488466000
H	-5.856490000	2.499531000	-4.028543000
H	-4.490497000	2.404025000	-2.902773000
C	3.828320000	4.296808000	-0.879593000
H	4.573997000	4.438790000	-1.669212000
H	3.507846000	5.300340000	-0.561562000
H	2.948661000	3.802187000	-1.309792000
C	4.656976000	2.068585000	-3.287186000

H	4.058756000	1.155472000	-3.423261000
H	4.974672000	2.409655000	-4.284858000
H	4.007050000	2.841284000	-2.868552000
C	-7.780556000	1.408721000	-2.415457000
H	-8.356560000	0.534561000	-2.087684000
H	-8.080592000	1.634013000	-3.450877000
H	-8.073789000	2.262819000	-1.785123000
C	6.861531000	2.998934000	-2.424935000
H	6.395043000	3.909032000	-2.028293000
H	7.185350000	3.214930000	-3.455155000
H	7.761055000	2.790573000	-1.824799000
B	-0.065949000	-2.224161000	0.016814000
C	8.035571000	0.211125000	2.464565000
H	8.638749000	-0.339576000	3.203646000
H	7.757770000	1.181104000	2.905172000
H	8.667470000	0.404133000	1.583742000
C	5.940293000	-0.864543000	3.350985000
H	5.053108000	-1.477262000	3.132163000
H	5.607471000	0.074728000	3.818740000
H	6.545034000	-1.402500000	4.096947000
C	5.586743000	4.382130000	0.896180000
H	5.965640000	3.967789000	1.842504000
H	5.271276000	5.420792000	1.082772000
H	6.420516000	4.405291000	0.179612000
C	-4.267354000	2.219095000	3.591519000
H	-4.923995000	1.430723000	3.990281000
H	-4.144573000	2.971377000	4.385686000
H	-3.279309000	1.779109000	3.389675000
C	-6.656569000	-2.219359000	1.286357000
H	-5.707685000	-2.679390000	0.972943000
H	-7.399957000	-3.025501000	1.374401000
H	-6.520580000	-1.803637000	2.294182000

C	-7.469594000	-1.955606000	-1.036257000
H	-7.935834000	-1.334389000	-1.808663000
H	-8.188615000	-2.752236000	-0.792700000
H	-6.584730000	-2.444385000	-1.462007000
C	-8.495728000	-0.583624000	0.783434000
H	-8.367331000	-0.105574000	1.766149000
H	-9.241966000	-1.386299000	0.891962000
H	-8.905289000	0.167777000	0.092655000
C	6.659389000	0.629282000	-3.129552000
H	7.650009000	0.443640000	-2.689194000
H	6.819868000	0.901840000	-4.183207000
H	6.089976000	-0.312632000	-3.117394000
C	-6.224648000	3.519864000	2.692752000
H	-6.675813000	4.016029000	1.819531000
H	-6.093479000	4.274129000	3.484708000
H	-6.933436000	2.760924000	3.058353000
C	-3.905284000	3.998122000	1.856994000
H	-2.904883000	3.607270000	1.615325000
H	-3.781199000	4.745700000	2.655267000
H	-4.292020000	4.524856000	0.971535000

## 5. References

- 1 <https://omics.pnl.gov/software/molecular-weight-calculator> (30.03.2021).
- 2 O. J. Scherer and T. Brück, *Angew. Chem. Int. Ed. Engl.*, 1987, **26**, 59.
- 3 M. Gonsior, I. Krossing and N. Mitzel, *Z. anorg. allg. Chem.*, 2002, **628**, 1821.
- 4 P. Romanato, S. Duttwyler, A. Linden, K. K. Baldridge and J. S. Siegel, *J. Am. Chem. Soc.*, 2010, **132**, 7828–7829.
- 5 W. Steinkopf, H. Dudek and S. Schmidt, *Ber. dtsch. Chem. Ges. A/B*, 1928, **61**, 1911–1918.
- 6 O. Behaghel and H. Seibert, *Ber. dtsch. Chem. Ges. A/B*, 1932, **65**, 812–816.
- 7 A. K. S. Chauhan, P. Singh, A. Kumar, R. C. Srivastava, R. J. Butcher and A. Duthie, *Organometallics*, 2007, **26**, 1955–1959.
- 8 (a) H. Sitzmann, P. Zhou and G. Wolmershäuser, *Chem. Ber.*, 1994, **127**, 3–9; (b) M. D. Walter, C. D. Sofield, C. H. Booth and R. A. Andersen, *Organometallics*, 2009, **28**, 2005–2019.
- 9 F. Dielmann, E. V. Peresypkina, B. Krämer, F. Hastreiter, B. P. Johnson, M. Zabel, C. Heindl and M. Scheer, *Angew. Chem. Int. Ed.*, 2016, **55**, 14833–14837.
- 10 S. Humbel, C. Bertrand, C. Darcel, C. Bauduin and S. Jugé, *Inorg. Chem.*, 2003, **42**, 420–427.
- 11 Agilent Technologies Ltd, *CrysAlis PRO*, Yarnton, Oxfordshire, England, 2014.
- 12 O. V. Dolomanov, L. J. Bourhis, R. J. Gildea, J. A. K. Howard and H. Puschmann, *J. Appl. Crystallogr.*, 2009, **42**, 339–341.
- 13 G. M. Sheldrick, *Acta Cryst. A* 2015, **71**, 3–8.
- 14 (a) G. M. Sheldrick, *Acta Cryst. A* 2008, **64**, 112–122; (b) G. M. Sheldrick, *Acta Cryst. C*, 2015, **71**, 3–8.
- 15 C. Riesinger, G. Balázs, M. Bodensteiner and M. Scheer, *Angew. Chem. Int. Ed.*, 2020, **59**, 23879–23884.
- 16 N. Burford, P. J. Ragogna, R. McDonald and M. J. Ferguson, *J. Am. Chem. Soc.*, 2003, **125**, 14404–14410.
- 17 M. J. Frisch, G. W. Trucks, H. B. Schlegel, G. E. Scuseria, M. A. Robb, J. R. Cheeseman, G. Scalmani, V. Barone, B. Mennucci, G. A. Petersson, H. Nakatsuji, M. Caricato, X. Li, H. P. Hratchian, A. F. Izmaylov, J. Bloino, G. Zheng, J. L. Sonnenberg, M. Hada, M. Ehara, K. Toyota, R. Fukuda, J. Hasegawa, M. Ishida, T. Nakajima, Y. Honda, O. Kitao, H. Nakai, T. Vreven, J. A. Montgomery Jr., J. E. Peralta, F. Ogliaro, M. Bearpark, J. J. Heyd, E. Brothers, K. N. Kudin, V. N. Staroverov, T. Keith, R. Kobayashi, J. Normand, K. Raghavachari, A. Rendell, J. C. Burant, S. S. Iyengar, J. Tomasi, M. Cossi, N. Rega, J. M. Millam, M. Klene, J. E. Knox, J. B. Cross, V. Bakken, C. Adamo, J. Jaramillo, R. Gomperts, R. E. Stratmann, O. Yazyev, A. J. Austin, R. Cammi, C. Pomelli, J. W. Ochterski, R. L. Martin, K. Morokuma, V. G. Zakrzewski, G. A. Voth, P. Salvador, J. J. Dannenberg, S. Dapprich, A. D. Daniels, O. Farkas, J. B. Foresman, J. V. Ortiz, J. Cioslowski and D. J. Fox, “*Gaussian 09*”, Revision E.01, Gaussian Inc., Wallingford CT, 2013.
- 18 (a) P. A. M. Dirac, *Proc. Roy. Soc. Lond. A*, 1929, **123**, 714–733; (b) J. C. Slater, *Phys. Rev.*, 1951, **81**, 385–390; (c) S. H. Vosko, L. Wilk and M. Nusair, *Can. J. Phys.*, 1980, **58**, 1200–1211; (d) C. Lee, W. Yang and R. G. Parr, *Phys. Rev. B*, 1988, **37**, 785–789; (e) A. D. Becke, *Phys. Rev. A*, 1988, **38**, 3098–3100; (f) A. D. Becke, *J. Chem. Phys.*, 1993, **98**, 5648–5652.
- 19 (a) F. Weigend and R. Ahlrichs, *Phys. Chem. Chem. Phys.*, 2005, **7**, 3297–3305; (b) F. Weigend, *Phys. Chem. Chem. Phys.*, 2006, **8**, 1057–1065.
- 20 J. Tomasi, B. Mennucci and R. Cammi, *Chem. Rev.*, 2005, **105**, 2999–3093.
- 21 (a) J. P. Perdew, K. Burke and M. Ernzerhof, *Phys. Rev. Lett.*, 1996, **77**, 3865–3868; (b) J. P. Perdew, K. Burke and M. Ernzerhof, *Phys. Rev. Lett.*, 1997, **78**, 1396; (c) C. Adamo and V. Barone, *J. Chem. Phys.*, 1999, **110**, 6158–6170.
- 22 F. Jensen, *J. Chem. Theory Comput.*, 2015, **11**, 132–138.

- 23 (a) B. Metz, H. Stoll and M. Dolg, *J. Chem. Phys.*, 2000, **113**, 2563–2569; (b) K. A. Peterson, D. Figgen, E. Goll, H. Stoll and M. Dolg, *J. Chem. Phys.*, 2003, **119**, 11113–11123; (c) D. Rappoport and F. Furche, *J. Chem. Phys.*, 2010, **133**, 134105.
- 24 T. Lu, F. Chen, *J. Comput. Chem.*, 2012, **33**, 580–592.
- 25 (a) S. Dapprich and G. Frenking, *J. Phys. Chem.*, 1995, **99**, 9352–9362; (b) M. Xiao and T. Lu, *J. Adv. Phys. Chem.*, 2015, **04**, 111–124.
- 26 (a) D. Feller, *J. Comput. Chem.*, 1996, **17**, 1571–1586; (b) K. L. Schuchardt, B. T. Didier, T. Elsethagen, L. Sun, V. Gurumoorthi, J. Chase, J. Li and T. L. Windus, *J. Chem. Inf. Model.*, 2007, **47**, 1045–1052; (c) B. P. Pritchard, D. Altarawy, B. Didier, T. D. Gibson and T. L. Windus, *J. Chem. Inf. Model.*, 2019, **59**, 4814–4820.
- 27 (a) E. D. Glendening, C. R. Landis and F. Weinhold, *J. Comput. Chem.*, 2013, **34**, 1429–1437; (b) E. D. Glendening, C. R. Landis, F. Weinhold, *J. Comput. Chem.*, 2013, **34**, 2134.
- 28 (a) P. v. R. Schleyer, C. Maerker, A. Dransfeld, H. Jiao and N. J. R. van Eikema Hommes, *J. Am. Chem. Soc.*, 1996, **118**, 6317–6318; (b) Z. Chen, C. S. Wannere, C. Corminboeuf, R. Puchta and P. v. R. Schleyer, *Chem. Rev.*, 2005, **105**, 3842–3888.